INTERNATIONAL SOCIETY FOR
SOIL MECHANICS AND
GEOTECHNICAL ENGINEERING

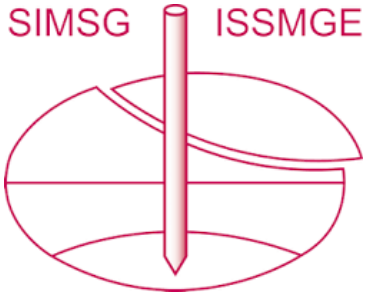

This paper was downloaded from the Online Library of the International Society for Soil Mechanics and Geotechnical Engineering (ISSMGE). The library is available here:

https://www.issmge.org/publications/online-library

This is an open-access database that archives thousands of papers published under the Auspices of the ISSMGE and maintained by the Innovation and Development Committee of ISSMGE.

Shallow Foundations and Pavements

Fondations peu profondes et chaussées

Chairman/Président: A. CROCE (Italy)
Deputy Chairman/Président adjoint: J. E. HURTUBISE (Canada)
General Reporter/Rapporteur général: E. E. DE BEER (Belgium)

Panel Members/Membres du Groupe de discussion
H. BOROWICKA (Austria)
Y. KOIZUMI (Japan)
R. L'HERMINIER (France)
J. A. J. SALAS (Spain)

Chairman: A. CROCE (Italy)

Ladies and Gentlemen. To open this session, I would like to introduce Mr. J. Hode Keyser, of the Department of Public Works of the City of Montreal who will speak on Engineering Geology and Public Works in Montreal. Mr. Hode Keyser.

(*Mr. Hode Keyser's lecture appears on pp. 114–33.*)

CHAIRMAN CROCE

I would like to express our gratitude to Mr. J. Hode Keyser for his fine and very interesting lecture. I would like to take this opportunity to stress the interest of such lectures, and I think that we have to be grateful to our Canadian colleagues of the Organizing Committee who have made them available. I propose now to adjourn for two minutes.

(*There followed a brief intermission.*)

CHAIRMAN CROCE

The General Reporter for this session is Professor de Beer. Professor de Beer's outstanding contributions to the field of soil mechanics are well known to all of us. We have read his General Report and now Professor de Beer will summarize the parts of this report which deal with the subjects to be discussed this morning. Professor de Beer.

Rapporteur général: E. E. DE BEER (Belgique)

Les organisateurs du Congrès ont prévu deux sessions pour la Division 3 qui groupe les problèmes se rapportant aux fondations directes et aux revêtements. A première vue une répartition logique semblait être de consacrer la session du matin aux problèmes de fondation et celle de l'après-midi aux revêtements. Toutefois des 48 rapports introduits, 33 se rapportent aux problèmes de fondation et 15 aux problèmes de revêtement. On pouvait donc craindre un certain deséquilibre entre les deux sessions.

Les problèmes de fondation directe peuvent être groupés essentiellement sous trois rubriques: 1) ceux concernant la capacité portante limite; 2) ceux concernant les tassements; 3) ceux concernant la répartition des réactions du sol sous la semelle de fondation. Afin de tâcher d'obtenir une meilleure répartition entre les deux sessions, il a été finalement convenu que la session du matin serait consacrée aux problèmes de la capacité portante limite et de la répartition des réactions sol-fondation, tandis que celle de l'après-midi traiterait des problèmes de tassements et de celui des revêtements.

Dans la séance de ce matin je dois dès lors vous présenter un bref aperçu de la partie de mon Rapport général traitant des problèmes de capacité portante limite et de la répartition des réactions sol-fondation.

CAPACITÉ PORTANTE LIMITE

De tous les rapports introduits il n'y a qu'un seul qui traite du problème de la capacité portante limite de sols purement cohérents. *Bent Hansen (3/15)* présente une méthode approchée pour des problèmes en déformation plane et qui tient simultanément compte des conditions statiques et cinématiques. Tous les autres rapports traitent des problèmes de capacité portante limite des sols pulvérulents.

Il est su que des essais sur semelles filantes de petites dimensions posées à la surface d'un sable donnent pour le facteur de portance N_γ des valeurs nettement supérieures aux valeurs théoriques. Différentes explications ont été avancées pour cette divergence. Lors d'une conférence à Essen, le professeur Meyerhof a conclu en disant que si on introduit dans les formules exactes les valeurs exactes des paramètres caractéristiques du matériau, on obtient la réponse exacte. On peut dès lors classer les explications avancées en deux catégories.

1) Une première catégorie part de l'hypothèse que les formules ou déductions théoriques obtenues pour des matériaux rigido-plastiques à volume invariant restent valables, à condition d'y introduire les paramètres caractéristiques du sol: (*a*) Une première explication donnée est alors que l'angle de cisaillement en déformation plane aurait une valeur environ 10 pour-cent supérieure à celle en déformation triaxiale. C'est l'explication de Brinch Hansen et de Meyerhof. (*b*) Une autre explication est que pour une compacité donnée d'un sol pulvérulent la courbe intrinsèque n'est pas une droite caractérisée par des valeurs constantes de c et de Φ, mais bien une courbe tournant sa concavité vers l'axe des contraintes normales. (*c*) Une troisième explication introduit les phénomènes de dilatance dont l'influence n'est pas nécessairement la même dans un essai triaxial, un essai de cisaillement direct, et dans les phénomènes de refoulement sous une semelle. Cette influence est notamment étudiée dans le rapport de *Feda and Pruska (3/10)*. Ce point mérite certainement une plus ample attention.

2) Une deuxième catégorie abandonne les résultats de la théorie des milieux rigido-plastiques à volume invariant, et part de l'adoption de surfaces de glissement jugées correspondre aux formes expérimentales. Depuis le Congrès de

Paris ont paru les contributions de Balla et de Hu. Dans la même catégorie on peut ranger la contribution de *Gorbunov-Possadov (3/11)* présentée au présent congrès. Une remarque générale concernant les méthodes se rapportant à cette 2e catégorie est qu'elles ne sont en général pas statiquement correctes, et que d'autre part les résultats que l'on obtient à partir d'une surface de glissement plus ou moins arbitraire sont fortement influencés par des variations même fort légères de la surface, de sorte que l'on ignore en fait où ils se situent par rapport à la réalité.

En définitive il existe pour l'instant des méthodes fort différentes pour déterminer la capacité portante limite. Il me paraît dès lors du plus haut intérêt de discuter au cours de cette séance des différentes méthodes, afin de clarifier les idées à ce sujet. Pour ma part je voudrais attirer l'attention sur les points suivants:

1) Les essais décrits dans le rapport de *L'Herminier, et al. (3/25)* montrent que la différence entre les valeurs expérimentales et théoriques du facteur de portance N_q est de loin moins importante que celle entre les valeurs expérimentales et théoriques du facteur de portance N_γ. Or si les différences constatées étaient dues à une différence entre les angles de cisaillement de déformation plane et triaxiale, on dévrait s'attendre à un même ordre de grandeur pour la différence des valeurs expérimentales et théoriques de N_q et N_γ. Les résultats des essais français semblent donc infirmer l'explication basée sur la différence des angles en déformation plane et triaxiale.

2) Les essais décrits par *Milovič (3/30)* indiquent que les valeurs obtenues par la méthode de Balla s'écartent pour certains sols de la réalité.

3) Les différences trouvées pour des semelles de petites dimensions ne sont pas nécessairement valables pour les semelles réelles. Une des raisons est que le phénomène de rupture progressive, lié d'ailleurs aux phénomènes de variation de volume (dilatance positive ou négative) n'est pas reproduisible à l'échelle. A ce sujet je puis renvoyer aux essais effectués par le Dr Muhs à Berlin, et aussi à la contribution de *Lee (3/23)* qui décrit des essais sur plaques de dimensions relativement grandes.

En dehors du problème de semelles soumises à des charges statiques se pose aussi de plus en plus le problème de semelles soumises à des charges *dynamiques*. Deux contributions importantes ont été introduites à ce sujet, celle de *Triandafilidis (3/44)* qui s'occupe du cas de sols purement cohérents et celle de *Vesič et al. (3/45)* qui s'occupent des sols pulvérulents. Dans le dernier cas les essais effectués montrent que la capacité portante limite de sable est fonction de la vitesse de chargement, et qu'à vitesse de chargement croissante la capacité portante limite décroît d'abord, pour remonter ensuite et atteindre un maximum sous des mises en charge quasi instantanées. Le problème de la capacité portante limite sous des actions dynamiques, vu son intérêt pratique croissant, me semble dès lors être aussi un point intéressant de discussion.

Deux contributions, notamment celles de *Mandel (3/27)* et de *West and Stuart (3/46)*, traitent de l'influence de la présence de semelles avoisinantes sur la capacité portante limite. Pour autant que la superstructure permet de reprendre les moments et les efforts tangentiels, les coefficients de majoration peuvent être importants lorsque l'entredistance des semelles devient relativement faible. Dans certains cas particuliers la prise en considération de cette influence peut dès lors amener à une économie appréciable. Ce raffinement pourrait alors être introduit dans la méthode décrite par *Kany (3/20)*, indiquant, comment à partir des normes allemandes, on peut déterminer la solution la plus économique pour une fondation directe sur semelles multiples.

Certains rapporteurs, notamment *L'Herminier, et al. (3/25)* et *Livneh (3/26)* traitent du problème de la capacité portante limite au cas d'un sous-sol composé de couches multiples, dont un cas particulier est celui d'une couche portante d'épaisseur limitée, et terminée inférieurement par un interface où l'adhésion est nulle. *Kany (3/20)*, dans son mémoire, décrit aussi une façon empirique pour déterminer la capacité portante limite au cas où celle-ci est influencée par des couches de caractéristiques différentes. Comme de tels problèmes se présentent assez fréquemment aux praticiens, ils constituent sans aucun doute un sujet intéressant de discussion.

D'autres problèmes ont été encore traités par les rapporteurs; ainsi *Feda and Pruska (3/10)* ont considéré l'influence des pressions hydrodynamiques sur l'apparition d'une première zone plastique, *Mintskovsky (3/31)* détermine la capacité portante limite de fondations terminées inférieurement en forme de cône, *Granger (3/12)* s'occupe de l'équilibre des parois de réservoirs d'eau, tandis que *Penman and Watson (3/36)*, ainsi que *Mehra and Natarajan (3/29)* traitent de l'application de la méthode de préconsolidation par surcharges temporaires et de l'emploi de drains de sable pour accroître la résistance au cisaillement et assurer ainsi une sécurité suffisante par rapport à la capacité portante limite. Ce sont là certes aussi tous des sujets très intéressants.

Eu égard au temps disponible, je puis en définitive proposer comme sujets principaux de discussion, se rapportant à la capacité portante limite, les sujets suivants.

1) Validité des différentes méthodes de calcul théoriques pour la détermination de la capacité portante limite sous des fondations directes. Comparaison des valeurs calculées par les différentes méthodes et les données expérimentales obtenues par des essais à l'échelle réduite et en vraie grandeur.

2) Capacité portante limite au cas d'un sous-sol composé de couches multiples ou de sols anisotropes.

3) Influence de la vitesse de chargement sur la capacité portante limite, incluant donc les chargements dynamiques.

4) Influence de semelles avoisinantes sur la capacité portante limite.

RÉPARTITION DES RÉACTIONS DU SOL SOUS LES SEMELLES DE FONDATION

En dehors des problèmes de la capacité portante limite et des tassements, se pose souvent au cas de semelles de grandes dimensions et de radiers généraux celui de la détermination de la répartition des réactions du sol sous le massif de chargement.

Les méthodes de calcul peuvent être classées en deux catégories: la première groupe les méthodes basées sur l'introduction d'un coefficient de raideur, constant ou variable; la deuxième celles qui assimilent le sol a un matériau caractérisé par un module d'élasticité constant ou variable.

On ne peut se dissimiler que chacune des deux catégories est basée sur une simplification des propriétés du sol. Cela ressort e.a. clairement des résultats des essais décrits par *Lee (3/23)*. Les modèles mathématiques dont on dispose (coefficient de raideur ou module d'élasticité constant) s'écartent donc plus ou moins fortement des propriétés réelles des sols.

Dans une étude remarquable *Zaretsky and Tsytovich (3/48)* établissent les équations générales du problème plan permettant de trouver la répartition des constraintes sous une semelle infiniment rigide et chargée de charges quelconques,

posée sur un terrain à volume invariant et dont la loi de déformabilité est non linéaire et continûment variable avec la profondeur. Cette contribution montre elle aussi que les répartitions obtenues à partir d'une loi de déformabilité linéaire et d'un module de compressibilité constant peuvent dans certains cas s'écarter notablement de la réalité.

Une autre contribution fort intéressante est celle d'*Egorov (3/9)* qui traite du problème des tassements, du déversement et de la répartition des réactions sous une semelle en forme de couronne, considérée comme infiniment rigide et établie sur un massif semi-infini à module d'élasticité constant. Le cas des semelles circulaires pleines et des semelles filantes constituent des cas particuliers du problème traité.

La répartition de réactions ne dépend d'ailleurs pas uniquement de la raideur de la semelle, et des propriétés de déformabilité du sol de fondation, mais aussi de la raideur de la superstructure et de celle des liaisons entre le radier et la superstructure. Une méthode fort élégante et qui est en principe applicable quelle que soit la loi de déformabilité du sol de fondation, pourvu qu'elle soit linéaire, est donnée par *Sommer (3/42)*.

Enfin *Chae, et al. (3/5)* traitent de l'influence de la vitesse d'application des charges sur la loi de répartition des réactions du sol.

Il apparaît que les méthodes du coefficient de raideur sont de plus en plus abandonnées en faveur de celles basées sur un module de déformabilité.

Cependant pour obtenir des méthodes de calcul définitivement valables, il est indispensable de connaître plus exactement les paramètres caractérisant la déformabilité des sols. A cet effet il est nécessaire de passer à une confrontation des résultats des différentes méthodes de calcul de la répartition des réactions du sol avec les résultats de mesures.

Je vous propose dès lors cette confrontation comme dernier point de discussion de la session de ce matin.

(*Professor de Beer's General Report appears on pp. 242–55.*)

CHAIRMAN CROCE

I thank the General Reporter, on your behalf, for his very fine and excellent summary. Now we can pass on to the panel discussions.

Panelist: H. BOROWICKA (Austria)

As time is short I won't go into too much detail, but will consider the ultimate bearing capacity of shallow footings from a more general and practical point of view. Actually we have to deal with two questions closely related to each other: the method of computation to be applied in a special case and the magnitude of the shear parameters to be introduced into the computation. As the computation is very sensitive to the magnitude of the shear parameters, the two questions cannot be dealt with separately.

As far as shear strength is concerned we must always have in mind that stresses in soils are only fictitious average values and do not exist in reality. Therefore, the failure condition we use in soil mechanics can never have the meaning of an exact physical law but must be considered as a relationship based on the principle of probability. Taking this fact into account, we realize clearly that the shear parameters are seldom exact and constant values. Apart from scattering, which cannot be eliminated, the type of shear test and even the test procedure has a certain influence on the test result. In addition, I should like to point out that the shear parameters might change in nature as time passes. Since a relatively small deviation in the magnitude of the shear parameters has a considerable influence on the result of computation, the computed bearing capacity is only a rough estimate.

As far as the method of computing the bearing capacity itself is concerned, there are two basic cases with simple and clear conditions: (1) Sudden loading of a fine-grained soft and fully saturated soil having such a low permeability that pore water pressures cannot dissipate; and (2) loading of a soil in such away that no pore water pressures have to be taken into account.

The first case refers particularly to soft saturated clays. The shear strength is to be assumed as one-half of the unconfined compressive strength of the clay. The apparent angle of internal friction determined by quick undrained triaxial tests equals zero. The pore water pressures which are caused by quick loading are already considered by the assumption made on the shear strength. From many failures which have actually occurred with soft saturated clays, results show that this method is fairly correct. The method was extended by Dr. Skempton to partly saturated clays by introducing apparent shear parameters determined by quick undrained triaxial tests. In the case of stiff or hard clays the method becomes somewhat doubtful. In these cases, conditions are similar to those in hard rocks in which the average shear strength cannot be determined by tests using small samples. In the case of foundations on clay prone to slippage we must be very careful, particularly if horizontal forces are involved.

The second case refers to coarse-grained soils such as gravel and sand, and also to fine-grained soils after the dissipation of pore water pressures. There are several formulae to compute the ultimate bearing capacity. In principle, these methods do not differ very much. They all use two shear parameters and obtain the ultimate bearing capacity as the sum of three terms, but there are great differences in the results of the computations. As these methods have been compared and discussed several times, there is no need to do so now.

We should never forget that all these formulae are based on small-scale tests frequently of very small dimensions. So far, we do not know whether extrapolation of these tests to prototype dimensions is permissible and, if so, to what extent. Because of this uncertainty it might be better to pay more attention not to the discrepancy of the results from various formulae but to the limit of validity of each individual formula and to the shear parameters to be introduced.

As long as we do not have a more positive proof or justification it would be wise to consider the computed bearing capacity a fictitious value which ideally should be the correct one but which in fact may deviate considerably. In spite of this, the computation of the bearing capacity is not useless; it should be done and is actually very helpful. But the work of the expert or engineer does not terminate with this computation. Based on his personal experience he has to judge whether in the case under consideration the real bearing capacity might be higher or even lower than the computed one.

In dense soils we do not have an opportunity to check the computed bearing capacity because, unfortunately, failures will not occur. But then we should not worry too much that we do not know the true safety factor in such a case.

I wish to call attention, however, to foundations on loose and extremely loose soils. Professor Terzaghi pointed out that no general shear failure will occur in such a case but that the footing will sink into the ground without a well-defined break in the load-settlement curve. He proposed to reduce the shear parameters to two-thirds in the case of a loose

soil. But he did not tell us where the limit is at which the reduction must be made. There should also be a transition zone in which the reduction factor decreases from one- to two-thirds. In addition, we should ask whether the proposed reduction is sufficient in the case of an extremely loose sand. Tests carried out by Dr. Bjerrum showed that the angle of internal friction of very loose sand may drop considerably. These tests suggest that the reduction to two-thirds taken from the angle of internal friction of loose sand under normal conditions might not be enough in some cases.

I know at least one case in which a small bridge abutment was sinking continuously into the ground at a rate of one cm per month at a load which was one-half the bearing capacity value computed by Terzaghi's local shear failure formula for loose sand. This sinking was accompanied by heaving of the ground surface 20 to 150 m away. (This shows that heaving can take place at very great distances from the footing.) Immediately adjacent to the bridge the soil surface settled. This is an effect that usually cannot be observed in small-scale tests.

In conclusion I wish to summarize the main points of this discussion.

1. The shear parameters with which we have to work are not absolute and true, but only probable values with a certain confidence limit.

2. On fine-grained soft saturated soils, the bearing capacity values for sudden loading are usually reliable.

3. On coarse-grained soil, on the other hand, various formulae yield differing results. Even more important than these discrepancies are the limits within which these formulae are valid and the magnitude of the shear parameters to be introduced.

4. These methods cannot be applied in loose and extremely loose soils. Here another phenomenon appears which Terzaghi called local shear failure or sinking into the ground. He gave some hints how to handle this problem but further studies are still necessary.

Panelist: R. L'HERMINIER (France)

Dans son Rapport général, Monsieur le Professeur de Beer a mis en évidence la grande dispersion des valeurs de N_γ obtenues suivant les auteurs. C'est ainsi que pour un angle de frottement interne $\varphi = 40°$, N_γ varie de 38 (Sokolovsky) à 192 (Gorbunov-Possadov). De telles différences proviennent d'un certain nombre de facteurs. (1) Les fondations sont considérées comme lisses ou rugueuses, souples ou rigides. (2) Les auteurs se sont efforcés d'obtenir des schémas d'écoulement statiquement valables ou bien ont mis l'accent sur la détermination des lignes de glissement à partir des données expérimentales, c'est-à-dire à partir des trajectoires décrites par les grains du milieu sableux. (3) Enfin les limites du noyau élastique, qui se forme sous la semelle, ont un tracé différent suivant les auteurs—soit rectiligne, soit curviligne; certains préfèrent la simplicité du calcul à l'exactitude mathématique. Pour éclairer ces différent aspects du problème, nous allons examiner le schéma classique d'une semelle rugueuse, et le comparer au schéma d'écoulement obtenu par la méthode des caractéristiques.

FONDATIONS RUGUEUSES: SCHÉMA CLASSIQUE ET SCHÉMA RÉSULTANT DE L'EMPLOI DE LA MÉTHODE DES CARACTÉRISTIQUES

Dans le schéma classique (voir la fig. 1) les lignes de glissement inférieures de la première famille limitant le domaine plastique sont tangentes en A suivant l'axe vertical de la semelle. Un dièdre de sol compacté d'arêt A, dont les

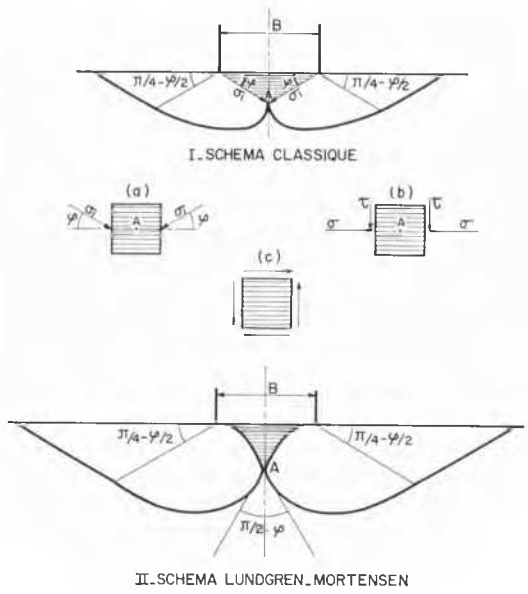

FIG. 1. Fondations rugueuses: schéma classique et schéma résultant de l'emploi de la méthode des caractéristiques.

plans extrèmes passent par les bords de la fondation, a une ouverture égale à $\pi - 2\varphi$. Ce sol compacté comporte un noyau central élastique limité par les lignes de glissement inférieures de la première famille prolongées du point A à la surface de la fondation. Le surplus du dièdre est un équilibre plastique. Sur les bords du dièdre, les contraintes sont verticales et tangentes aux lignes de glissement de la première famille. Sur un élément plan vertical centré sur A, les contraintes σ_1 situées de part et d'autre de cet élément sont inclinées de l'angle φ sur l'horizontale et symétriques par rapport à l'axe vertical de la semelle (fig. 1a). Il en résulte que la décomposition des deux contraintes σ_1 en contraintes normales et contraintes tangentielles donne le schéma "b" sur les faces verticales d'un petit cube élémentaire centré sur A. Les contraintes tangentielles sont toutes les deux dirigées verticalement vers le bas—ce qui est en contradiction avec le schéma "c" d'équilibre des forces, qui exige que les contraintes tangentielles forment deux couples égaux et de sens contraire. Le schéma classique n'est donc pas statiquement valable dans la zone du point A.

Au contraire dans le schéma d'écoulement déterminé par la méthode des caractéristiques, ces lignes de glissement inférieures de la première famille ne sont pas tangentes en A, mais forment entre elles un angle égal à $\pi/2 - \varphi$, c'est-à-dire un angle $(\pi/4 - \varphi/2)$ avec la verticale. Les contraintes principales en A sont l'une horizontale, l'autre verticale de telle sorte que l'objection présentée pour le schéma classique tombe d'elle-même. D'ailleurs les caractéristiques limitant le domaine plastique ont été précisément choisies de telle sort qu'elles soient inclinées sur la verticale de l'angle $(\pi/4 - \varphi/2)$ à leur point d'intersection avec l'axe de la semelle—ce qui fixe la position du point A.

En ce qui concerne l'aspect cinématique du problème, l'étude expérimentale des trajectoires décrites par les particules de sol montre que ces trajectoires sont verticales sur le pourtour du noyau élastique. Si l'on admet—et ce n'est qu'une hypothèse—que les caractéristiques des contraintes et les trajectoires des grains sont confondues, le schéma classique répond bien aux données expérimentales, alors que le

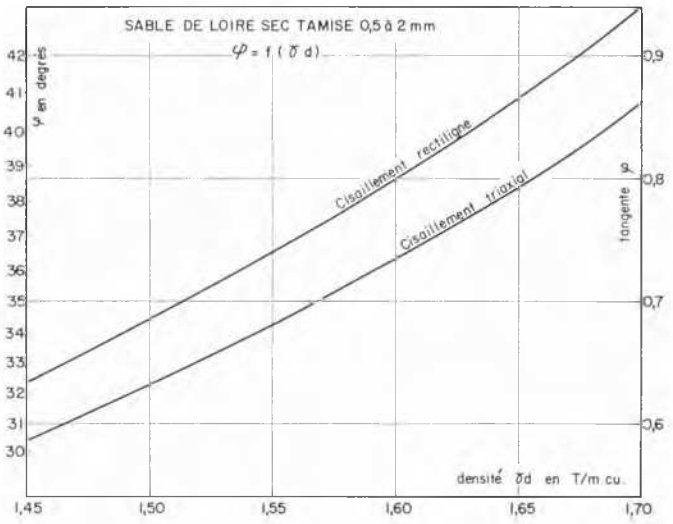

FIG. 2. Sable de Loire sec, tamisé 0.5 à 2 mm. L'angle de frottement interne φ en fonction de la densité γ_d.

schéma résultant de l'emploi de la méthode des caractéristiques prêts à discussion puisque les lignes de glissement de la première famille ne sont pas dirigées suivant la verticale à leur point de rencontre avec le noyau élastique.

Toutefois, il est bon de rappeler que l'on ne connait pas les conditions cinématiques générales à satisfaire pour mettre un milieu pulvérulent en état d'équilibre limite. Elles doivent résulter de la relation entre contraintes et déformations dans un tel milieu lorsque l'état d'équilibre est atteint. Mais cette relation est inconnue à l'heure actuelle.

Gorbunov-Possadov (3/11) donne un nouveau schéma d'écoulement en système plan basé sur les résultats expérimentaux, c'est-à-dire sur les trajectoires verticales des grains de sable aux abords de la semelle.

L'auteur définit successivement à partir de la fondation et en s'éloignant progressivement de cette dernière: (a) Un dièdre de sable compacté sous la semelle. Ce dièdre se subdivise en un noyau élastique lié à la semelle et en une zone

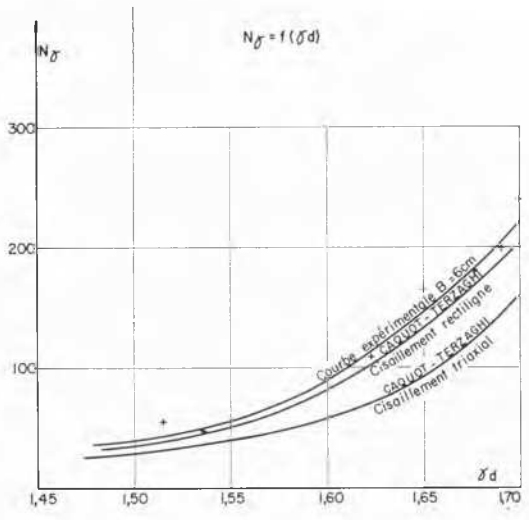

FIG. 3. Valeurs expérimentales et théoriques de N_γ en fonction de la densité γ_d pour une semelle filante de 6 cm de largeur.

constituant le surplus du dièdre, mais en équilibre plastique. La totalité du dièdre délimite l'ensemble de la zone compactée. (b) Une zone de transition, également en équilibre plastique, comprise entre le dièdre de sable compacté et la zone terminale des lignes de glissement (partie en équilibre de Rankine et partie calculée suivant la méthode des caractéristiques). L'auteur a établi ce schéma d'écoulement avec le souci constant de rester dans le cadre des données expérimentales.

Au sujet de ce schéma, le Rapporteur général formule les remarques suivantes: (1) Les vitesses dans les zones plastiques sont dirigées suivant les lignes de glissement actives. Mais cette hypothèse peut être controversée. (2) Dans la partie plastique du dièdre, l'axe vertical constitue une enveloppe des lignes de glissement de la première famille. L'auteur s'est efforcé de rendre la solution statiquement valable "mais certaines singularités notamment le long de l'axe de symétrie en font douter." On retrouve ici les objections présentées au sujet du schéma classique.

Nous serions heureux de connaître le point de vue de l'auteur. Quoi qu'il en soit, Gorbunov-Possadov fournit les valeurs les plus élevées du terme N_γ.

VALEUR DE L'ANGLE DE FROTTEMENT À PRENDRE EN CONSIDERATION

Le sable utilisé à Paris au Centre expérimental de la rue Brancion est à l'heure actuelle du sable sec tamisé de Loire (dimensions des grains 0,5 mm à 2 mm).

Ce sable vient de faire l'objet d'essais de cisaillement systématiques en fonction de sa densité, soit par cisaillement rectiligne, soit par cisaillement triaxial (fig. 2). Il ressort des résultats obtenus, qu'à densité égale, l'angle de frottement interne est, dans la gamme des densités expérimentées plus élevé d'environ 3° pour le cisaillement rectiligne. Comme le précise le Rapporteur général, les auteurs dans leur ensemble seraient d'accord pour estimer que le cisaillement rectiligne fournit des angles, supérieurs d'environ 10 pour-cent à ceux résultant du cisaillement triaxial normal. (Avec le sable de Loire, nous avons obtenu 8 pour-cent.)

Il ressort de ce qui précède qu'à chaque densité correspond deux angles de frottement, et par conséquent deux valeurs théoriques de N_γ par application d'un des schémas d'écoulement. Nous avons pris la moyenne des valeurs, d'ailleurs très voisines, fournies par les schémas d'écoulement Terzaghi et Caquot (fig. 3).

D'autre part, nous avons représenté sur la même figure, les valeurs expérimentales de N_γ obtenues en laboratoire à l'aide d'une semelle filante de 6 cm de largeur. Le tracé des courbes montre que, sous réserve d'adopter l'angle de frottement obtenu par essai rectiligne, il y a une bonne concordance entre les résultats expérimentaux et les résultats théoriques.

Toutefois, il ne semble pas que cette conclusion puisse faire l'objet d'une certaine généralisation.

En effet, les différents auteurs qui se sont intéressés à ce problème ont constaté que les résultats expérimentaux fournissent pour N_γ des valeurs égales à plusieurs fois la valeur de N_γ théorique.

En adoptant 10 pour-cent de majoration sur l'angle de frottement déterminé au triaxial, on obtient pour N_γ les pourcentages d'augmentation suivants: 57 (φ triaxial, 30°); 79 (φ triaxial, 35°); 115 (φ triaxial 40°). Ces pourcentages apparaissent faibles par rapport à ceux résultant de l'expérience sauf pour $\varphi = 40°$. En effet nous avons obtenu avec du sable de Leucate trois fois la valeur théorique de N_γ pour

φ compris entre 30° et 35°, et deux fois seulement cette valeur pour $\varphi = 40°$.

Certains chercheurs ont exprimé la crainte que la courbe intrinsèque des sables ne présente une concavité marquée vers l'axe des contraintes normales, et que de ce fait la résistance au cisaillement soit plus faible pour des contraintes élevées que celles résultant de la droite de Coulomb, généralement déterminée pour des contraintes normales inférieures à 10 kg/cm.ca. Nous donnons (fig. 4) la courbe

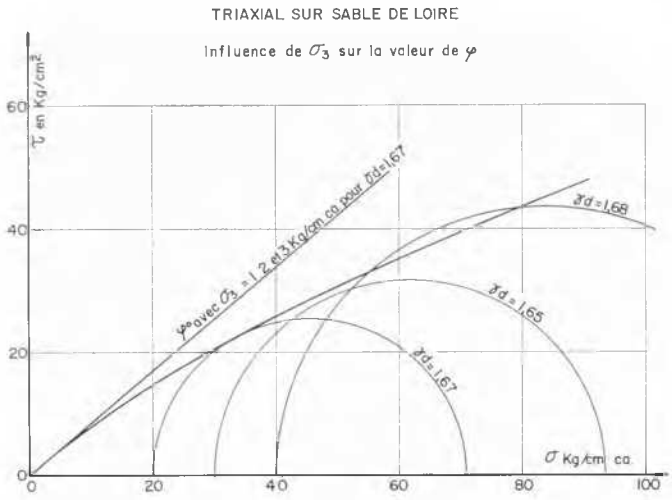

FIG. 4. Courbe intrinsèque du sable de Loire.

intrinsèque du sable de Loire (pour une densité de 1,65–1,68 tonnes m.cu.) jusqu'à des valeurs de la contrainte normale de l'ordre de 80 kg/cm.ca. Cette courbe montre que pour les valeurs habituelles des contraintes, concernant les fondations superficielles ou semi-profondes, et compte tenu du coefficient de sécurité généralement admis, on peut considérer que la droite de Coulomb reste applicable.

SEMELLE UTILISÉE PAR LE CENTRE EXPÉRIMENTAL DE PARIS POUR L'ÉTUDE DES FONDATIONS SUPERFICIELLES

Le modèle (fig. 5) a été conçu pour étudier le problème de la portance des semelles filantes superficielles verticales ou inclinées avec un ancrage pouvant atteindre quatre fois la largeur de la semelle, dans une cuve à faces parallèles dont elle occupe toute la largeur.

La semelle est rigide, encastrée et ne possède qu'un seul degré de liberté suivent l'axe de déplacement du modèle. Elle est divisée en trois parties: deux parties extérieures de garde et une partie centrale de mesure. Ceci pour éviter de prendre en compte les perturbations dues aux parois. La partie centrale sensible de mesure à 3 cm de longueur pour une longueur totale du modèle égale à 20 cm.

Cette partie sensible libre par rapport aux parties de garde est équipée de deux micro-dynamomètres dont la déformation maximale est de 2/100ème de mm. Ces dynamomètres de même capacité de charge sont disposés symétriquement par rapport à l'axe de la semelle, normalement à son plan. Ils permettent de déterminer le point d'application de la composante normale et sa valeur. De plus, l'un des deux anneaux dynamométriques est équipé de lames de flexion qui permettent de mesurer le moment résultant de toute force horizontale appliquée dans le plan inférieur de la semelle.

Enfin la hauteur et la nature de matière des parties de garde ont été choisies de façon qu'elles présentent le même module de déformabilité que la partie centrale. On peut

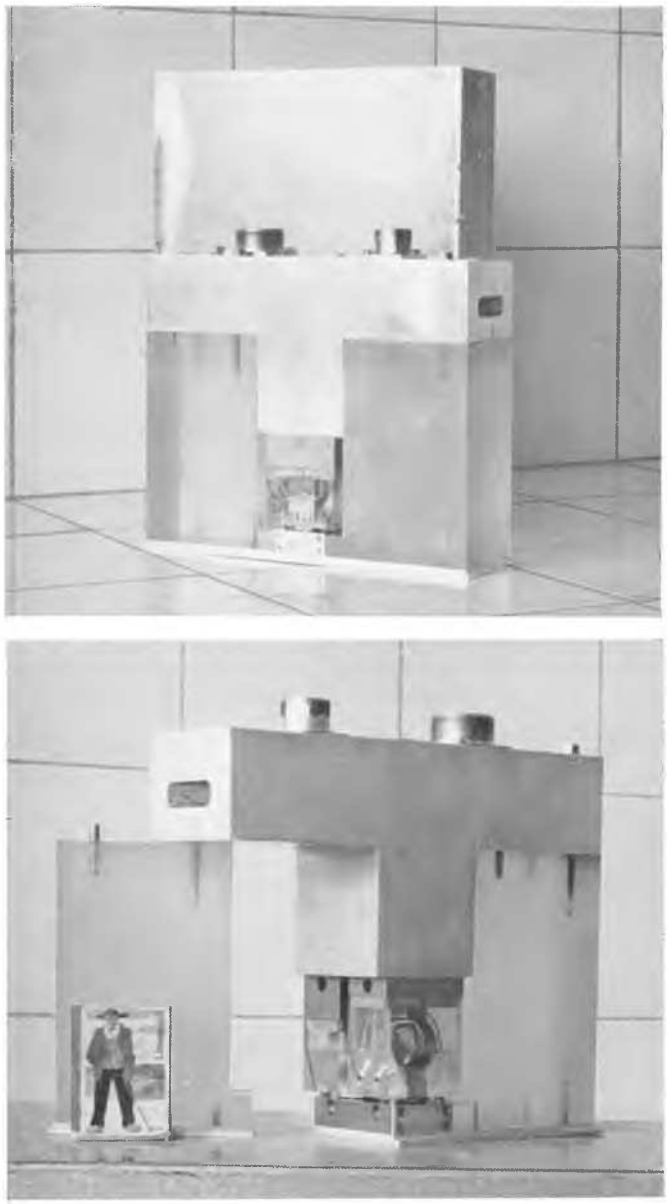

FIG. 5. Semelle utilisée par le Centre expérimental de Paris pour l'étude des fondations superficielles.

assurer que parties de garde et partie sensible constituent, au point de vue déformation, un ensemble homogène et que toutes trois subissent le même déplacement.

CONCLUSIONS

La détermination théorique du term N_γ (suivant un schéma à la fois statiquement valable et cinématiquement possible demeure un problème posé. En l'état actuel de la question, seul un schéma du type Lundgren-Mortensen (fig. 1) est à retenir.

En adoptant une majoration de 10 pour-cent sur l'essais triaxial normal on obtient des valeurs de N_γ qui se rapprochent des valeurs expérimentales surtout pour des angles de frottement voisins de 40°. Il n'en est pas de même pour des angles plus faibles comme nous l'avons vu. Mais il s'agit de petites semelles expérimentées en laboratoire. Il faut demeurer prudent pour les semelles de dimensions normales.

Panelist: Y. KOIZUMI (Japan)

I should like to start my discussion by considering the problem of the progressive failure of multi-layered soils. The actual soil which we encounter is neither homogeneous nor isotropic; it is anisotropic or multi-layered. Thus, when applying the bearing capacity theory established for homogeneous soils to such a soil, the foundation engineer must

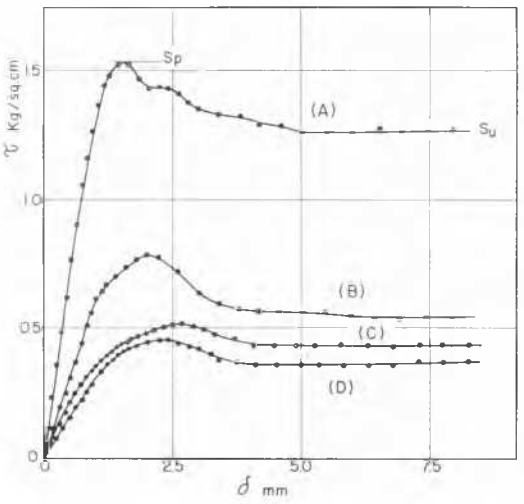

FIG. 6. Results of shear box tests with sensitive clays.

rely, to a greater or lesser extent, upon his judgment. The ultimate bearing capacity of multi-layered soils is commonly estimated using the average shear parameters of soils within the failure zone, if their soil properties are not widely different. The depth of the failure zone is usually taken as equal to or about twice the foundation width. Such design practice may occasionally lead to overestimation of the ultimate bearing capacity of multi-layered soils, especially in cases involving overconsolidated or sensitive clays.

Fig. 6 shows the results of shear box tests with several highly sensitive clays (S_r = 20 to 60). As the clay is strained, it builds up an increasing resistance. But, under a given effective pressure, there is a definite limit to the resistance the clay can offer, and this is the peak point strength s_p. If the test is continued, then we find that as the displacement increases the resistance decreases gradually to the ultimate strength s_u. The difference between these two values is also considerable for overconsolidated clays and dense sands.

Even in a homogeneous soil, a failure surface under a foundation would not occur simultaneously throughout its entire length, but would start at points of maximum strain and develop progressively. In practice this progressive effect may be unimportant if the soil is uniform. But when the ground consists of different soils with different stress-strain relationships, failure occurs much more progressively or it proceeds in one soil layer after another. The ultimate bearing capacity of layered soils may thus be overestimated if the shear parameters are taken from the peak point strength for each of the layered soils. The degree of overestimation depends on the difference in shear and deformation parameters among the layered soils, and also on the thickness and sequence of the layers.

As an example of the simplest case, we performed plate loading tests with two layered clays whose shearing characteristics are shown in Fig. 6. Undisturbed soil blocks were taken at several excavations by means of steel tubes 40 cm in diameter, and two-layered specimens were made by combining these clays. Great care was taken to avoid disturbance. Loading tests were also made with the individual clays. The loading plate was 5 cm in diameter. The observed ultimate bearing capacity values of the two-layered soils were considerably lower in Cases B and C than those obtained from Button's method (Button, 1953), and much lower than those calculated by the conventional practical method. The discrepancy seems to vary according to the method of calculation and the sequence of soil layers. The progressive effect would appear to contribute, at least partially, to lowering the bearing capacity of the layered soils.

Another contributing factor influencing the overestimation of the ultimate bearing capacity of layered soils is the sliding surface. Sliding surfaces which occur in a layered soil may be not single or continuous but composite or discontinuous. Actual failure will take place along one of the potential sliding surfaces which has a minimum bearing capacity.

When the ground consists of soils with widely different properties, the effects of these factors affecting the ultimate bearing capacity are more pronounced. Consider a case in which a sand layer is underlain by a soft clay deposit. When load is applied, the sand layer certainly contributes to spreading it onto the underlying clay as long as both layers remain in an elastic state. When the shearing stress at any point in the layers reaches a yielding stress, the sand layer will be punched down and rupture will take place in the underlying clay. Tcheng (1957) observed that punching occurred vertically when loose cohesionless material with a thickness less than $1.5B$ (B = width of footing) is placed on a very soft cohesive material. In general, the angle of punching surface depends largely upon the thickness and density of the sand layer, and the deformability and shearing strength of the clay. In a case of two-layer clays in which the upper layer is about six times as strong as the lower layer (Fig. 7c), it has been found that the punching occurred exactly vertical through the upper layer.

Since the sliding surfaces in stratified soils with widely different properties are affected by so many factors, further studies in this area should be made on the basis of observations of sliding surfaces in model tests.

I would now like to draw your attention to the fact that the bearing capacity of layered clays can decrease on both sides of a foundation some time after application of load, as already pointed out by Bishop and Bjerrum (1960) and Kenney (1964). In the case of layered clays, which occasionally have a much larger permeability in the horizontal direction than in the vertical, pore water tends to move from the centre of the foundation towards the edges. Such water movement can cause pore pressure increases and swelling in zones near the edges of the foundation. Therefore, in this case the most unstable condition can occur some time after loading, whereas in isotropic soils a critical condition occurs always immediately after loading. Several examples of the failure have been shown for large foundations by some investigators.

I would like to mention the bearing capacity of soils involving thin sand layers or sand lenses, when they are subjected to a vibrating load such as earthquake or machine vibration. Since the sands contained in a clay deposit are usually in a loose state, they can liquefy due to vibration and cause serious disturbance in the surrounding clay. This has been explained by Professor Seed as the cause of landslides during the Alaskan earthquake of 1964. I observed similar

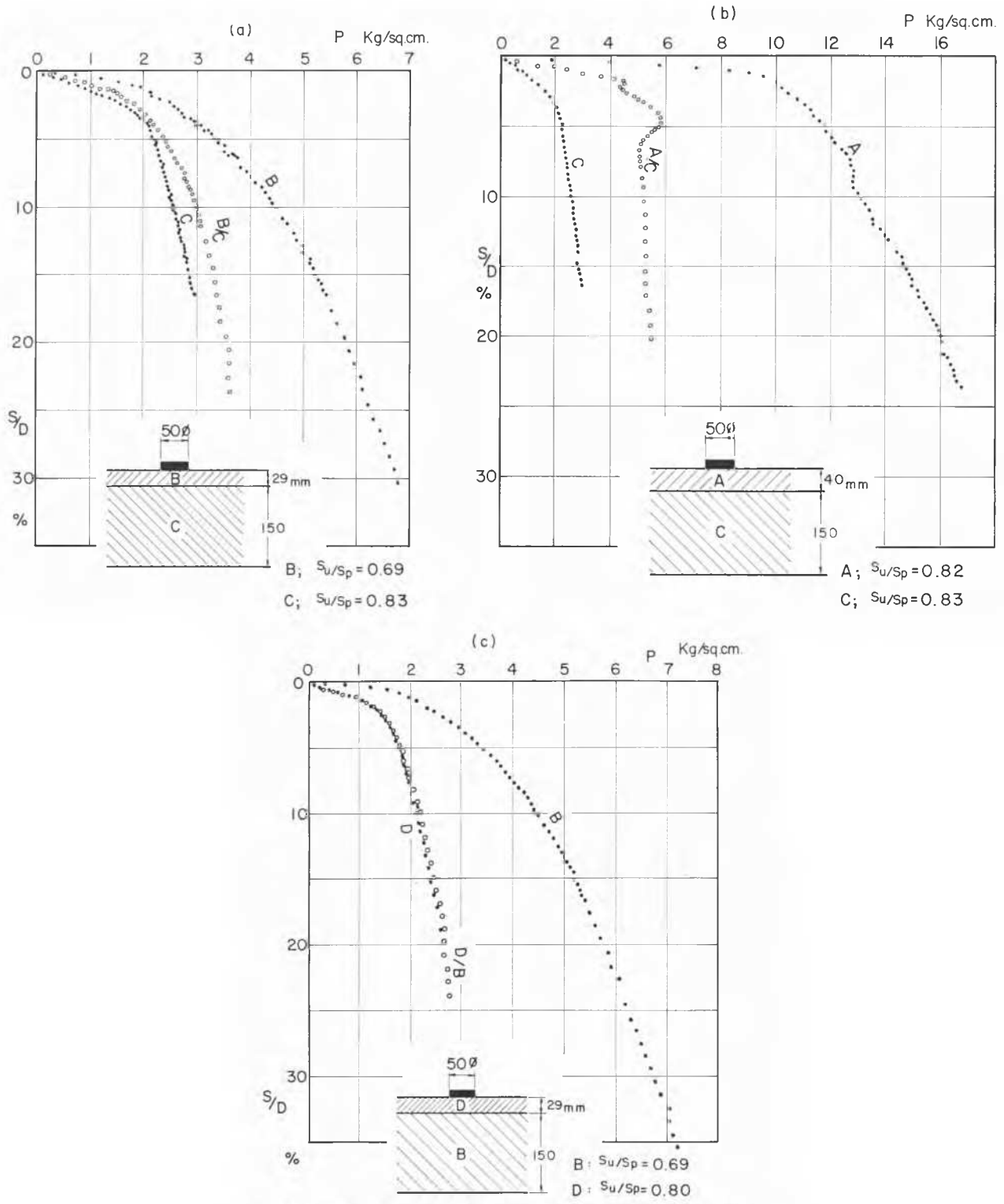

FIG. 7. Plate loading tests with two-layered and individual clays.

phenomena in the Niigata earthquake of 1964. Two days after the earthquake we made a boring to take soil samples by a thin-wall tube sampler with a fixed piston. A sample taken from a depth of 5 m was silty clay with sand seams. When the sample was extruded from the sampler, clear water spouted out of the sand seams and the clay around them was found completely disturbed. The sensitivity of the clay is about 10. When sampling was repeated 3 months later, no more excess pore water pressure was found in the sands, and the clay had regained some of its structural strength, although it had not returned to its undisturbed strength.

Lastly, I would like to add some brief words with respect to the stratifying condition of sand layers for liquefaction. A large-scale liquefaction of sand layers occurred during the Niigata earthquake of 1964. The city of Niigata is situated on a thick sand deposit. Severe damage was concentrated in the region in which loose saturated sand layers extended from near the ground surface to great depths. Except in the top 5 m, liquefaction, in my opinion, resulted when the loose

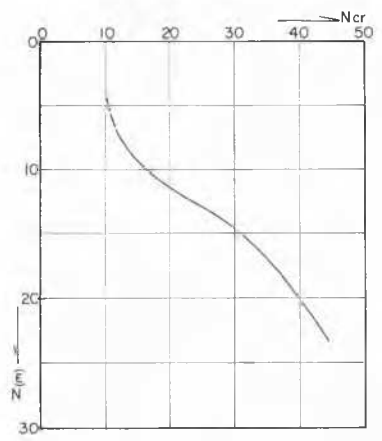

FIG. 8. Relation between critical void ratio (N_{cr}) and depth below surface (z).

saturated sands with void ratios higher than the critical void ratio were subjected to vibration and the escape of pore water pressure was prevented. In order to obtain the critical void ratio with depth, the standard penetration tests were made about two weeks after the earthquake at about 20 locations in the city where the same tests had been conducted before. A comparison was made between the penetration resistances, N values, as measured at the same points before and after the earthquake. An intermediate N value which did not change during the earthquake was determined as the N_{cr} which corresponds to the critical void ratio at that depth (Koizumi, 1964). The critical N value is plotted against depth in Fig. 8. It appears that the distribution of damage to buildings could be fairly well explained by this curve. Surcharge with any material can certainly reduce damage to structures due to liquefaction. According to the investigation of the relationship between damage and N value distribution connected with the N_{cr} curve, it seems that when the top 6 m or so does not liquefy during the earthquake, this contributes very much to a decrease in damage, even when the underlying sands are very loose. The thickness of the top layer required to prevent damage due to liquefaction might depend, to some degree, on the thickness of the zone of liquefaction (Ohsaki, 1965).

REFERENCES

BISHOP, A. W., and L. BJERRUM (1960). The relevance of the triaxial test to the solution of stability problems. *Proc. A.S.C.E. Research Conference on Shear Strength of Cohesive Soils,* pp. 437–501.

BUTTON, S. J. (1953). The bearing capacity of footings on a two-layered cohesive subsoil. *Proc. Third International Conference Soil Mechanics and Foundation Engineering,* Vol. 1, pp. 332–34.

KENNEY, T. C. (1964). Pore pressures and bearing capacity of layered clays. *Proc. A.S.C.E.*, SM4, July.

KOIZUMI, Y. (1964). Changes in density of sand subsoil caused by the Niigata earthquake. Symposium on Niigata Earthquake.

OHSAKI, Y. (1965). *Damage to buildings in the Niigata earthquake.* Report of the Building Research Institute of Japan.

TCHENG, YU. (1957). Fondations superficielles en milieu stratifié. *Proc. Fourth International Conference Soil Mechanics and Foundation Engineering,* Vol. 1, pp. 449–52.

Panelist: J. A. J. SALAS (Spain)

Very often we judge the results of soil mechanics in a hypercritical way, probably because all of us who have felt the appeal of soil mechanics have hypercritical minds. We have followed the lure of a realm in which all mathematical reasoning has to be immediately followed by close experimental checking. This school of thought for the treatment of the problems set before us by the soil, we have come to call soil mechanics. This hypercritical attitude is sound, provided that it does not lead to a lack of spirit inducing us to fall into empiricism, with the inaccurate slogan of "Nature does not know Mathematics." But the fact is that nature is Mathematics itself: Mathematics materialized in the spin of the most elemental among its particles. We can be sure that whatever efforts we make to better the abstractions by which we try to represent the soil will be rewarding.

In this respect, we cannot forget that soil is anisotropic. If it is a sedimentary soil, it is anisotropic because of the seasonal variations in deposition. If it is an intrusive rock, it will probably be jointed. If of metamorphic origin, then anisotropy results from a combination of both causes. When we consider seepage we never forget anisotropy. We also have to take it into account when considering failure matters. It is impossible to ignore it in some types of soils and rocks. The study of the failure of anisotropic soils is not far advanced. This is especially true when considering the influence of anisotropy on plastic failure lines, bearing capacity, and the general safety factor.

I cannot, of course, present here a thorough treatment, nor even a decisive contribution. Nevertheless, a few months ago, we had to solve a special problem: a small dam, 25 m. high, which had to be founded on very suspicious ground formed by thin layers of marl and sandstone. I am going to tell you how the problem was solved by Dr. Uriel, the engineer in my laboratory who was put in charge of the problem.

The soil was considered as a "homogeneous jointed medium," that is, a medium consisting of a homogeneous matrix with cohesion and internal friction defined by ϕ and c, but one in which there is a single system of joints or diaclases along which the strength is defined by ϕ_D and c_D. In such a medium, failure occurs along surfaces that cut the layers constituted by the matrix, or along the joints according to the direction of the principal stresses. In this last case the failure will be called orthoplastic and the region in which this type of failure occurs, the orthoplastic region.

Fig. 9 shows, in a polar representation, that the apparent variation of the internal friction angle of a jointed medium is a function of the α angle that the major principal stress forms with the direction of the joints. If the α angle is contained between the said limits, orthoplastic failure occurs. Beyond these limits, the slide lines cut the less resistant planes obliquely. This result, which had been deduced by theoretical considerations, is now confirmed by the experimental results shown to us yesterday by Mr. Armand Mayer in his lecture on rock mechanics.

Eq 5 of Fig. 10 indicates in a general way the limiting

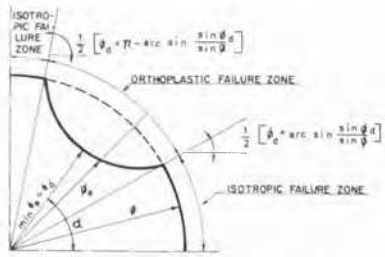

FIG. 9. Polar diagram of the angle of friction of a monodiaclased rock.

condition for which failure does not distinctly occur in either of these two ways.

In a study of the failure of a ground wedge undergoing the application of external forces p and q, by the method of the characteristic lines, regions have been found in which failure occurs through the layer, and we call them isotropic regions. There also exist orthoplastic regions in which the condition of plasticity is determined by Eq 3 which expresses in an analytical way the condition graphically represented in Mohr's plane; a line, drawn through the pole, parallel to the joint plane, cuts Mohr's circle on the very line of intrinsic resistance of the joints. These regions can be studied using, for instance, Sokolovsky's theories.

Eq 3, together with Eqs 1 and 2 which concern stress equilibrium, determines two systems of differential equations, the solution of which is direct, leading to Eq 4. If, at a boundary, the functions f_1 and f_2 which appear in these equations are known, the complete solution of the stress distribution in an orthoplastic region can be obtained.

Dr. Uriel has solved the failure problem for a special case by assuming the following three conditions:

1. The H and H' magnitudes are equal. This condition may seem arbitrary, but the fact is that for rocks with defects a tendency has been observed for the tangent of ϕ and the cohesion to vary roughly proportionally to the matrix and to the defects. In another respect, the information relating to these constants will probably be so reduced that the adaptation of the line of intrinsic resistance can be made without any supplementary error.

2. The ground of the sliding wedges is weightless. Contrary to what one would think, this simplification is not very important in rock mechanics and in many other cases (deep foundations, abutments, etc.) where the stress level is very

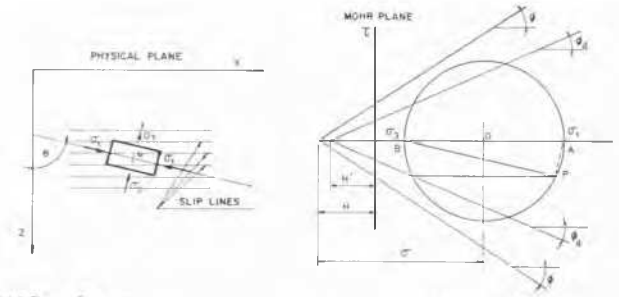

FIG. 10. Plastic equilibrium conditions in a diaclased soil.

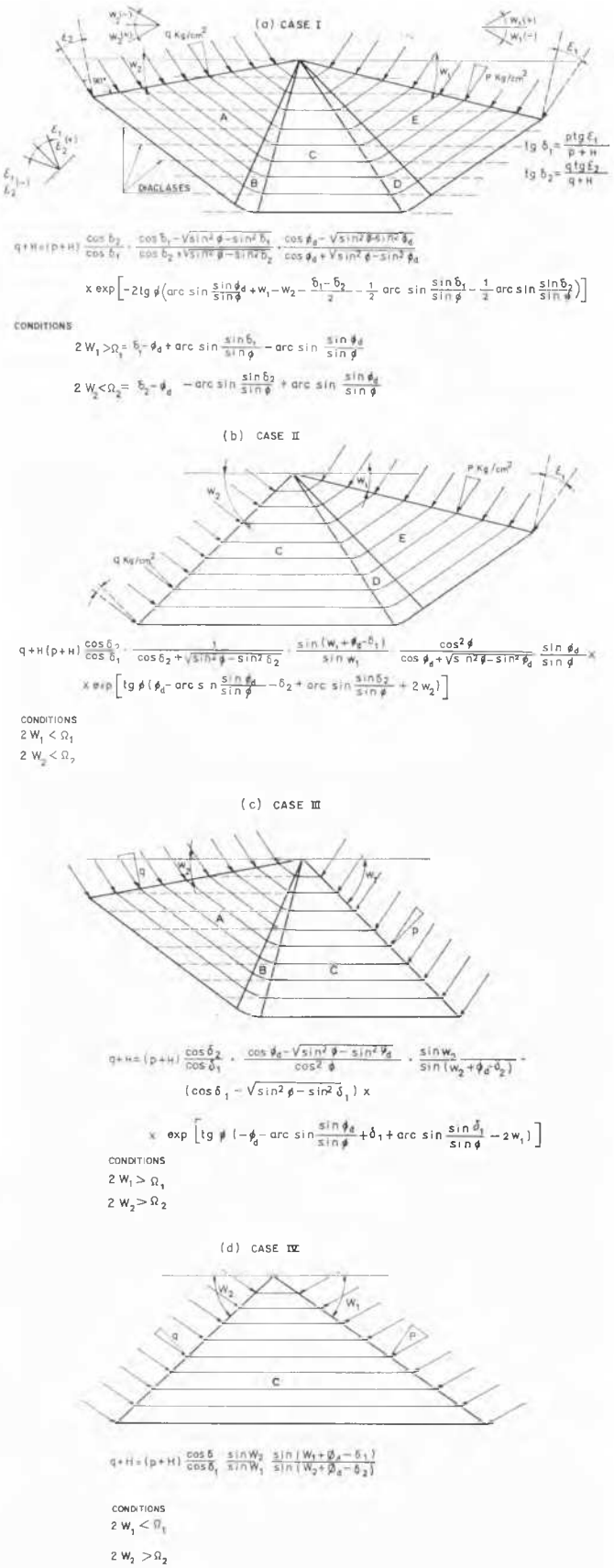

FIG. 11. Isotropic and orthoplastic regions of failure. (a) Case I, (b) Case II, (c) Case III, (d) Case IV.

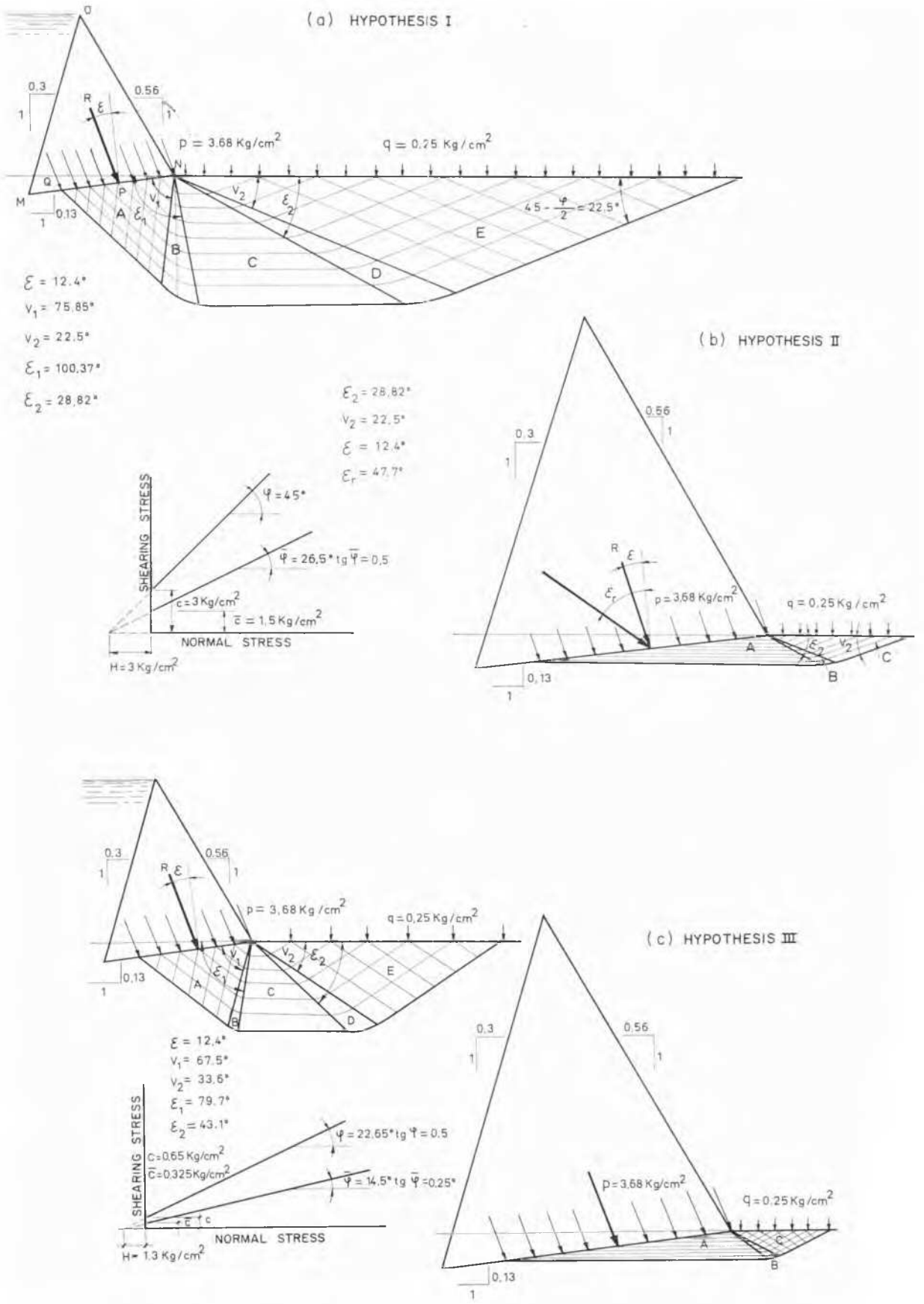

FIG. 12. Types of failures in a dam foundation. (a) Hypothesis I, (b) Hypothesis II, (c) Hypothesis III.

high or where the movement occurs nearly in a horizontal plane.

3. Having used the method of characteristics, it is implicit that the ground is supposed to constitute a rigido-plastic solid. This limitation is not so important in the case of rock as in the case of clay or of granular materials.

In this way failure occurs in different ways for different cases. Presented in Fig. 11a is the case in which there are five regions, four of them being isotropic and one orthoplastic. Indicated in the same figure are the conditions which must be fulfilled for this to occur. In Figs. 11b and 11c two isotropic regions have disappeared, and finally, in Fig. 11d the orthoplastic region remains alone.

But we were talking of a dam. Where is this dam? Here it is in Fig. 12. What type of failure threatens it? The interesting point I want to make is that the expected type of failure depends on the definition adopted for the safety factor, and then, the expected ultimate load also depends on this same definition.

We can take as the safety factor the inverse of the ratio between the real force (sum of the weight of the dam, the pressure of water, and the uplift) and the force with the same direction and application point which would produce the failure. This is hypothesis I (Fig. 12a) which leads, in our case, to a safety factor of 47. We can assume that only horizontal forces increase, following the concept of the "shear friction factor" introduced by the U.S. Bureau of Reclamation. This is hypothesis II (Fig. 12b) with a safety factor of 5.02. Finally, we can take as safety factor the number by which one has to divide the parameters which define the lines of intrinsic resistance. In the present case, since there are two lines of intrinsic resistance, there are four parameters. It would not be reasonable to have the same safety factor for the four parameters, since knowledge about their safe value is very different for the four of them. The safety in regard to the friction in the matrix material, for instance, cannot be compared to the cohesion in the joints which can be so much affected by the action of water. The problem, as can be seen, has an infinite number of solutions, but in the present case, the answer given was that with a safety factor of two as regards friction, the safety factor for cohesion was 4.6, which seemed sufficient. The actual failure in this case was practically within the limit between the two possible ones drawn in Fig. 12c. This shows how the definition of the safety factor, already very important in the case of homogeneous ground, is much more important in the case of anisotropic ground, where forms of failure as varied as the ones here described, can be met.

I want to introduce a second point of discussion, the pressure distribution under foundations. It is very well known, and yesterday it was confirmed, that settlements in stiff clays are several times smaller than the ones calculated with the classical theories and the help of the oedometer. This is true even if we apply successively the Schmertmann and the Skempton and Bjerrum corrections. (In some regions of Spain, and particularly in Madrid, stiff clays are the general rule, and the classical methods nearly useless for the calculation of possible settlements.) In our opinion these discrepancies depend to a great extent on dilatancy. This includes not only the considerations on stress paths that we have been shown yesterday, but also the aspect of pressure distribution in the interface between soil and foundation.

Dilatancy depends on shearing stresses, and it is necessary to recall how little we know about correlation between calculated and actual shearing stresses under foundations. We very often forget to consider the rigidity of the foundation when calculating settlement. For instance, it is usual to calculate the settlement of the "characteristic points" without taking account of the same. These practices are based on the fact that mean settlements do not differ very much between a rigid foundation and in a uniformly loaded area, if they are placed on a hypothetical Boussinesq half-space. But this cannot be true in the case of a half-space of a dilatant material. In other words, at the time of calculating the pressure distribution, how rigid is a foundation?

In many foundation designs we look on the one hand at the calculations of bending moments and stresses that the structural engineer has made on the hypothesis that the structure behaves as an elastic continuum. On the other hand, the soils engineer admits the possibility of differential settlements say of 0.3 or 0.5 per cent of the distance between columns. In most cases these are high enough to produce the failure of the structure as calculated by elastic methods. Fortunately structures behave plastically. It seems that the time has come to begin openly to take into account this fact and not to calculate foundation beams and rafts in an elastic way, while admitting that they can support deformations that are several times those that they could withstand if behaving elastically. (This does not apply in principle to structures that support predominantly live loads, as for instance crane beams, where it seems convenient to secure an elastic state of deformation.)

CHAIRMAN CROCE

Thank you gentlemen. We will now have a short recess.

(*There followed a brief intermission.*)

CHAIRMAN CROCE

The oral discussors who have been chosen are Bent Hansen (Denmark), H. Muhs (Germany), A. Rabinovici (Switzerland), B. Prange (Germany), T. Tassios (Greece), H. Militzer (Germany), R. A. Ashbee (Great Britain), A. P. Sinitzyn (U.S.S.R.).

BENT HANSEN (Denmark)

Professor *Gorbunov-Possadov (3/11)* has given an ingenious calculation of the boundary to the rigid body of sand beneath a strip foundation loaded to failure by a vertical and central load.

The basic assumptions seem to be incorrect, however. Because of the symmetry there cannot be shear stresses along the axis AB in Fig. 3 of the paper, and the stresses can hardly be assumed to be zero at the point A; at least this is

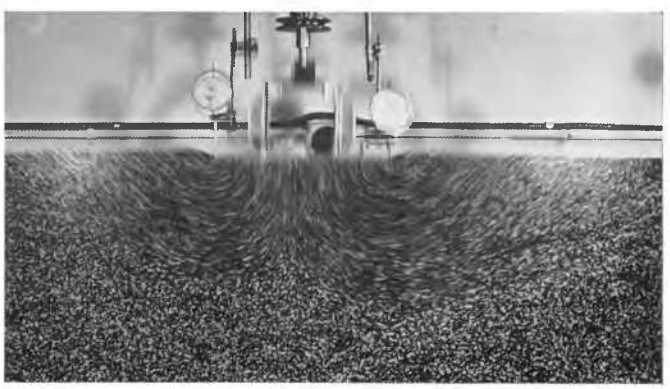

FIG. 13. Displacement field under a strip foundation. Photographed in a pin model ($\phi = 23°$).

incompatible with the stress calculation along the slip line connecting A with the surface OE.

Also, the stress distribution is only used to determine the shape of the boundary to the rigid body. Outside this boundary, the stress distribution is calculated by means of the classical theory of plasticity. The boundary to the rigid body acts in this calculation as a perfectly rough wall. It will therefore be an envelope of slip lines. This calculation would be correct if the rigid body was made of concrete. Being a sand body, it will not be stable against the stresses acting along its boundaries. The stress distribution used to find the shape of the body is not relevant in this respect, because it does not give the same stresses along the boundary as does the stress distribution from the slip line field outside the body.

Therefore, the bearing capacity calculated from this latter stress distribution will be too high. I believe that the Lundgren-Mortensen stress distribution, presented to the Zürich Conference in 1953, which is at least statically possible, gives the best approximation presented as yet to the theoretical bearing capacity of a strip foundation.

In a Master's thesis presented by Damgaard to the Technical University of Denmark in 1951, in which this solution was calculated for the first time under the guidance of Professor Lundgren, the field of strain characteristics was also roughly indicated, assuming coinciding principal stress and strain directions and constant volume. A calculation on the basis of the displacement field seems to show that the Lundgren-Mortensen solution is in fact also kinematically possible, at least when there is no surface loading.

Fig. 13 shows a field of displacement observed in the pin model of the Danish Geotechnical Institute. It corresponds closely to the theoretical field when the angle of internal friction for the pin material, which is 23°, is introduced in the calculation. In this picture the rigid body is clearly distinguished from the radial and surface zones. In the latter zones the particle movements form an angle with the horizon which is very nearly 45°.

Incidentally, the lines one can see on the picture, that is the trajectories of particle movements, are neither slip lines (stress characteristics) nor strain characteristics, except in part of the surface zones. The field of displacements does not even cover the whole rupture figure. This figure contains zones, in the rigid body beneath the foundation as well as in the rigid body outside the moving sand mass, that are stressed until failure but are not deformed after the final state of failure has been reached.

In conclusion, it seems that the Lundgren-Mortensen solution is both statically and kinematically possible. It is therefore a mathematically correct solution. Discrepancies between theoretical and observed bearing capacities are not, therefore, a result of the theory, but rather to the determination of friction angles in the laboratory. This fact has been recognized by the new Danish Code of Practice for Foundation Engineering, in which it is specified that the friction angle measured by triaxial tests should be increased by 10 per cent before it is used in full-scale problems of plane strain.

H. Muhs (Germany)

The General Reporter, Professor de Beer, has given in his contribution to this conference a report about the influence of the phenomenon of progressive rupture on the bearing capacity and the equations for its numerical determination. He treated this problem in connection with our tests in Berlin to investigate the failure behaviour of sand under footings with a flat foundation. I think it will be of interest to you to hear something more about our observations of this phenomenon.

Performing large-scale model tests with footings, 0.5–1 m wide and 0.5–2 m long, embedded at a shallow depth (maximum 0.5 m) into fine to medium sand varying in density from rather low to very high, we found that considerable settlements of the footings and corresponding movements in the surrounding stratum were needed to reach the state of rupture, particularly the real failure load. Fig. 14, for

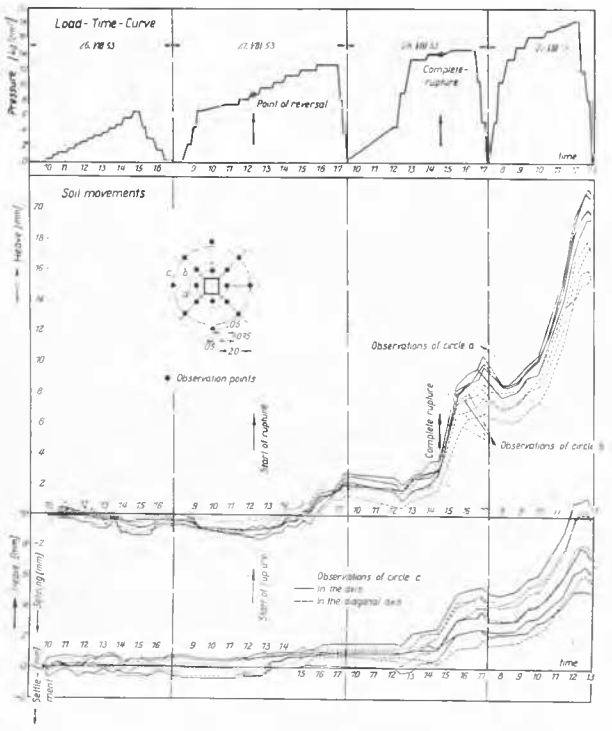

FIG. 14. Settlement and heave of sand.

example, shows in the first part of the loading test the settlements of the surface around the footing, in the second part how the settlements change over into a heave, and in the third part failure has occurred and the sliding mass is now moving very steeply upward.

In the second part of the loading what we call the failure of the soil occurs. But there is generally no distinct load at which the bearing capacity of the stratum is overcome. This is especially true of the general case where the footing has a circular or square shape and is not directly on the surface. The second part of the test—the part between the first heaving movements at the surface and evident failure—extends over a rather long period.

Progressive heaving of the surface around a test footing is shown in Fig. 15A. In this test the water level at the start was exactly at the surface and was not changed; therefore the zone with the upward movements is easily recognized. Fig. 15B shows the same footing after the total failure was reached and there is an obvious difference compared with Fig. 15A. It is nevertheless difficult to say what is really the bearing capacity in such cases: the load causing the first upward movements will be too low and the load causing the final movement, the outpressing of the sliding mass, will be too high.

A

B

FIG. 15. Progressive failure as evidenced by increasing heave of sand around footing.

But there is another difficulty. With regard to the movements in the sand mass before failure, we have to consider that these displacements in a non-constant–volume soil will cause a change of porosity and therefore of the original shear strength. Furthermore we cannot expect that these displacements will take place at the same time and to the same extent at all points. With the gradual increase of the load, the bearing capacity is not immediately mobilized at all points of the sliding area, but at first only where the shearing forces are the largest, from which points the alteration of the soil properties extends to other points. This gradual progression causes modifications of the original strength of the sand along the sliding surface and is known as the phenomenon of progressive rupture. In our first test report in 1954 we pointed out that because of this phenomenon we cannot expect a uniform shearing resistance along the total sliding surface. Furthermore, equations which have to work necessarily with a constant shear value must not be expected to yield good agreement with test results or with reality where this phenomenon takes place (for instance, in sand, or generally in non-constant–volume soils).

Last year we repeated a test to demonstrate that the progressive rupture really does exist and how it functions. A series of long vertical glass tubes each with a diameter of 6 mm were inserted in the sand on both sides of a rectangular footing. The tubes were closed at the lower end and filled with coloured water, which could be observed on the surface (Fig. 16). During the first period of the test the water level did not change in any of the tubes. That means that under the first loads the lateral displacements were limited and so small that no tube was broken by the moving and then sliding part of the soil mass. In a later stage of the test the water in the first tube near the footing disappeared, as the soil movement of the sliding part was so large that the glass tube was broken by shearing or bending forces in the sand, but the other tubes at this stage were still stable. They were broken one after another in a progressive manner as the load was gradually increased.

FIG. 16. Progressive failure as evidenced by loss of liquid in glass tubes.

The line of sliding (Fig. 17), easily distinguished by the vertical cylinders of dark sand which were inserted into the sand strata before the test and cut out after the test, shows the size of the deformations in the same vertical plane in which the glass tubes stood during another test. The horizontal displacements are rather large. They amount to 9 cm and are due to the total settlement of the footing of 14 cm, whereas the settlement at failure was only approximately 2 cm. It is evident, that a real shear zone with very marked relative displacements in the sand mass was produced by the test, and furthermore that in this shear zone the phenomenon of progressive rupture took place. That means that the void ratio and hence the effective shearing resistance of the sand was changed in a progressive way in this zone during the test beginning in the vicinity of the footing. All of you know that shear deformation alters the density of sand by dilatation in a dense sand and compaction in a loose sand, and

FIG. 17. Section showing line of failure beneath footing.

that there is a very strong relation between the density and the angle of internal friction, which can lie between 30° and about 45°, according to the original void ratio.

It is obvious that under these circumstances no equation based on a constant shear value along the total sliding area can meet the real conditions where progressive rupture is acting. Its influence depends on the deformation before the failure and will be larger when the settlement of the footing is relatively large. As the settlement of a footing is larger under big footings, and also larger when the footing is not founded directly on the surface but is embedded in the stratum, the influence of progressive rupture will be much greater under large than under small footings. Most model tests in the past were performed at the surface of a test box with small or even small model footings (sometimes of a size of a cigarette packet). Under these test conditions only very small settlements took place before failure which may explain why the influence of progressive rupture has been neglected so far.

I believe that it will be nearly impossible to introduce this influence in the equations for the bearing capacity, and it is my opinion therefore that these equations cannot be solved on a purely theoretical basis but that they need data yielded by experiments with larger footings so that the effects of this theoretically insurmountable problem are contained in the results.

A. Rabinovici (Switzerland)

La présente participation à la discussion consiste dans un bref exposé d'une étude expérimentale concernant les plaques sur sol élastique.

En suivant les derniers developpements des méthodes élaborées dans le calcul des dalles appuyées sur le sol, on se rend compte que les chercheurs ont adopté l'hypothèse de Boussinesq comme base de calcul plutôt proche de la réalité du sol. Le traitement qui en découle reste cependant difficile et, jusqu'à présent, beaucoup de problèmes n'ont pas trouvé de solution. Pour cette raison, les méthodes d'approche offrent dans certains cas des solutions satisfaisantes et accessibles à l'ingénieur praticien.

C'est ainsi que nous connaissons les méthodes du Dr. Grasshoff, Jemoschkin, et Gorbunov-Possadov qui se sont proposés de remplacer le diagramme continu de la charge de réaction par un polygone étagé (dalles circulaires) ou bien d'exprimer la ligne de déformation par une loi mathématique (dalles circulaires et rectangulaires). Les résultats ont toutefois montré que, tout en se basant sur la même hypothèse du semi-espace élastique, des divergences apparaissent dans les résultats obtenus. D'autre part, ainsi que le Dr. von Guten l'a montré, les moments de fléxion, pour les dalles circulaires et carrées, symétriquement sollicitées, sont peu sensibles à la variation de la charge de réaction. Si on admet une charge de réaction uniformément répartie pour une dalle circulaire chargée au milieu, au lieu du diagramme classique correspondant à la dalle infiniment rigide, on obtient une différence de 10 pour-cent de la valeur du moment de fléxion maximum.

Il paraît donc utile de confronter les résultats théoriques par des essais sur modèles. Nous avons essayé de réaliser une étude expérimentale sur modèles réduits en appliquant la méthode Moiré. Cette méthode semblait adéquate à ce propos, car elle offre la possibilité de calculer le moment de flexion, grandeur utile dans la pratique. Voilà brièvement l'idée de cette méthode (fig. 18).

Un modèle réduit de l'élément à étudier (A) est fait de perspex noir miroité et appuyé en position verticale sur une

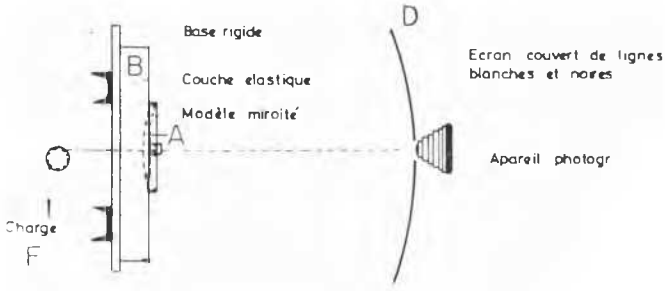

FIG. 18. Montage expérimental.

couche élastique de caoutchouc (B). Sur l'écran (D) est déssiné un réseau régulier de lignes équidistantes blanches et noires, qui se reflète sur le modèle. Par l'application des poids (F), sa surface se déforme, l'image du réseau se distord et elle est prise sur le même négatif. L'interférence du réseau déformé avec l'original crée des franges qui représentent des lignes d'égale pente dans une direction choisie, donc des lignes $\partial w/\partial x =$ constant. Le calcul de la variation de ces lignes offre les valeurs de la courbure des points considérés à l'aide desquelles on calcule les moments de fléxion:

$$M = -D\left(\frac{\mathrm{d}^2 w}{\mathrm{d}x^2} + \mu \frac{\mathrm{d}^2 w}{\mathrm{d}y^2}\right)$$

où $w =$ déflexion de la dalle.

L'object du présent mémoire était d'étudier la relation entre les moments de flexion et la rigidité des dalles pour les charges concentrées disposées au centre, la couche élastique restant toujours la même. D'autre part, on a comparé les résultats obtenus pour les dalles circulaires et carrées de même rigidité et dimensions. Finalement, un essai a été fait pour observer le comportement des dalles rectangulaires.

DESCRIPTION DES ESSAIS ET RÉSULTATS

Trois dalles circulaires de diamètre $d = 20$ cm et trois dalles carrées de côté $b = 20$ cm ont été étudiées. Leurs moments d'inertie ont été choisis de sorte qu'elles puissent représenter les rigidités souvent rencontrées. La couche élastique d'épaisseur 50 mm est identique pour tous les essais et son module d'élasticité $E_s = 12$ kg/cm.ca. De même, la surface de répartition de la charge concentrée appliquée au

TABLEAU I. DONNÉES DES ESSAIS

ESSAI	DALLE	DIMENSIONS cm	CAS DE CHARGE
1	CIRC.	ϕ = 20 h = 0,32	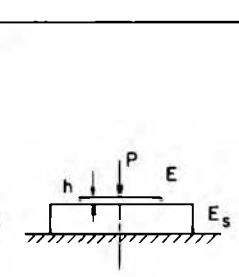
2	CIRC.	ϕ = 20 h = 0,50	
3	CIRC.	ϕ = 20 h = 0,95	
4	CARREE GRANDE ETANDUE	b = 40 h = 0,32	
5	CARREE	b = 20 h = 0,50	
6	CARREE	b = 20 h = 0,95	
7	CARREE	b = 20 h = 1,25	
8	RECTAN.	20 x 15 h = 0,95	
9	RECTAN.	20 x 10 h = 0,95	
10	RECTAN.	20 x 10 h = 0,32	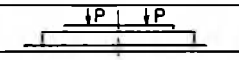

centre est de 1.0 cm.ca. Les données concernant les modèles sont résumées dans le tableau I. Afin d'accorder aux résultats un caractère général et pour faciliter la délimitation entre les différentes catégories de fondation, l'indice de rigidité relative a été employé K_s.

Reprenons le dans la forme introduite par Schultze: $K_s = 1/12 \times E/E_s(h/R)^3$, où E, E_s = module d'élasticité du matériau de la dalle et du sol, h = épaisseur de la dalle, d,b = diamètre ou côté de la dalle, R = rayon de la dalle. A cause de l'espace limité, deux essais uniquement sont représentés ici: No 2 et No 5 (figs. 19 et 20).

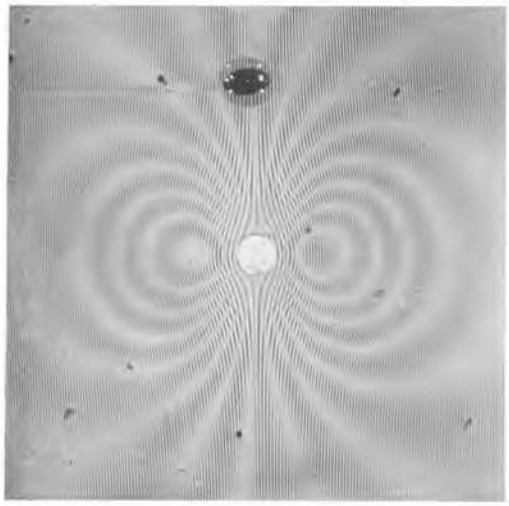

FIG. 19. Résultat type.

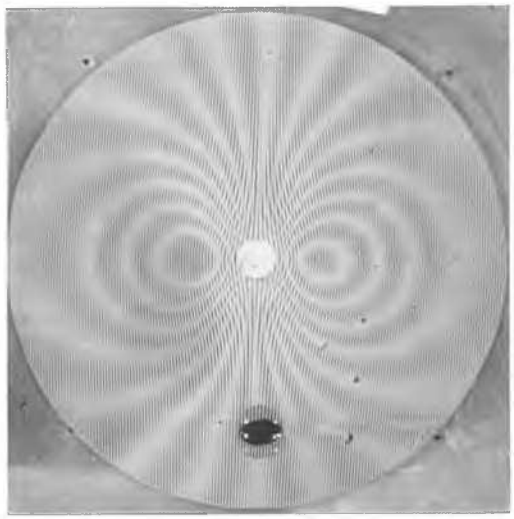

FIG. 20. Résultat type.

CONCLUSIONS

1. L'examen des franges Moiré pour tous les essais révèle des contours fermés. Ce fait indique un changement de signe de la pente qui se situe sur un cercle concentrique à la charge sous forme d'onde. La ligne de déformation présente une courbure concave sous la charge et une courbure convexe plus loin. En effet, les moments M_r et M_x calculés le long d'un diamètre à travers la charge (fig. 21) passent des valeurs positives autour de la charge, aux valeurs négatives. Cette observation sera importante dans l'accumulation des influences provenant de plusieurs charges en un point donné.

2. La notion de la longueur caractéristique joue un rôle important dans la définition de la rigidité des dalles. Elle est donnée par l'expression: $L = \sqrt[3]{(2D/K)}$, $D = Eh^3/12(1 - \mu)^2$, $K = E_s/(1 - \mu_0^2)$, où μ = coefficient de Poisson. En effet, on constate que pour les dalles rigides, cette valeur approchée est d'environ $0{,}7R$ tandis que pour les dalles fléxibles elle est d'environ $R/3$. On pourrait donc, à l'aide de la longueur caractéristique, estimer le dégré de rigidité et par conséquent le comportement statique de la dalle.

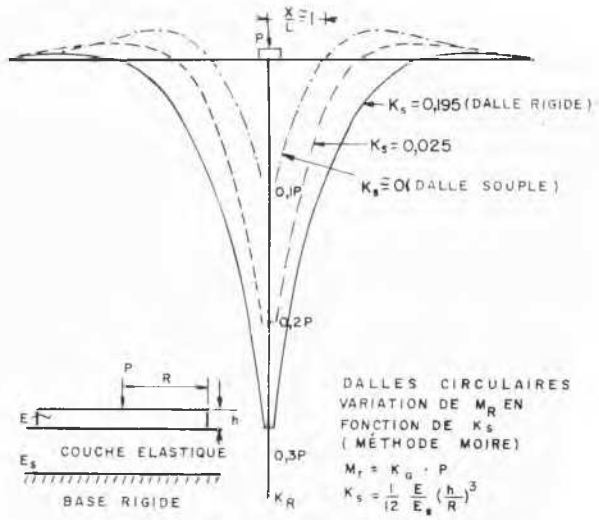

FIG. 21. Moments calculés.

3. Les diagrammes du moment radial obtenu et la corrélation établie entre ces moments et la longueur caractéristique suggère l'idée d'assimiler chacune des dalles circulaires étudiées aux dalles de grande étendue de même rigidité cylindrique D. En effet, admettons les dalles de rayon donné comme étant des dalles de grande étendue et calculons les diagrammes du moment radial en fonction de l'abscisse relative x/L (L variable); nous observons une concordance entre les valeurs théoriques et expérimentales ainsi que entre les régions de moments positifs et négatifs. D'autre part, le calcul des mêmes dalles, d'après les méthodes mentionnées plus haut comme étant des dalles de diamètre déterminé, amène des écarts. Ce fait laisse entrevoir la possibilité de simplifier le calcul des moments de flexion.

4. Le comportement des dalles circulaires et carrées de même rigidité et dimensions ne présente pas de différence. Ce fait apparaît comme une conséquence de la discussion sur les moments de flexion. C'est ainsi que nous retrouvons la concordance avec les résultats obtenus par le Dr. von Guten dans les dalles circulaires et carrées de mêmes dimensions et chargées uniformément.

5. Une tentative a été faite pour comparer le comportement des dalles dont les rapports des côtés sont 1/1, 1/1,5, 1/2 et chargées par une charge concentrée disposée au milieu. On constate que pour le rapport 1/2 les dalles rigides se comportent comme des poutres, donc se déforment dans la direction longitudinale uniquement, tandis que les dalles flexibles maintiennent l'effet des dalles dans le même rapport. Ceci provient également de la signification de la longueur caractéristique.

B. PRANGE (Germany)

I would like to make a few comments on the problem of pressure distribution underneath shallow foundations. Most

approaches to the solution of the problem of pressure distribution in a half-space are based on the theory of elasticity and especially on the assumption of a shear-stress-free surface, thus involving perfect lubrication of the contact zone. This, of course, is not true with most foundations. However, only a few contributions to this Conference deal with the problem of shear stress distribution underneath foundations due to friction or interaction of foundation and subsoil. It was pointed out very early by Froehlich that the stress distribution in the half-space is very much affected by shear stresses in the contact zone. Recent tests by different authors, which obviously showed the effect mentioned, had often been considered incorrect due to false test conditions. There was, however, until now no exact explanation for the remarkable stress concentration under foundations found in many tests. Since the design of a foundation depends on the pressure distribution, but also on the shear stress distribution in the contact zone, it is of importance, from an engineering point of view, to know the influence of surface friction, as Professor Salas pointed out during the Panel Discussion.

During our studies concerning bearing capacity and stress distribution underneath shallow foundations on sand we found that the bearing capacity and the stress distribution were very much influenced by the shear stresses in the contact zone. The investigation of the stress distribution in the half-space was done by means of telemetric pressure cells operating on the same principle as the telemetric pore pressure cells mentioned in paper (*2/33*) of these proceedings. The evaluation of the theoretical calculations and the test results are shown in Fig. 22 (see Prange, 1965). It may be noticed that the stress concentration around the load axis reaches values about twice the stresses calculated on the assumption of a shear-stress-free contact zone. The problem of stress redistribution due to shear stresses is similar to the one connected with end restraint of triaxial test samples

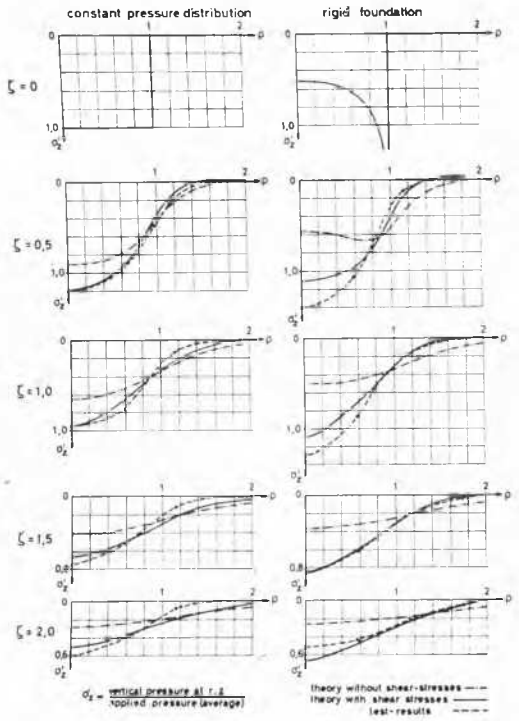

FIG. 22. Pressure distribution underneath circular foundations.

due to end-cap friction. This problem is recognized by many authors and has led to the application of lubricants between the sample and the end cap to perform triaxial tests in correspondence with the theory. The problem was theoretically investigated by Egger (1965), whilst Prange (1965) dealt with the similar problem of foundations. For further investigation of both problems, tests will be performed in our institute to measure the stress distribution within the triaxial test sample, in addition to the end-cap friction, as well as the shear stresses underneath foundations on sand.

I want to point out, however, that the problem of shear-stress distributions must gain our interest and further research should be done theoretically, as well as by testing. Refined theories and sophisticated tests lead to correct results only when all parameters involved are taken into consideration.

REFERENCES

PRANGE, B. (1964). *Druckmessdose mit drahtloser Messwertübertragung sowie Messergebnisse über die Spannungsverteilung im Untergrund.* Berlin, Vorträge der Baugrundtagung.

——— (1965). *Ein Beitrag zum Problem der Spannungsmessung im Halbraum.* Veröffentilichungen des Instituts für Bodenmechanik und Grundbau der Technischen Hochschule Karlsruhe, Heft 18.

EGGER, P. (1965). *Die Abhängigkeit des Spannungszustandes im Druckversuch von den Auflagerungsbedingungen.* Veröffentlichungen des Instituts für Bodenmechanik und Grundbau der Technischen Hochschule, Karlsruhe, Heft 19.

T. TASSIOS (Greece)

I would like to comment on Dr. Sommer's most valuable contribution, paper *3/42*, concerning the exact solution of the problem of the participation of the superstructure's rigidity in the behaviour of foundation beams.

There is an increasing need among practising engineers for a better understanding of the function of foundation beams. Three aspects of the problem have been considered to date: (a) soil stress distribution underneath a foundation beam; (*b*) participation of the superstructure; (c) distribution of loads into two directions in the case of a grid of beams in a raft foundation. As this last problem will not be the subject of actual discussion, I would simply like to remind you that relatively little work has been done on this theme and that a symposium dealing with it would be very helpful for engineers.

As far as the first problem is concerned there exists many solutions based on different assumptions about the law of soil reactions, but the problem of how to choose the appropriate law of soil reactions in each specific case still remains. In this connection it is opportune to remember that in cases of thin soft layers on rock, the Winkler theory, in spite of its non-scientific conception, is much more realistic than the methods based on the theory of the elastic half-space.

Looking now at the problem of the superstructure's participation, I would like to say how much I have appreciated the exact and precise solution presented by Dr. Sommer. Unfortunately, in everyday practice we cannot afford similar numerical work, in spite of the use of electronic computers. Also, the well-known uncertainties about the correct evaluation of many other factors of the problem ask, in my opinion, for a rather rough estimation of the role that the superstructure's rigidity can play.

In this connection a very rapid method would be to consider an average value of the initial deflection (Y_o) of a characteristic point of the foundation beam, considered in isolation, and to suppose the superstructure to be reacting to that deflection by developing an unknown system of forces

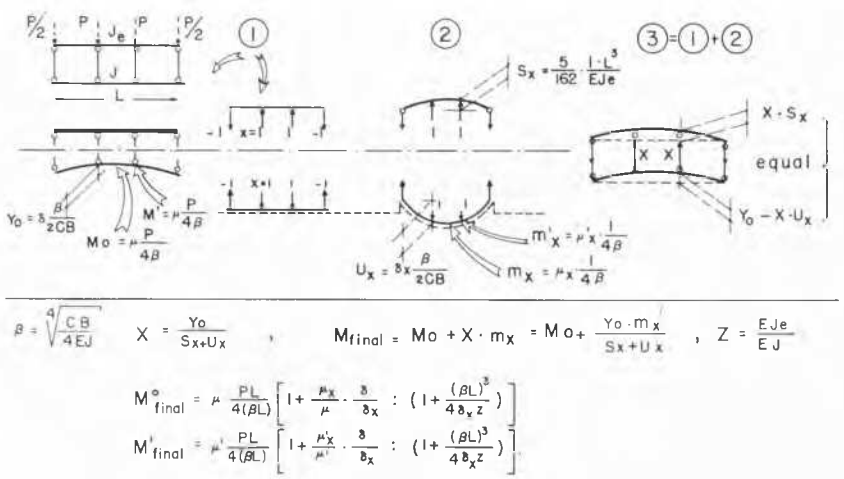

FIG. 23. Analysis of bending moments and deflections of a foundation beam.

"X" (Fig. 23). For $X = 1$, one can find the corresponding deflections S_x and U_x of the superstructure and the foundation beam respectively. Expressions for these deflections can readily be found on the basis of tabulated values for a certain law of soil reaction. Now, as the final deflections $(Y_0 - XU_x)$ of the beam and (XS_x) of the superstructure will be equal, one can find the leading value of the load X induced by the superstructure to the foundation beam. Finally, a closed formula for the corresponding maximum bending moment M_0 is given; and this is the moment which is opposed to the initial moment in the centre of the beam.

For reasons of discussion only, we have used here the easily tabulated, but generally incorrect, theory of subgrade reaction but the same can be applied with any other tabulated law of soil reactions. In Fig. 24 typical numerical coefficients for use in the above formula of Fig. 23 can be found.

Finally, Fig. 25 shows in full lines the values of this bending moment, M_0, as a function of the relative stiffness, K, between foundation and soil, and the ratio, Z, of rigidities between the superstructure and the foundation. For the translation of K to βL of the Winkler theory the following relation has been used: $C = (\sigma/y) = E_s/L$, where L is the smallest dimension of the building. Appropriate evaluation of this relationship in other cases should lead to some different figures.

From Fig. 25 a number of conclusions can be drawn. First of all, Dr. Sommer's values of moments are positive, but the moments derived from the theory of subgrade reaction are in this case negative. Thus, the error committed from the use of an improper method would be catastrophic. However, from the point of view of the superstructure, the general trend of the curves is quite the same, and the same holds, for the percentage of the alleviating moments. Never-

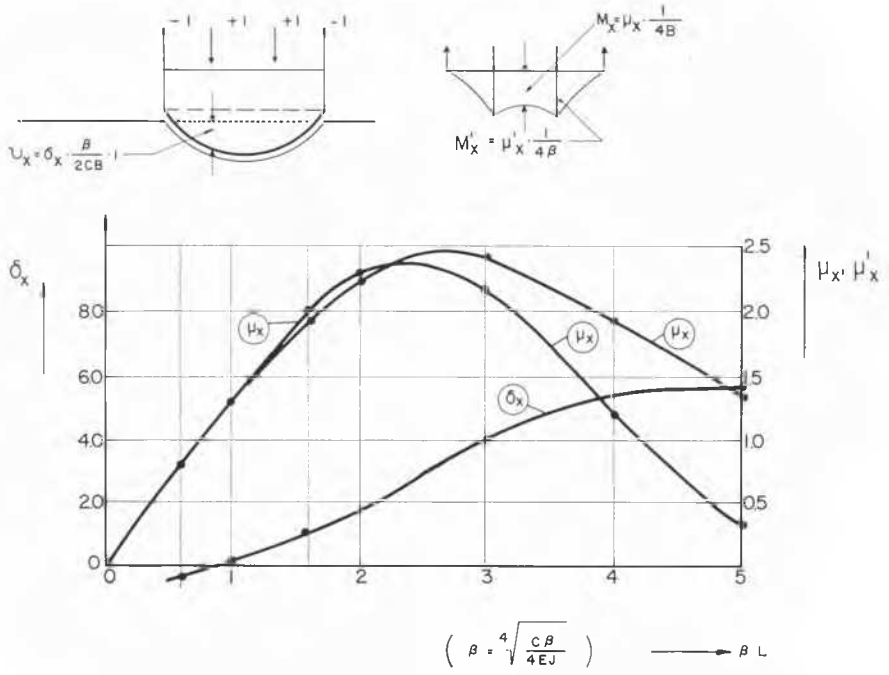

FIG. 24. Graphical presentation of numerical coefficients.

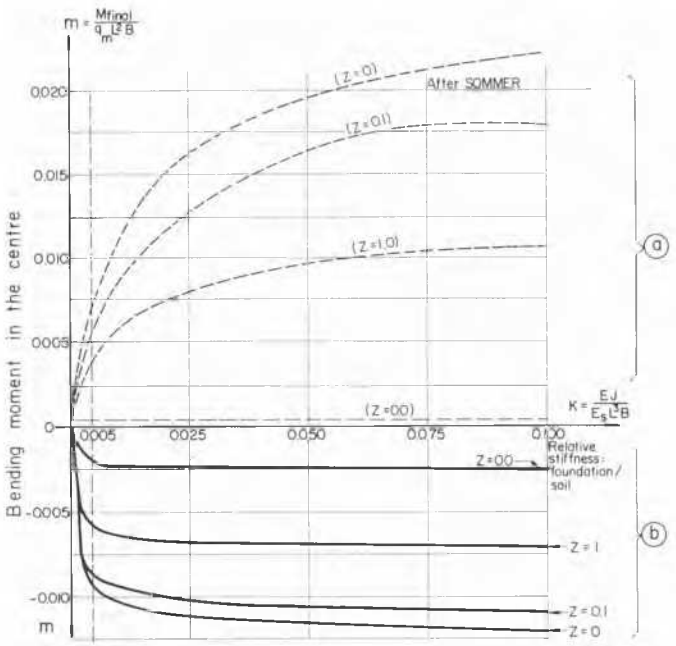

FIG. 25. Final bending moments in the middle of the foundation beam according to two different methods of analysis: (a) elastic half-space (E_s); (b) subgrade reaction (C).

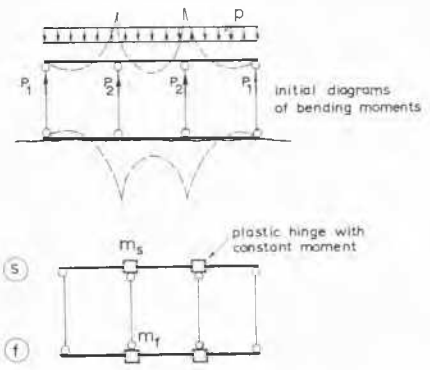

FIG. 26. Bending moment diagrams.

theless, one will probably think that this kind of computation refinement is not very realistic when the errors due to the adopted method of analysis itself can be much greater. On the other hand, it is well known that elastic solutions are extremely sensitive to small variations of any one of the uncertain parameters entering the problem. From this point of view, *ultimate methods* of design yield more reliable and realistic solutions.

As the first plastic hinges appear at the supports, both in the superstructure and the foundation beam (Fig. 26), the superstructure's rigidity will not be able to react to a further increase of differential settlements in the foundation. At that stage of the plastic behaviour of the structure and the soil, elastic deflections of the foundation beam could be ignored and the settlement curve could be considered as formed of linear parts, and an approximately linear soil stress distribution can be accepted, properly adjusted to every specific case by means of a shape factor, v. Although this shape factor will largely depend on the actual soil conditions, its maximum possible value ($v = \infty$ or $v' = \infty$, see Fig. 27) corresponds to certain limit values of bending moments

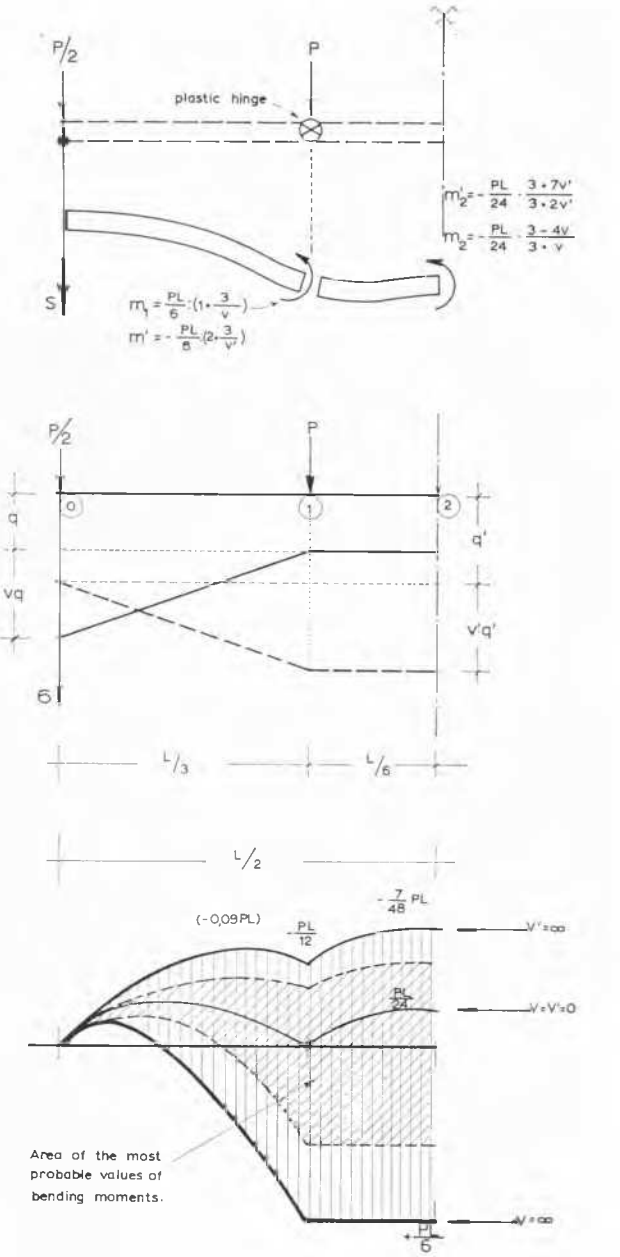

FIG. 27. Details of bending moments in a foundation beam.

which are indicated on the diagram of Fig. 27. As a matter of fact, the form of soil stress concentration will gradually change during the soil plastification process from the v to the v' type of distribution, a self-stopping phenomenon which contributes to a larger factor of safety. This is the reason why extreme values of moments will not result (see shadowed area in Fig. 27). The order of magnitude of the expected maximum moments will be approximately equal to $\pm$ 0.10 PL, however, or in terms of Fig. 25 $\pm$ 0.03$q_m BL^2$. This moment has to be equal to the ultimate moment capacity of the reinforced concrete section of the foundation beam, in which symmetrical reinforcement has always to be provided.

A further development of such a method will contribute, in my opinion, to a better, simpler, and more realistic analysis of foundation structures.

H. MILITZER (Germany)

In order to determine the homogeneity of the pavement of roads and runways of airfields, the thickness and physical characteristics of those pavements, and also the same characteristics for the subgrade, we developed a vibratory technique in the Institut für angewandte Geophysik of the Bergakademie Freiberg (German Democratic Republic). The instruments are also able to locate cracks inside concrete structures.

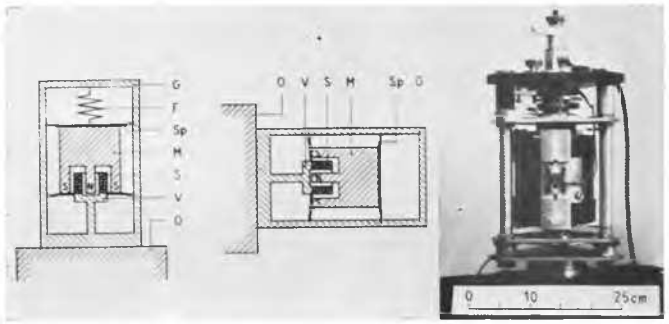

FIG. 28. Vibrator. G, box; F, spring; Sp, spider; M, magnet; S, coil; V, peg for connection; O, subject under investigation.

The left-hand side of Fig. 28 shows the schematic sections of the vibrator when used in the vertical and in the horizontal positions. The right hand side of Fig. 28 shows a photograph of the instrument. At this time I will not describe the instrument in detail; its basic principle is an electrodynamic exciter. The frequency range of the vibrator is between 20 and 10,000 cycles per second. If the thickness of the subject under investigation is small in comparison to the length of the excited elastic waves—for example, in the case of road and airfield pavements or spread foundations of a building—so-called flexure waves are always obtained. Flexure waves in every instance show normal dispersion; that means the propagation velocity of the flexure waves increases with the frequency. If we know the dispersion curve we are able to determine for example the thickness, provided the density, Poisson's ratio, and the elastic modulus of the material have been previously established by some other method. Obviously it is possible to obtain one of the other physical characteristics in a similar manner if the thickness and the other remaining values are known.

Fig. 29 shows a dispersion curve obtained for a concrete pavement. The curve drawn represents the theoretical curve, and the points marked are the values obtained by measurement.

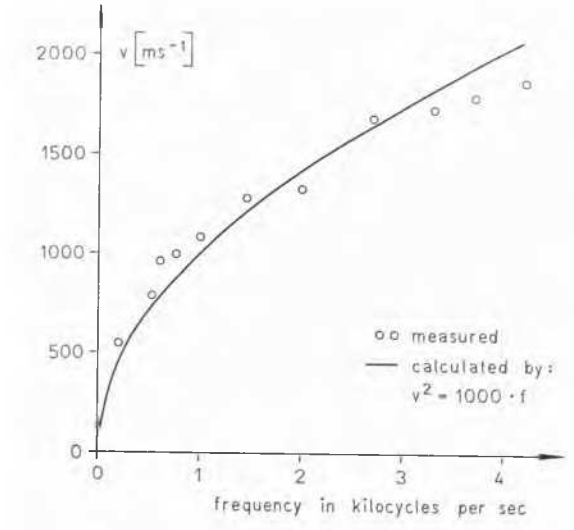

FIG. 29. Dispersion curve for a concrete pavement. (V = propagation velocity of flexure waves.)

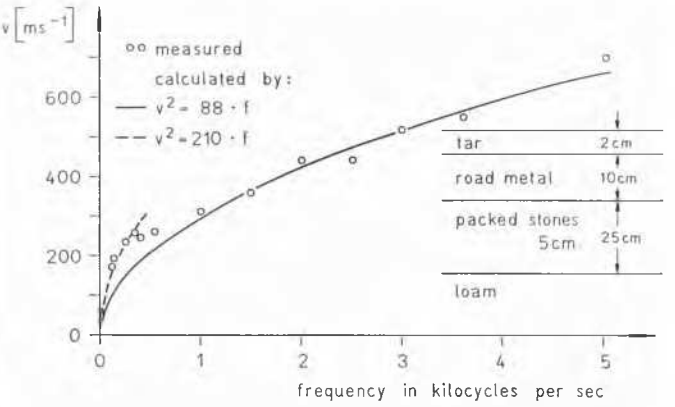

FIG. 30. Dispersion curve for road consisting of different layers. (V = propagation velocity of flexure waves.)

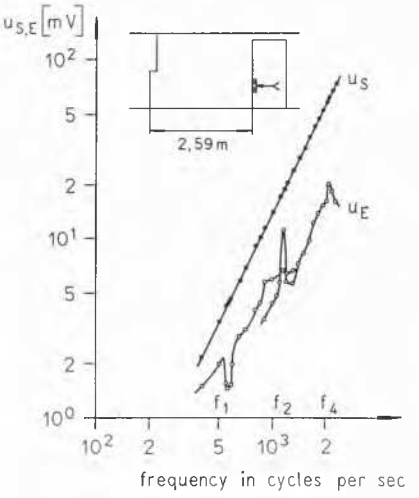

FIG. 31. Resonance curve.

It is also possible to obtain information on the thickness or the elastic modulus of the different layers of the road. For example, Fig. 30 shows the result of such a measurement obtained on a road built with the layers shown on the right-hand side of the figure. The evaluation of results is more complex in this case. The dispersion curve may possess two or more single branches, as is represented in Fig. 30 by the continuous and broken line.

In the case shown in Fig. 31 the object was to determine the thickness of wall built of bricks. The wall was excited periodically and the resonant frequencies were measured. The lower curve represents such frequencies. If the velocity of elastic waves is known the thickness or the distance to cracks inside the concrete structure can be obtained with the help of the measured resonant frequency values.

We believe the methods and the instruments developed by our Institute are a good contribution to the solution of some of the engineering problems discussed here to-day.

R. A. ASHBEE (Great Britain)

I would like to extend the use of "progressive failure" and "residual shear strength" to rigid foundations. In doing this I may be guilty of some gross oversimplifications; the results, however, do lead to some interesting conclusions.

Professor Skempton has shown how the shear strength of a soil drops after failure to a residual value. The shear strength is, of course, the maximum stress that can be supported at a particular strain.

We assume that a clay bank fails eventually because the soil strength has been falling with time. The shear stress in a bank is not uniform. When stress and strength become equal, local shear failure takes place, the ability of the soil to support stress drops, and redistribution of shear stress follows. The shape of the new curve will depend on the stress-strain characteristics of the soil, but there can be a fall to the residual value. Failure of the bank occurs when the soil can no longer accommodate the redistribution of stress.

An important point is that the loss of strength will be most serious with those soils which are most sensitive to disturbance. We conclude from this that a cutting slope through virgin clay will eventually undergo a more rapid type of failure than an embankment made of remoulded, less sensitive soil. We must expect an exactly similar loss of strength with a rotational failure of a foundation. Here the local shear failure will be initiated by the building since maximum soil strain will always be closest to the driving force. Another feature which encourages local shear failure is differential consolidation. The building surcharge is on one side of the shear surface only, tending to cause consolidation mainly on that side.

This local shear failure associated with differential consolidation is, I think, an important mechanism with many applications. First, consider the shear box test. Local shear and consolidation will take place at every rigid contact surface. On these sheared surfaces only the residual shear strength of the soil can be mobilized. The peak shear strength is only being realized at a number of isolated points of impending failure. This test can never measure the full shear strength of a clay; it is of course ideally suited to the measurement of residual shear strength. Rate of loading will also influence this test result, consolidation being encouraged by slow loading. Another point; with a soft clay there is probably adhesion on the exposed shear box surfaces, thus the effective area is increasing instead of decreasing as usually assumed. I think this combined action of local shear and consolidation plays some part in the settlement of any foundation on a compressible soil.

To obtain a mathematical answer calls for a simple model, and in Fig. 33 I have assumed a circular foundation generating a cylindrical shear failure surface. The thickness of material D_1 is compressed to D_2, and the shear failure extends to the full depth of differential movement. Lateral soil displacements have been ignored. Because of the high edge stresses under a rigid footing, this failure surface can be initiated at very low foundation loads. For calculation purposes we use average pressure, starting at the average foundation bearing pressure w. This decreases as load is taken by shear on the cylinder. At the limit of shear penetration an average residual pressure q remains which maintains the sheer stresses below that level. This is a considerable oversimplification but I think on the face of it that the Leaning Tower of Pisa is an example of this mechanism, the symptoms being settlement with little or no surface distortion.

The consolidation process involved is time dependent and so a rigid solution must also be time dependent. On the basis of a simple model, a circular base generating a cylindrical failure surface, two approximate limiting solutions are possible (Fig. 34). The first solution assumes that all the

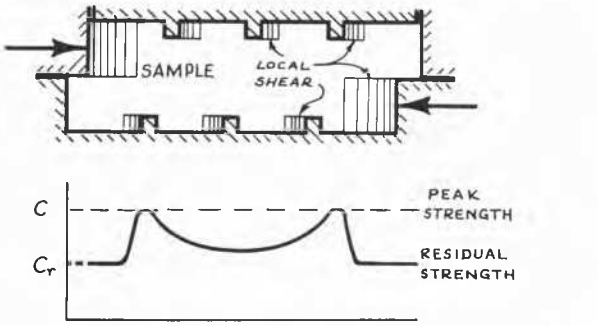

FIG. 32. Possible shear stress distribution in the shear box.

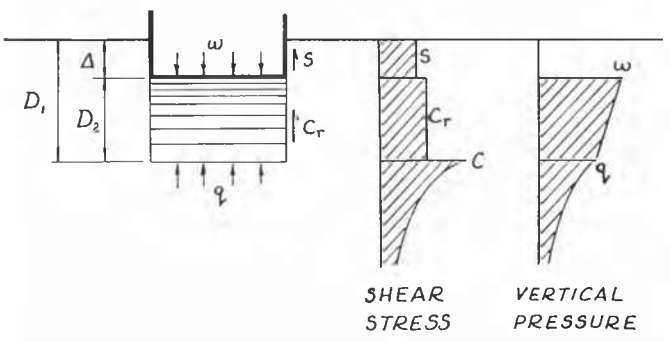

FIG. 33. Local shear and consolidation.

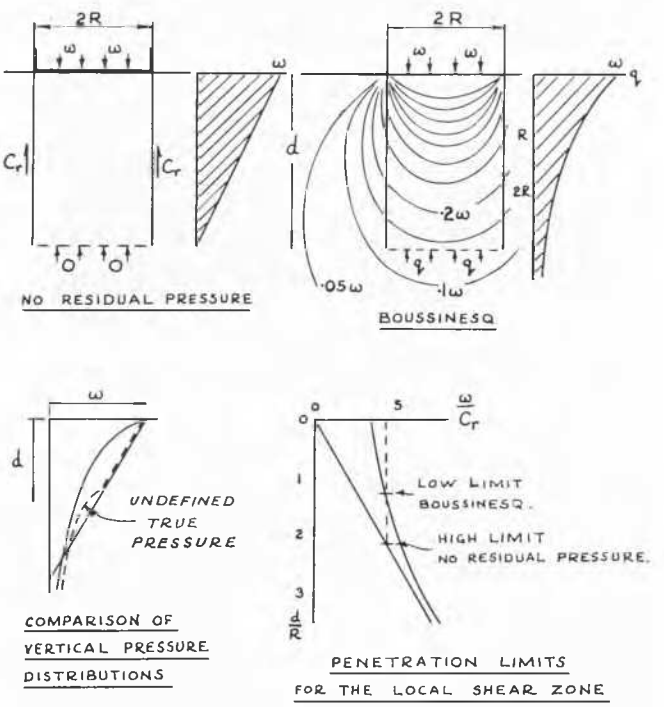

FIG. 34. Limiting solutions for circular base generating a cylindrical failure surface.

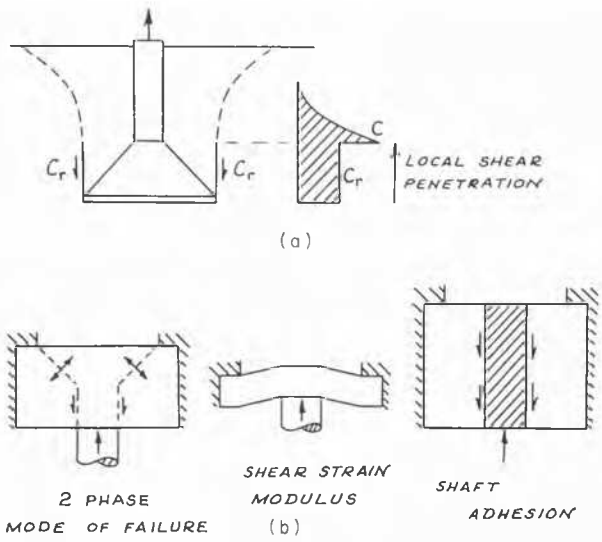

FIG. 35. Example of transition to an alternative failure mechanism. (a) Uplift foundation; (b) punching shear test.

FIG. 36. Field test on an undercut foundation.

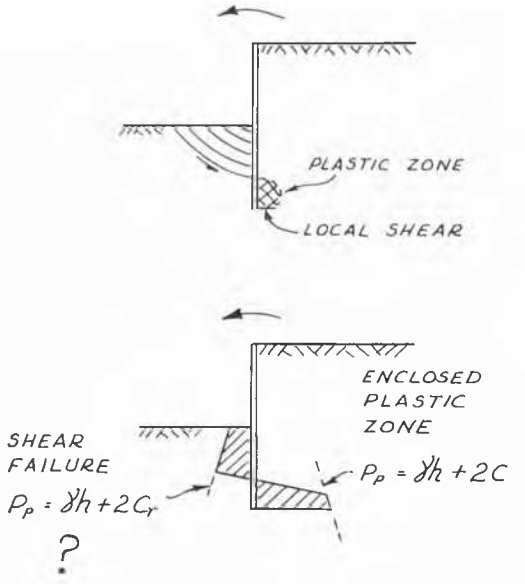

FIG. 37. Passive pressure.

foundation load is supported by shear on the cylindrical failure surface. That is, there is no residual pressure at the limit of shear penetration. This approach must give an overestimate of penetration, because there must in fact be a residual pressure. The second solution makes use of the elastic bulbs of vertical pressure to determine residual pressure at the limit of shear penetration. The average pressure q is taken over the projected area of the foundation at the required depth. The balance of forces provides a solution which must give an underestimate of penetration, since the effect of introducing a cylindrical surface of weakness is to increase the vertical stresses at any depth below the actual footing. This mechanism shows how foundation movement can be dependent on both shear strength and compressibility. It may, however, only form part of a general mode of failure.

Sometimes a transition to an alternative failure mechanism takes place. An example of this transition is an uplift foundation in a clay soil (Fig. 35). Local shear failure is generated by the foundation, but the build-up of stress beyond the limit of shear penetration is restricted by the presence of the free surface at ground level. The transition is to a tensile mode of soil failure near ground level.

We have been able to study this type of behaviour in the laboratory using a "punching shear" soil test. In this test a plunger is thrust upwards through a disc of clay. The two types of soil failure can be seen on the 2-inch-thick punching shear sample, true shear in the lower part of the sample changing to tensile failure above. This tensile failure can be inhibited by using air pressure to simulate overburden.

Fig. 36 shows a field test on an undercut foundation. A trench has been cut into the zone of failure. The failure surface can be seen; it reaches ground level at 45°, which corresponds well with the angle found in the punching shear test.

The same logic can be applied to the calculation of passive pressures (Fig. 37). It would seem that if passive pressure is controlled by a free surface, there is a possibility of a progressive mode of failure. In such a case the residual shear strength will be the controlling soil property. If no free surface is involved the conventional value is used.

In these examples it is the linear translatory strain after failure which governs the drop of strength to the residual, and it is this actual translation on each slip surface which must be considered in any application.

A. P. SINITZYN (U.S.S.R.)

In the U.S.S.R. the design of a plate based on an elastic half-space has been developed on an extensive scale by B. N. Gemochkin, M. M. Filonenko-Borodich, M. I. Gorbunov-Possadov, and others. In this discussion the problem of determining the collapse load of the plate is dealt with. The elastic foundation is specified as a two-layered model.

The upper layer is of limited thickness and follows the Winkler hypothesis; it is supported by an elastic half-space. The vertical reactions developed between the plate and the foundation are taken into consideration. For design purposes the plate is considered to be separate from the foundation and the reactions, represented by generalized or discrete groups are applied on the contact plane.

These generalized forces are calculated by means of the system of linear equations obtained under contact conditions between the plate and foundation. The equation coefficients are determined as generalized deflections of the plate and the settlements of the foundation due to single group forces. The solution of continuous equations is carried out by means of an electronic computer and as a result the reactions on the contact area of the plate and foundation are estimated. The bending moments in the plate are calculated on the assumption that the plate is separated from the foundation and loaded with external forces and reactions of the foundation in the contact area. If a region of plastic deformations arises in the plate, the rigidity of the plate will decrease and the reactions and bending moments will change their values. Beyond the elastic limit the deflections of the plate are studied step by step.

At first investigations are made in the elastic field; this helps to determine the position of the linear plastic hinges in the plate. The next step consists of a new design of the basic system, in which the plate is considered to contain plastic hinges. The deflections of the plate are now determined for this rearranged system. New reaction forces and bending moments are calculated in the elasto-plastic plate by solving the general equation.

The meaning of the term ultimate load-carrying capacity in this problem differs from the usual one. The development of one or many linear plastic hinges in the plate will not realize the whole load-carrying capacity of the structure because the elastic foundation will support the plate. Now the collapse load will be determined by standardization of the maximum structural deflection. When plastic hinges develop, the deflection of the rigid plate increases rapidly. This increase depends upon the geometrical dimensions of the plate and the elastic properties of the plate and the foundation. In a flexible plate the development of the first plastic hinge does not involve any substantial increase of deflection. The elastic layer between the plate and the elastic half-space will affect the distribution of reactions in the elastic foundation and cause the decrease of reactions concentrated at the end of the plate. When the elastic limit is exceeded, the plate deflections will increase due to the layer deformation. The collapse load of the infinite plate acted upon by a concentrated force can be approximately determined by the assumption that the plate deflections are in the form of a conical shell with linear plastic hinges on its surface and a circular plastic hinge on its base.

Setting the work of external force $P_{\lim}$ equal to the total work of the moments in the hinges and reactions of the foundation we obtain:

$$P_{\lim} = M_{pl}\int_0^{2\pi}\left[1 + 2\frac{1}{r^2}\left(\frac{d_r}{d\theta}\right)^2 - \frac{1}{2}\left(\frac{d_r^2}{d\theta^2}\right)^2\right]d\theta + M_{pl}\int_0^{2\pi}\left[1 + \frac{1}{r^2}\left(\frac{d_r}{d\theta}\right)\right]d\theta + \int_0^r\left[\frac{q(r-\rho)}{r}2\pi_\rho\right]\left(\frac{r-\rho}{r}\right)d_\rho \ldots \quad (1)$$

The minimum rate of the collapse load $P_{\lim}$ is obtained when the first two integrals in Eq (1) are equal to 4.

$$[P_{\lim}]_{\min} = 4\pi M_{pl} + \frac{1}{12}\pi r^2(q_{\max} - q_r) + \frac{1}{3}\pi r^2 q_r, \quad (2)$$

where M_{pl} = plastic moment per unit length of hinge, r = distance from load $P_{\lim}$ to circumferential hinge, $q_{\max}$ = intensity of foundation reactions under the load, q_r = intensity of foundation reactions at a distance r. The strip acted upon by the concentrated load in the middle of the span will be investigated, and the rate of $P_{\lim}$ computed for various values of the limiting deflections $Y_{\lim}$. In dimensionless form it was presented by means of the deflection Y_0 and the load P_0 corresponding to the elastic limit. The non-linear relation between $P_{\lim}$ and $Y_{\lim}$ will be obtained, which depends on the physical properties of the strip and the foundation, and which is expressed in terms of the parameter:

$$\alpha = E_0/E[l/b\,(l/h)^3 10^{-3}], \quad (3)$$

where E_0 = deformation modulus of foundation, E = elastic modulus of strip, l, b, and h = span, width, and thickness respectively of strip.

$$P^*_{\lim} = P_{\lim}/P_0 = (0.14 + 0.80\alpha^{1.2})\,Y^{*\,(2-\alpha)}_{\lim}, \quad (4)$$

valid under the following conditions:

$$2 \leqslant Y^*_{\lim} \leqslant 5 \text{ and } 0 < \alpha < 1. \quad (5)$$

After developing the first plastic hinge a change of position and magnitude of subgrade reactions will take place. These reactions will depend on the rigidity of the plate and the foundation and on the applied load. The problem will become non-linear. The subgrade reactions and the deflections increase rapidly at the acting point of the load. The deflections of a rigid plate ($\alpha = 0$) beyond the elastic limit increase faster than the applied load does. The collapse load $P_{\lim}$ depends on a given maximum deflection $Y_{\lim}$ and on the rigidity of the plate as it is shown in Fig. 38.

One can see in this figure that the rigid plate has a smaller load-carrying capacity when the deflection $Y_{\lim}$ is large. It is important to note that the load-carrying capacity of the

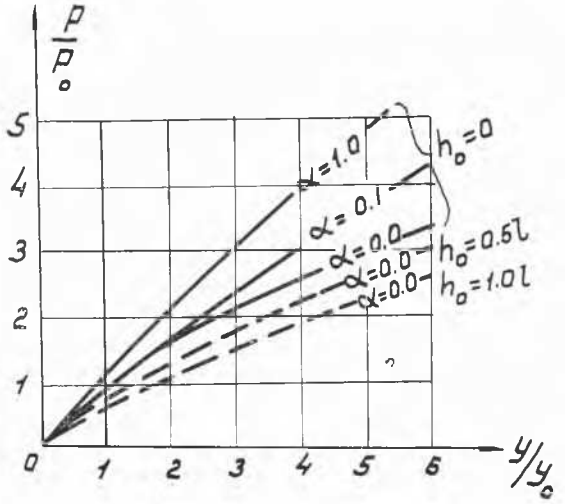

FIG. 38. Relationship between collapse load, maximum deflection, and rigidity of plate.

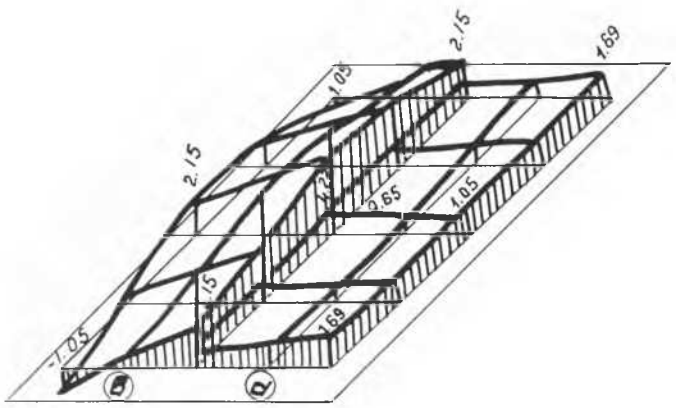

FIG. 39. Variation of subgrade reactions beneath a square rigid plate: (a) within the elastic range; (b) beyond the elastic limit.

plate can increase, while its rigidity decreases or the subgrade modulus increases. The optimum value of the parameter, α, corresponding to the plate with higher collapse load can be determined. Beyond the elastic limit the subgrade reactions change their value all over the surface of the plate. This is shown in Fig. 39 (a, within elastic range; b, beyond elastic limit), for a square rigid plate acted upon by a concentrated load in the middle of the span. If four linear plastic hinges occur, the subgrade reactions at the centre of the plate will be six times larger than in the elastic range. These theoretical results are in good agreement with the test data.

RAPPORTEUR GÉNÉRAL DE BEER

Des discussions de ce matin je dois tâcher de tirer certaines conclusions. Il me semble qu'une première conclusion est que le problème de la capacité portante limite des sols n'a jusqu'ici pas reçu de solution définitive. La limitation de la signification des méthodes actuellement disponibles a été clairement indiqué par le professeur Borowicka. Il a surtout attiré notre attention sur la non validité des formules au cas de sables très peu compacts. Je voudrais relier ce problème à celui de la compacité critique; en effet un sable, saturé d'eau, ayant une compacité inférieure à la valeur critique doit être considéré comme étant en équilibre instable et est donc en principe impropre à servir de base pour une fondation. La limitation de la signification des formules ne doit pas nous étonner. D'une part les propriétés mécaniques des sols sont beacoup plus complexes que la loi simple de Coulomb ne laisse supposer; d'autre part les théories disponibles sont basées sur un certain nombre d'hypothèses simplificatrices qui s'écartent plus ou moins profondément de la réalité.

Il nous faut tâcher d'obtenir des solutions qui sont statiquement et cinématiquement admissibles et le Dr Bent Hansen nous a clairement montré que certaines solutions présentées ne répondent pas à cette double condition.

Vu la complexité du problème il faut nécessairement faire intervenir certaines données expérimentales si l'on désire aboutir à une solution. M. L'Herminier nous a décrit certains essais de laboratoire qui apportent des données intéressantes pour mieux circonscrire le problème.

Toutefois on ne peut se dissimuler que les essais effectués sur semelles de petites dimensions doivent être transposés avec prudence au cas des semelles réelles. Cela a été clairement souligné aussi par le professeur Borowicka.

C'est pourquoi je suis d'avis qu'il faut multiplier les essais en vraie grandeur, pour autant qu'ils soient exécutés avec toutes les garanties voulues et de telle façon qu'on puisse sérier les paramètres. Les essais effectués par la Degebo à Berlin avec des semelles de 1 m.ca de surface constituent un apport fort intéressant dans le problème de la capacité portante limite. Dans son intervention, le Dr Muhs a clairement indiqué le phénomène de progressivité de la rupture. Ce phénomène est intimement lié aux phénomènes de dilatance positive et négative. La question est de savoir si ce phénomène est indépendant de l'échelle.

Le Dr Muhs nous a d'autre part présenté certaines autres déductions intéressantes de ses essais, notamment en ce qui concerne les coefficients de forme. De ses essais il déduit que le coefficient de forme pour des semelles carrées, pour le facteur de portance N_q, est une fonction de la densité relative et est rapidement supérieur à 1,5. Des essais qui sont en cours au laboratoire à Gand confirment ces valeurs élevées.

D'autre part les essais fragmentaires dont nous disposons semblent aussi indiquer que le facteur de profondeur dans le terme de N_q est généralement sousestimé.

Si on veut interprêter correctement les résultats expérimentaux, il est absolument nécessaire de pouvoir sérier les variables; dès lors des essais systématiques à échelle réelle devraient être effectués en ce sens. Au lieu de dépenser des sommes importantes en répétant dans divers laboratoires des essais à petite échelle, ou des essais en vraie grandeur mais dans des conditions non idéales, il faudrait pouvoir aboutir à une conjugaison des efforts pour réaliser un programme d'essais en vraie grandeur conçu de telle façon que l'on puisse sérier les variables.

Il est d'ailleurs évident qu'entretemps les praticiens doivent pouvoir disposer d'un outil leur permettant de fixer une valeur située du côté de la sécurité pour la capacité portante limite. Il semble bieu qu'une telle limite puisse être actuellement trouvée pour les fondations directes courantes en utilisant les formules classiques, dans lesquelles on introduit pour le facteur de portance N_γ la valeur obtenue en adoptant un angle de frottement de 10 pour-cent supérieur à la valeur obtenue dans un essai triaxial normal et une valeur de N_q correspondant à un angle non majoré, tout en maintenant provisoirement les coefficients de forme et de profondeur, tels que définis par Brinch Hansen. Il est par ailleurs quasi certain que l'analyse d'essais en cours et encore à réaliser aménéront à une importante modification de certains de ces coefficients.

Le praticien se trouve souvent confronté avec le problème de fondations établies sur des sols composés de couches multiples et de sols anisotropes. Koizumi et Salas nous ont apportés certaines données nouvelles à ce sujet notamment par l'application de la méthode des caractéristiques à des problèmes comportant des couches ortho-plastiques. Ici aussi le praticien ne peut attendre qu'on lui ait apporté la solution exacte. Dans l'état actuel de nos connaissances il devra laisser travailler son bon jugement. Il se verra obligé de simplifier grandement le problème en introduisant des hypothèses de travail situées du côté de la sécurité. Les interventions très intéressantes de Koizumi et de Salas pourront utilement le guider dans le choix de ces hypothèses.

Le problème de la répartition des réactions sol-fondation a donné lieu à des interventions très intéressantes. Là aussi seules des données expérimentales sont à même de faire avancer nos connaissances. Je regrette que la limitation du temps n'a pas permis au Dr Leussink d'exposer les résultats qu'il a obtenus en couvrant pratiquement toute la surface d'une semelle avec des cellules de mesure des pressions et qui font apparaître les fortes concentrations de pressions aux

bords que l'on obtient dans des sables avec des semelles faiblement enterrées notamment lorsque la compacité est forte, et la charge notablement inférieure à la capacité portante limite.

D'autre part sous des déformations lentes le module de déformation du béton dont est constitué le radier et la superstructure peut être de loin inférieur à la valeur déduite d'essais normaux sur éprouvettes en laboratoire. Une tendance se dégage aussi pour calculer les radiers en plasticité.

Enfin se posent de plus en plus les problèmes de la capacité portante limite sous des charges dynamiques et vibratoires. Ce problème a d'ailleurs déjà été abordé dans la division précédente, consacrée à la détermination de la résistance au cisaillement. D'une façon assez surprenante *a priori*, il semble bien que ce problème, en ce qui concerne les sols pulvérulents, soit plus facilement abordable d'une façon théorique, que le problème de la capacité portante sous des charges statiques. Dans ce domaine un pas important a été réalisé, grâce aux sommes importantes et aux recherches systématiques effectuées dans les grands pays directement intéressés à ce problème. Il ne laisse pas de doute que si un même recherche systématique était concentré dans le domaine de la capacité portante limite sous des charges statiques, on pourrait aboutir à un même résultat positif.

CHAIRMAN CROCE

I wish to extend our thanks to the members of the panel, the General Reporter, and to the oral discussors for their excellent presentations. This session is over.

(*The remarks of the General Reporter for Session 4 presented to the Closing Session appear on pp. 593–4.*)

WRITTEN CONTRIBUTIONS

CONTRIBUTIONS ÉCRITES

A. I. DEMENTIEV (U.S.S.R.)

The paper by *Kiselev, et al. (3/21)* is devoted to the determination of the extent of a foundation's ultimate settlement on permafrost, since this value is one of the main factors influencing the stability of buildings being erected.

Foundation settlements are caused by the thawing of permafrost as a result of the heat emission of the building over the entire period of its maintenance. However, the extent to which this heat emission influences the settlement and the nature of soil changes due to its influence are not constant; they change with time. To determine the pattern of this process it is necessary to study a model of it for a long period of time.

The information presented herein reports observations made over many years of settlements on thawing permafrost. Several buildings in Zabaikalie were under observation over a period of 21 years, from 1941 to 1962. The buildings are situated on a soil formed by quaternary pebble-gravel deposits of 3.5 m thickness and with a sandy loam and loam stratum underlain by Jurassic clays. Beginning with the upper surface of the clays the soils were in a permanently frozen state down to 20–25 m. The buildings observed are brick, 80 m long, and with tape type rubble foundations laid 1.80 m deep, that is the foundations were laid in the active layer, above the permanently frozen strata.

Observations made over many years made it possible to determine not only the extent and rate of building settlement, but the pattern of the process as well. Fig. 40 shows the settlement of two of these buildings, curves 1 and 2 corresponding to the settlement of the opposite sides of the two-storey administration building and curve 3 to the settlement of the industrial building. The larger settlement of one side of the administration building (curve 1) is explained by a higher ice formation in the soils under that foundation. The settlement of the industrial building was not as great as it was constructed on more favourable conditions of permanently frozen soil.

However, in all cases the same pattern in the character of the building settlements was observed, the only difference being in the magnitude of the settlement. During the first years after construction of the buildings a markedly seasonal periodicity of settlements was observed: in the first half of a year the settlement decreased due to winter freezing of the soils; in the second half of the year the settlement increased

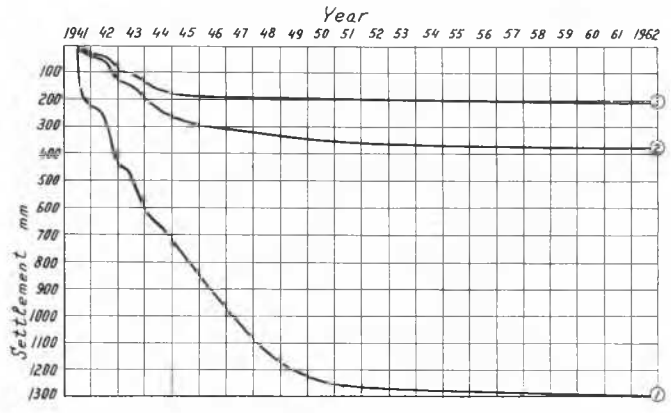

FIG. 40. Development of settlement as a result of soils thawing under the foundation of (1), eastern part of the administration building; (2), western part of the same building; (3), industrial building.

because of summer thawing of the soils. In the course of time the rate of settlement slowly decreased and approached complete stabilization.

The highest settlement rate was observed during the first year of the administration building's existence, and in some places it amounted to 27 cm per year (curve 1); from 1945 to 1950 the average settlement of the same part of the building amounted to 9 cm per year; and from 1950 to 1962 it amounted to 0.4 cm. per year. Thus the average annual rate of building settlement had decreased by approximately 70 times, as compared with the initial period, and during the very last years it became infinitesimal. It should be noted that the settlement of this part of the building was greatest in the region of objects observed: in a period of 21 years it amounted to 129 cm, 124 cm or 96 per cent of the total settlement occurring in the first ten years.

The settlements of the opposite side of the administration building (curve 2) and of the industrial building (curve 3) were considerably less, amounting to 37 and 21 cm respectively for the 21 years. However, in these cases the same regularity of settlement rate with subsequent stabilization is observed. In the first case complete stabilization of the settlement took place in 12 years, in the second case in 10 years, and in the third case in 6 years.

The results of the observations show that when calculating the settlements of foundations on thawing permanently frozen soils, not only the ultimate settlement should be taken into consideration but also the settlement rate which can achieve a very high value during the initial period of the building's existence. The actual information on foundation settlements can be used to determine the limits of deformation required of a building's constructive elements and to check the methods of calculating foundation settlement on thawing permafrost.

L. J. GOODMAN (U.S.A.)

This discussion is occasioned by the papers in Division 3 concerning storage tank foundations—*Jappelli (3/19)* and *Penman and Watson (3/36)*. The specific purpose of this discussion is to summarize the results of preloading a site underlain with highly compressible glacial lake deposits of varying thickness to permit the use of shallow foundation pads for oil storage tanks. Some brief attention is then devoted to preloading a site underlain with peat to support a light metal structure on shallow footing foundations. Included are post-construction settlement records for each case history.

CASE HISTORY 1

This case record illustrates the preloading of a site prior to construction of 4 fuel oil storage tanks. The original tank design called for a height of 48 ft and diameters from 70 to 125 ft. These dimensions were changed during the initial stages of the subsurface investigation programme in order to reduce the loading. The final design called for a tank height of 32 ft and diameters from 67 to 134 ft. The loading from each tank is approximately 2000 lb/sq.ft. which includes the weight of the tank and the storage of fuel. Each tank is enclosed by a fire dike and is connected to the truck loading station by piping. A minimum clearance of 50 ft is required between tanks.

The site is situated on a gentle sloping hillside, with the ground surface dipping to the south. Existing site grades varied from approximately El. 30.0 at the northern end to El. 14.0 at the southern limit of the tank installations. This necessitated a fairly extensive excavation programme in the northern half since the finished site grade varied between El. 15.0 and El. 14.0.

During the terminal part of the ice age, a glacial lake covered a considerable portion of the area. The lake basin accumulated silts and clays which covered the bottom to considerable depth. The inundation of the lowland was followed by successive lowering of lake levels with changes in the drainage pattern resulting in a layer of largely loose granular material—silts, sands, and gravel. A marshy environment followed the deposition of granular material adding some peat and marl which are overlain by present fill material. The natural material below the miscellaneous fill in this location forms a wedge-shaped deposit which has a thickness of approximately 74 ft at the southern end of the site and disappears before reaching the northern end. Water was encountered on the site at depths varying from 10 to 17 ft.

The preload decision was based on previous experience with field load-time-settlement relationships in similar soil deposits and cost comparisons with a short pile installation. It was estimated that a preload of 2000 lb/sq.ft. would require less than six months to develop expected settlement for the most severe case which was Tank 4's location. No attempt was made to secure undisturbed samples in this location for laboratory consolidation and shear tests in view of the erratic deposition of compressible materials.

The estimated cost of the preloading operation and select materials indicated for both frost wall and foundation pad requirements and additional site preparation for the tanks was less than $50,000 for all four tanks. The estimated cost of piling, including reinforced concrete pile caps was approximately $210,000. These cost data were based on the use of 20-ton short piles that would average 25 ft in length over the site.

A full preloading programme was followed for Tanks 2, 3, and 4 and a large-scale field load test was conducted in the southwest quadrant of Tank 1 to establish the need for any partial preload treatment for this tank location. Site preparation included compaction of the subgrade and the overlying gravel fill prior to placement of preload. The fill in Tank —4's location was obtained from Tank 1's excavation and placed in increments to the specified 17 ft in fourteen days. The load remained for approximately 2 weeks beyond October 30 on which date the settlements reached equilibrium. Four settlement plates were used to monitor the preload operation as shown in Fig. 41. A similar procedure was used for the remaining two tanks, 2 and 3.

Settlements for all tanks conformed closely to the thickness of compressible materials underlying the particular tank. All time limits for the settlements were less than the estimates.

Following the preloading programme, final site preparation for the oil storage tanks was carried out. This included a compacted granular base to serve as a foundation pad for each tank, with a clean sand and gravel frost wall along the perimeter of the tank.

Four settlement observation points were established around the exterior of each tank. Tanks 2, 3, and 4 were test-filled with water before they were used to store the fuel oil and gasoline. Four feet of fuel oil were stored in Tank 1 for six months, at which time the storage was increased to 30 ft ±. Settlement records since tank erection during the spring of 1961 indicated a maximum settlement of 1 in., which is well within tolerable limits.

CASE HISTORY 2

This case record illustrates the preloading of a site underlain with 3 to 5 ft of amorphous peat to permit the use of shallow footing foundations for support of a relatively light metal structure. The structure has plan dimensions of 40 by 60 ft and a foundation loading of 1000 lb/sq.ft., including a floor slab independently supported on grade.

The site lies in a lowland area, underlain with loose sediments of considerable thickness deposited in an eroded bedrock trough created by glacial action. The deposits are quite similar to those reported in Case History 1 with the exception of more uniform deposition in lateral directions and the peat layer commencing at contemplated foundation grade.

A limited construction budget precluded the use of either short piles driven into an intermediate zone of compact materials or removal and replacement of the peat. It was therefore decided to secure 5-in.-diam. Shelby tube samples of the peat for laboratory consolidation and shear testing to establish the feasibility of preloading.

Laboratory results yielded ranges of 2.58 to 2.84 for compression index, 5.23 to 5.48 for initial void ratio, 319 to 403 per cent for natural water content, 1.51 to 1.62 for specific gravity, and 42.5 to 75.2 per cent for organic content. Theoretical time-settlement studies indicated approxi-

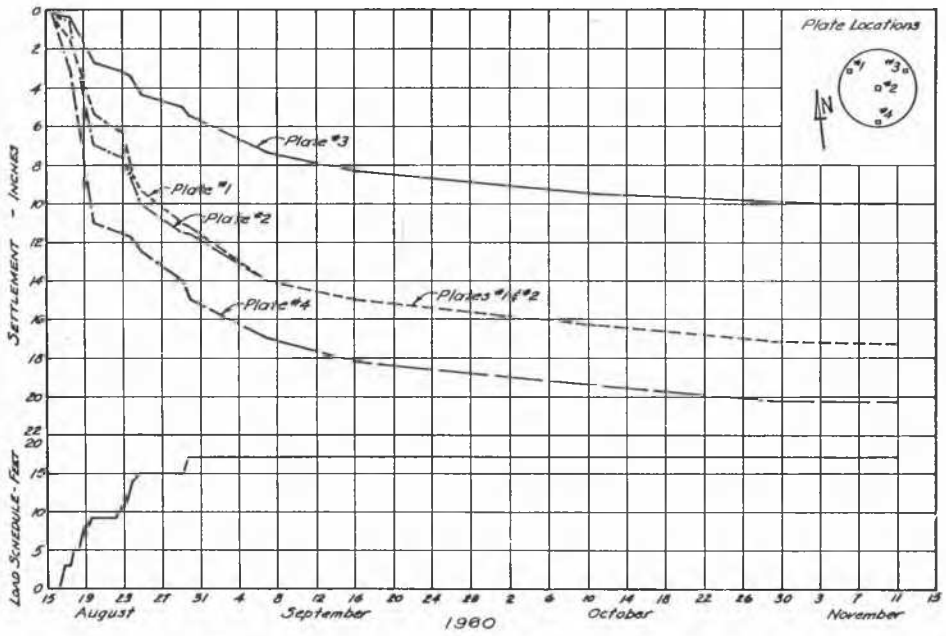

FIG. 41. Field time-settlement curves (Tank 4).

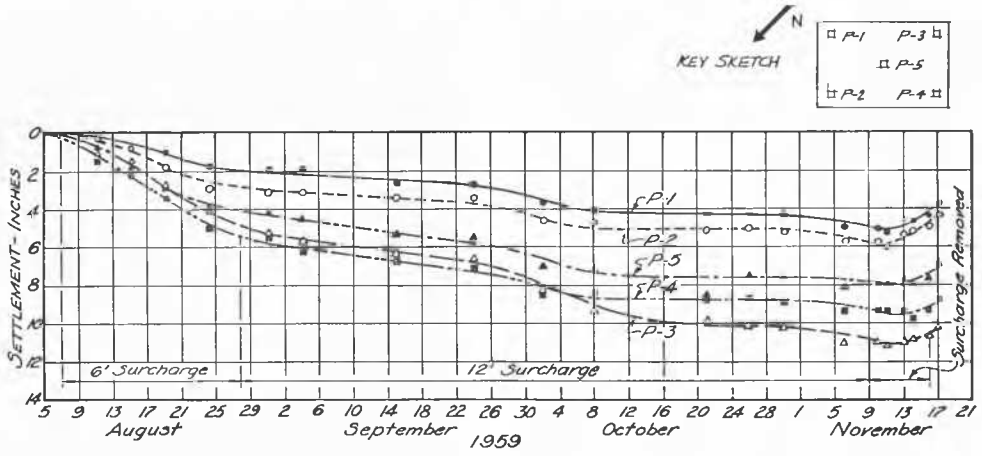

FIG. 42. Field time-settlement curves, Case History 2.

mately 6 months would be required to develop expected settlements due to the building loading of 1000 lb/sq.ft. if a surcharge of 500 lb/sq.ft. were placed over the simulated building preload. Computations for the subsoil stresses due to the building loads were made on the basis of the Boussinesq equations. The earth material used to develop expected settlements was end-dumped and spread by a bulldozer in essentially two 6-ft stages approximately 3 weeks apart.

Provisions for monitoring the settlement under this load were provided by 5 settlement plates which were located at the corners and at the centre of the building location. Vertical movement of the plates was observed at regular intervals and recorded as shown in Fig. 42 to evaluate actual time-settlement conditions. Fig. 42 also includes rebound data during and after the removal of the preload. It is noted that the actual settlement curves levelled off in a range varying from 5 to 11 in. after 3 months of loading in contrast to the theoretical predictions of 9¼ in. in 5⅓ months. This range of field recorded settlements is explained in part by the fact that the front of the site has a past history of some preloading. The rebound from the field settlements amounted to approximately 10 to 25 per cent. The higher percentage of rebound recorded for plates 1 and 2 was apparently due to some reported disturbance to these plates during removal of the preload.

Arrangements were made with the owner to make settlement observations both during and after construction. This was accomplished by placing settlement pins in both the columns and in the floor. As of this writing, no settlement due to a recompression of the peat has been noted. Construction was started in November, 1959. Maximum foundation loads have been in effect for 5½ years (October, 1965). Loading includes 1 ft of compacted granular fill to satisfy grade requirements.

REFERENCES

GOODMAN, L. J., and N. E. FALTYN (1965). Preloading results in tank foundation economies. *J. Construction Division, A.S.C.E.*, Vol. 91, CO-1.

GOODMAN, L. J., and C. N. LEE (1962). Engineering characteristics of some peat soils. *Proc. 8th Muskeg Research Conference,* National Research Council of Canada.

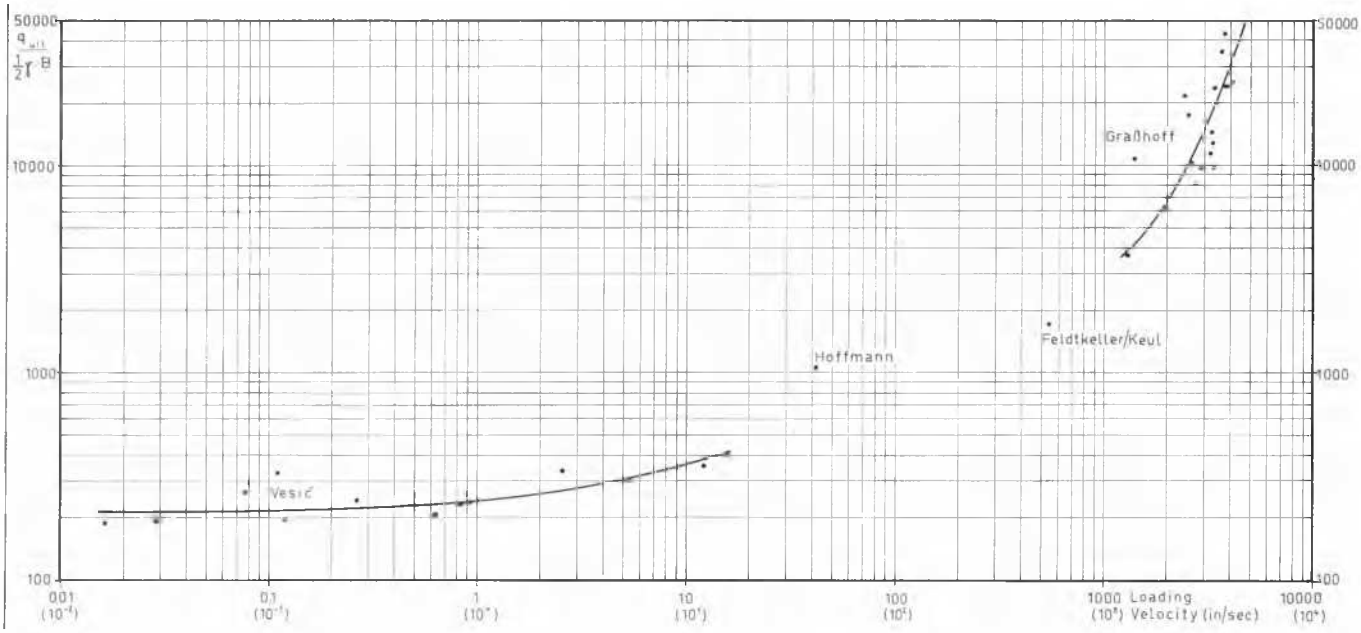

FIG. 43. Test results.

H. GRASSHOFF (Germany)

In paper *(3/45) Vesić, et al.* describe loading tests on dry and submerged sand bringing up the model footing at different velocities. The purpose of the tests was to show the dependence of the bearing capacity of sand on the loading rate. The tests have shown that in the case of very small loading rates (from about 10^{-3} to 10^{-2} in/sec) the bearing capacity at the beginning decreases, but in the case of growing velocities it increases to values which are larger than the static bearing capacity. As the tests were performed at a loading rate of only about 12 in/sec it may be assumed that the loading resistance is mainly caused by the static failure zone of the classic earth pressure theory. At greater loading rates—as obviously occur with problems of missile launching and blast resistant structures—the failure zone in sand can probably not be registered by means of the formulae of the earth pressure theory. The model footing will penetrate like a punch into the soil and the soil surrounding the penetrating object will show a zone of disturbance, possibly corresponding to the laws of rheology.

In 1944 I performed similar tests in which projectiles were catapulted into sandy soil with velocities between 1000 and 5000 in/sec (Grasshoff, 1947 and 1953). The penetrating projectile was photographed by means of a high-speed motion picture camera. The double differentiation of the penetration-time diagram led to the penetration-resistance curve. High values of resistance were measured. The main reason is to be seen in the acceleration resistance of the grains of sand. The measured resistance factors in dry sand are shown in Fig. 43. Also shown are the test values obtained by Vesić, *et al.* The test points follow a steeply rising curve.

The resistance factors of a ramming test by Hoffmann (1948) and of a falling test by Feldtkellar and Keul (1943) in dry sand are also shown in Fig. 43. The test points coincide with the course of the curve.

Excavation of the projectile in the penetration test very distinctly shows the punching effect and the quasi-liquid flow in the vicinity of the penetrated object (Fig. 44).

In the above-mentioned publications (Grasshoff, 1947 and 1953) I have tried to develop a law of dynamic resistance in the case of high velocities in which each part is dependent on a certain soil characteristic.

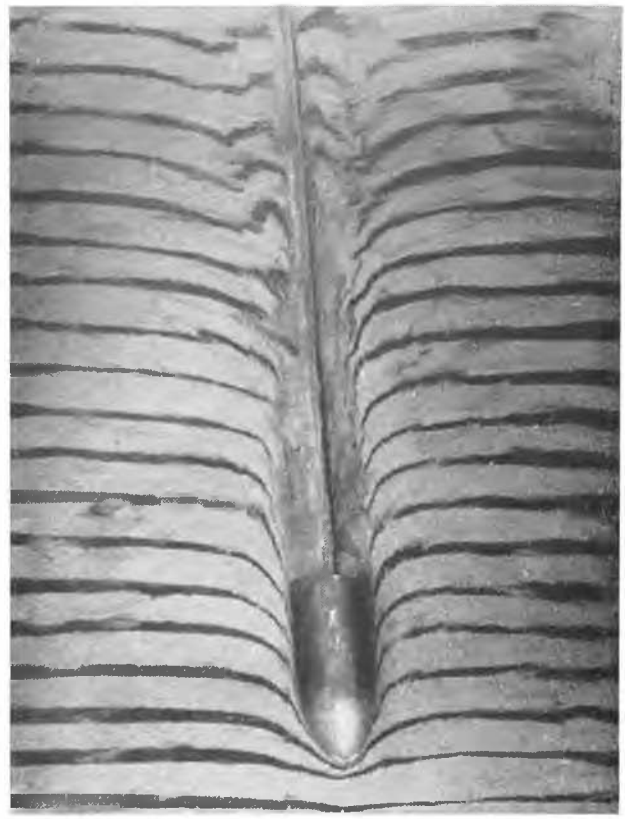

FIG. 44. Photograph showing projectile embedded in resisting medium.

REFERENCES

FELDTKELLER and KEUL (1943). *Fernregistrierungen von Aufschlagverzögerungen frei fallender Bomben.* Bericht Nr. 162 der Lilienthal-Gesellschaft.

GRASSHOFF, H. (1947). Messungen des dynamischen Widerstandes an Modellpfählen in Sandböden und Untersuchungen über seine Gesetzmässigkeit. Dissertation, Technische Hochschule Hannover.

——— (1953). Investigations of Values of the Dynamic Penetration Resistance to Model Piles in Sand and Clay, Obtained from Tests. *Proc. Third International Conference on Soil Mechanics and Foundation Engineering*, Vol. 2, pp. 000–00.

HOFFMANN (1948). Beitrag zur frage der statischen und dynamischen pfahltragfähigkeit. *Abhandlungen über Bodenmechanik und Grundbau*, pp. 150–6. Berlin-Bielefeld-Detmold, Erich Schmidt Verlag.

A. K. JAMAL (U.S.A.)

This is a discussion of paper *3/3* by *E. E. de Beer*.

The phenomenon of progressive rupture also occurs in the laboratory testing of sand in the conventional triaxial test. Observations similar to those of different degrees of settlement in the bearing capacity tests with different plate sizes, described by the author, have been made in triaxial tests performed on sand specimens of varying geometry.

Fig. 45a shows the maximum principal strain ϵ_z at failure, corresponding to peak deviator stress, plotted against initial specimen porosity, obtained from conventional drained triaxial tests on 4-in.-diam. specimens. The failure points shown are those for specimens 8 in. long and 10 in. long. It can be seen that for medium to dense sand specimens, the axial strain ϵ_z required to induce a plastic failure in the 8-in.-long specimens is higher than that required for the 10-in.-long specimens. On the other hand, for loose sand, the strain for 10-in. specimens is higher than that for 8-in. specimens. If the specimen diameter to length ratios of 0.5 (8 in. long) and 0.4 (10 in. long) are thought to correspond to different plate sizes in the bearing capacity tests, these results are very similar to those given by the author in his Fig. 3. The other shear parameters at failure obtained from the triaxial test, namely those of volumetric strain and the dilatation, Figs. 45b and 45c, show that for the shorter (8 in. long) specimens, a larger mass of sand is set in motion in reaching a limiting equilibrium state and the lateral strains induced are higher. Thus the deformations of these samples are characterized by extensive bulging.

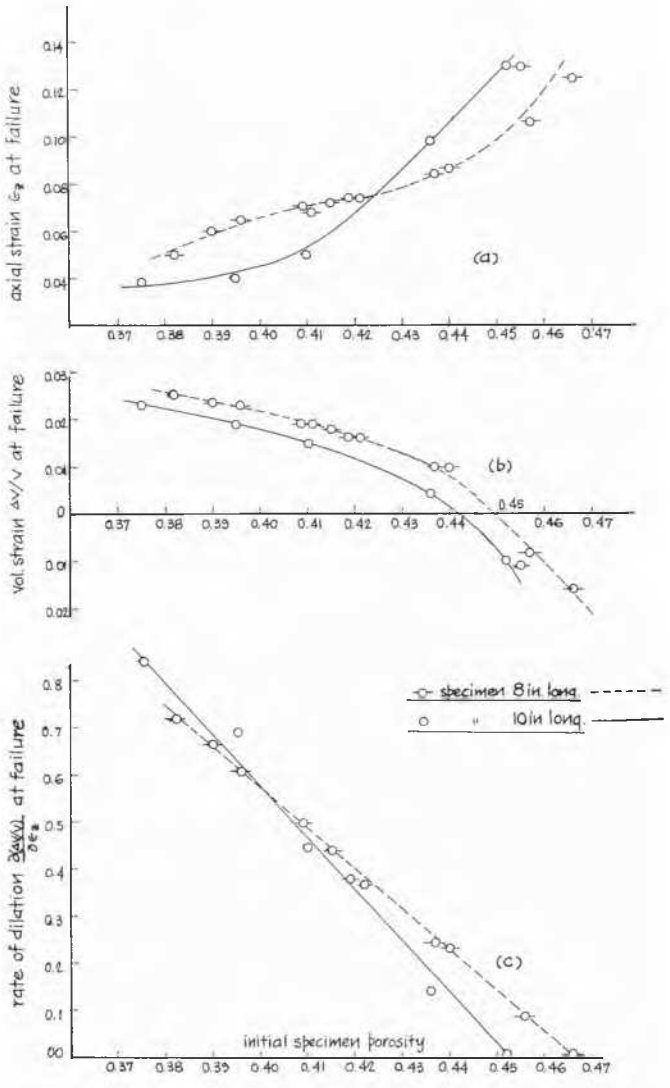

FIG. 45. Results of laboratory triaxial tests performed on loose to dense sand specimens.

It is a common observation that the characteristic failure plane at the periphery of the triaxial sample appears at a strain value which is higher than the strain corresponding to the peak deviator stress. Further, at this higher strain no further volume changes in the specimen take place and the sand mass flows as an ideal plastic body. The explanation of these observations is as follows.

From the state of isotropic, homogeneous mass which exists in a triaxial specimen consolidated under an ambient pressure, the application of a deviator stress results in an anisotropic condition being set up in the specimen. Non-uniform strains and stresses occur throughout the radial planes of the triaxial specimen, and there is a continual re-distribution of the strains and the stresses during the entire shearing process (*Broms and Jamal, 2/9*). A plastic state of failure, for the limiting condition of Coulomb's law, first occurs at the axis of the specimen and this plastic domain then progresses throughout the radial plane, reaching the outer periphery of the specimen last. Thus progressive rupture is occurring during the triaxial test, and the rate of advance of the plastic domain, or rupture is strongly influenced by test specimen geometry.

These and similar conclusions have been made from tests performed at Cornell University on hollow cylindrical specimens of sand. Papers for publication of these results are in the course of preparation.

L. LAPIDUS and W. STOROJENKO (U.S.S.R.)

At present the mechanical behaviour of cohesive soils under pulsating loading is receiving insufficient study. The investigations carried out by Seed, Chan, and McNeill (1961) are widely known but many questions connected with this problem are not clear, particularly that of soil strength. That is why a special apparatus for dynamic loading was designed in our laboratory. By means of this apparatus (Fig. 46) it was possible to carry out unconfined triaxial tests. In this apparatus electrical impulses are transformed into mechanical pulsating loads by means of a magnet. The amplitude, frequency, and duration of pulsating load can be regulated over a wide range. The stress was measured by means of a membrane gauge and registered by means of an oscillograph.

Disturbed samples of red-brown loam were compressed without lateral confinement. Their properties were as follows: $\gamma = 1.92$ grams/cu.cm., $w = 22.5$ per cent, $w_L = 32.6$ per cent, $I_w = 8.9$ per cent, $S_r = 0.72$. Special investigations showed that this soil does not possess thixotropic properties.

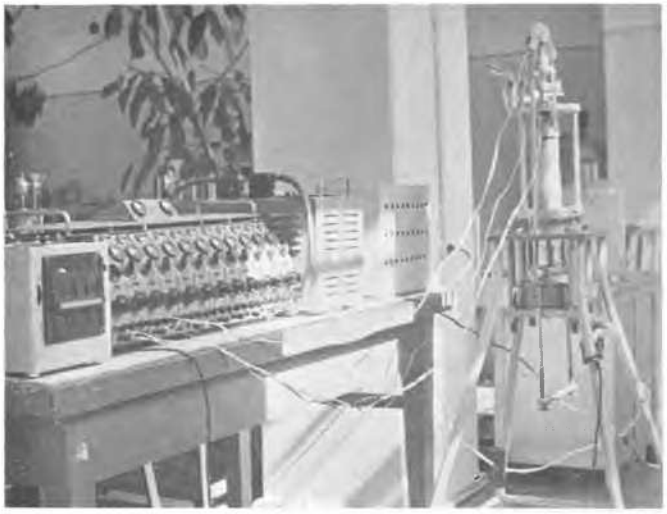

FIG. 46. Apparatus used for the study of the effect of dynamic loads on soil strength.

The dependence of the maximum load value on the number of cycles until failure of the sample was found experimentally. At first the breaking point under the action of static loading σ_s was found. Then some samples were subjected to dynamic loading with amplitude values less than the corresponding σ_s. The frequency of pulsation was equal to 1·Hz and the duration of each pulsation was equal to 0.1 sec. A good analogy was found between the fatigue strength of the red-brown loam and those of other materials (Fig. 47, and Freedman, 1952).

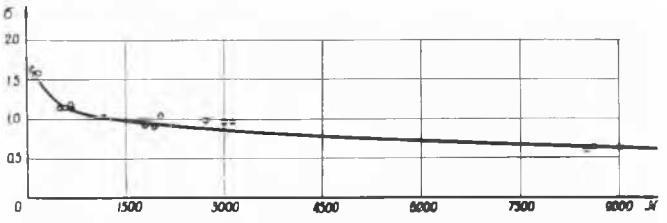

FIG. 47. Results of tests on red-brown loam.

The effect of the frequency of pulsation on the strength of the loam was also investigated. The maximum value of the pulsating stress was equal to 1.3 kg/sq.cm., the frequencies being 1·Hz and 4·Hz. The number of the cycles until failure was 5950 and 6000 respectively. Thus the effect of the frequency of pulsation on the loam strength in the frequency range 1–4 Hz is practically insignificant.

In order to study the effect of the interval between the action of the pulsating load on the strength some tests were carried out with loams which had different static strengths. The action of the pulsating load lasted one minute, and the duration of the interval was equal to 3 minutes. The maximum values of the pulsating stress were 0.8 kg/sq.cm. and 1.3 kg/sq.cm. If we assume the relation of the number of cycles until failure with intervals to that without intervals to be $k = N_1/N_2$, then, $k = 1.55$ when $\sigma_{max} = 0.8$ kg/sq.cm., and $k = 1.91$ when $\sigma_{max} = 1.3$ kg/sq.cm.

A series of tests was carried out in which the samples were subjected to the action of the pulsating loading until visible cracks appeared, after which dynamic tests were interrupted and the samples were tested statically to failure. Very good agreement between the strength of these samples

FIG. 48. Multi-surface sliding failure of a sample tested under dynamic loading.

and the static strength of the samples that had not been subjected to the pulsating loading was obtained.

It was found that the character of the failure was different under static and dynamic loading. Under static loading only one slide plane inclined at an angle of 58° to the horizontal was found. In the case of dynamic loading failure occurred in the form of multi-surface sliding (Fig. 48).

REFERENCES

FREEDMAN, A. B. (1952). *Mechanical properties of metals.* Moscow.

SEED, H. B., and C. K. CHAN (1961). Effect of duration of stress application on soil deformation under repeated loading. *Proc. Fifth International Conference Soil Mechanics and Foundation Engineering*, Vol. 1, pp. 341–5.

SEED, H. B., and R. L. MCNEILL (1957). Soil deformations under repeated stress applications. *Conference on Soils for Engineering Purposes.* Mexico City. A.S.T.M. Special Technical Publication 232.

H. MUHS (Germany)

In his paper to this conference *Gorbunov-Possadov (3/11)* has established theoretically the vertical and tangential reaction forces of the soil in the compacted core under a rigid rough footing. I want to inform you of some experimental data which were obtained by measuring these forces with a newly developed gauge.

In 1955–56 we performed some large-scale loading tests to determine the size and the distribution of the stresses within footings of non-reinforced concrete. While measuring the stresses in the footings we also measured the pressure at the base, that is the soil reaction in the vertical and horizontal planes. For this purpose we used existing Maihak gauges for the measurement of the vertical stresses, but we had to develop a gauge for the measurement of the horizontal stresses. The gauge and the results gained by these investigations are described by Bub (1963).

Because we had two kinds of gauges, which of course had to be fitted one beside the other, the vertical and hori-

FIG. 49. Gauge developed to measure horizontal and vertical stresses.

zontal stresses could not be measured at the same point, which proved a disadvantage in evaluating these tests. The evaluation was made rather difficult by the inevitable discrepancies in the results and by the fact that the friction-measuring gauge gives the product of $F\mu$ and not single values of F and μ. Nevertheless, we did find that considerable shear forces were acting at the base.

This problem is of importance not only for the bearing capacity but also for the stress distribution in the footings and even in the subsoil—for example, as regards the concentration factor of Fröhlich. Therefore in 1964 we performed a new series of tests avoiding the main disadvantage of the earlier investigations with two kinds of gauges for the measurement of the vertical and horizontal stresses. For this purpose we had to develop a new gauge allowing the combined measurement of these stresses (Fig. 49). Such a gauge must be able to separate a three-dimension force into its three components and to determine the size of each component.

The construction and the workings of the gauge will now be briefly described (Fig. 50). The three-dimensional force F acts on the circular plate (1), the roughness of which can be suited to that of the base of the footing. Plate (1) is placed in the gauge so as to be completely movable; it is connected to a very thin measuring cylinder (2) which on the other end is fixed to a rigid plate (3). All this forms the inner system. This inner system is linked by a ball bearing (4) to the base plate (5) so that displacements of the inner system in the x–y planes are possible and only the vertical component F_z is carried through the measuring cylinder (2) from the plate (1) to the base plate (5).

Now we come to the second system, measuring the horizontal components of F. For this purpose four rectangular beams (6) arranged vertically and at 90° to one another are built in under pre-stress into the base plate (5). These four beams transmit the horizontal components F_x and F_y of F again by a ball-bearing system (7) which lies on four even planes directly behind plate (1). Thus movements of the inner system (3) in the z direction are possible and only the horizontal components of F (F_x and F_y) are transmitted by the four beams. That means that three components F_z, F_x, and F_y are measured independently.

For the measurement of the vertical and horizontal forces, strain gauges are fixed to the cylinder and the four beams. In the cylinder only vertical stresses can be measured in the usual way, whereas in the beams bending stresses are acting and are measured by strain gauges on both sides of the

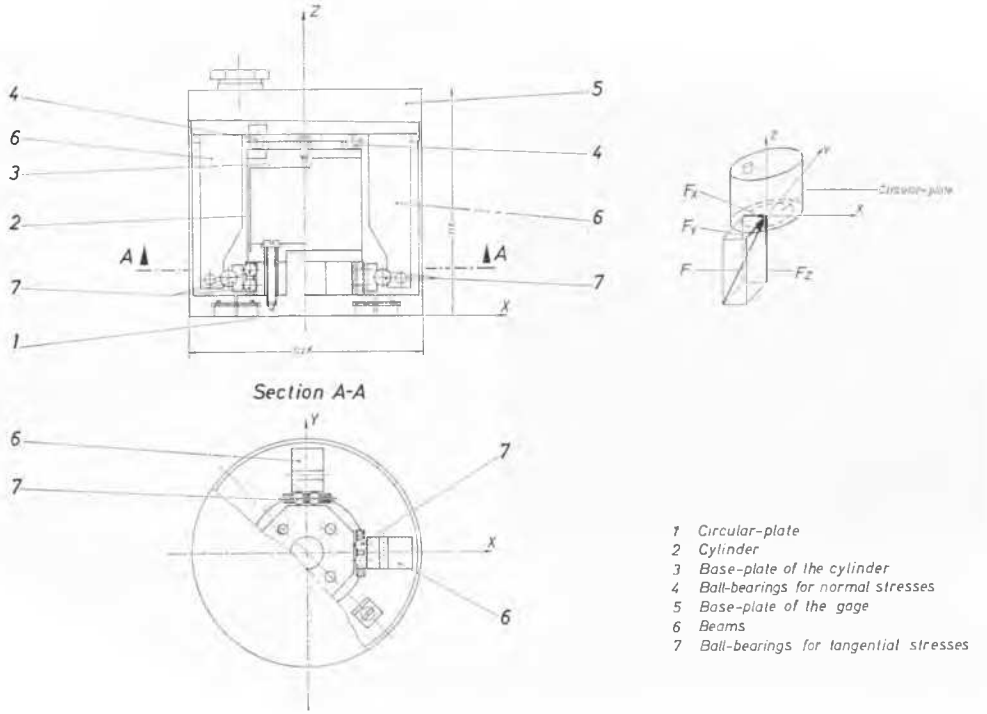

FIG. 50. Schematic details of interior of gauge.

beams. Fig. 51 shows the interior of the gauge, the inner cylinder and the four beams. After having calibrated the gauge under different conditions in a direct shear machine, four of these gauges were placed into the base of a footing 0.6 m wide and 1.2 m long (Fig. 52) and loading tests were performed with this footing in loose, medium dense, and dense sand (Fig. 53). The footing was either at the surface or 0.3 m deep in the three different fills and the water level was always at the surface to prevent any apparent cohesion in the sand. Thus the gauges were underwater during the investigations; they proved watertight for the two months which were needed for the performance of the tests.

FIG. 51. Photograph of interior of gauge.

I want to show you the result of one of these tests (Fig. 54). This test was carried out at the surface of the medium dense fill. The plot in the upper left corner gives the pressure-settlement curve for the first loading, the reloading, and the second reloading. Below this we see the normal stresses and on the right side of this the tangential stresses, both measured by the gauges at some characteristic loads.

FIG. 52. Location of gauges in base of footing.

The normal stresses under the first relatively low pressures are according to the theory of Boussinesq: that means the pressures in the middle part of the footing are smaller than in the outer parts. This distribution under higher loads changes over to a parabolic form and under the failure load we have a full, but unsymmetrical parabola, showing the lower pressure on the side where the failure occurred, which is quite understandable, because here the grains are moving and therefore unable to take over higher pressure.

The tangential stresses, for example the shear stresses, show an approximately uniform trend under all loads. They are always greater towards the outer regions of the footing and smaller towards the inner, which fits in with the displacement of the grains that takes place mainly near the edges of the footing where the slip surfaces are formed. The shear stresses were directed almost completely in the plus or minus x axis, particularly under higher loads.

By dividing the corresponding values of τ by σ the effective friction angles at the base can be calculated. They are given for the points A and D in the table in the right bottom corner of Fig. 54 and you can see that a much higher angle or a much higher friction is effective at the side where the failure took place; the angle ρ' is 25.4° here compared with 12.6° on the other side. Similar results were obtained in the

FIG. 53. Load test of footings in sand.

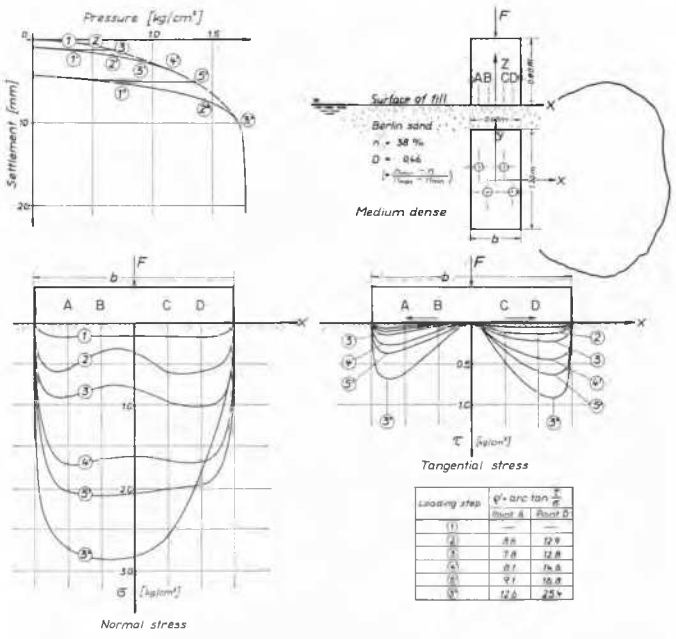

FIG. 54. Test results.

other tests, where the tangential stresses in the dense sand reached peak values of about 3 kg/sq.cm.

In the medium dense sand we can suppose an angle of internal friction of perhaps 37.5° or a coefficient of friction, μ, of 0.77. Comparing this value with the value $\mu' = \tan 25.4° = 0.47$ we can state that during failure the friction at the base of a footing, founded directly at the surface, amounts to about 0.6 of the possible maximum. This is a high value considering that a specially constructed and therefore rather smooth footing was used. Even higher values have to be expected when the concrete is poured directly into the soil, as is usually the case.

The effective friction and its maximum is not a constant value but depends on the foundation conditions, firstly on the embedding depth of the footing, and secondly on the density of the bearing stratum—that is on those factors which mainly determine failure and the corresponding soil movements.

With regard to the newly developed gauge it can be said that all four gauges worked well and have fulfilled all requirements. A larger number of gauges are now being used to measure the normal and tangential stresses around a subway tunnel to find out more about the effective friction forces here, which are important for the design of relatively thin-walled steel tubes.

H. Muhs (Germany)

In his paper to this conference *Milovič* (*3/30*) has considered the results of our large-scale loading tests, carried out in Berlin, and the bearing capacity factors, N, obtained in these tests. May I add some words about the determination of the factors N, providing that the failure loads themselves have been found experimentally. After some years of experiment, we disposed of quite a number of test results and were induced to try to determine the bearing capacity factors, N, according to the different failure loads of the different tests.

Doing this and using the general set-up of the bearing capacity formula we had to calculate six unknown factors, the three bearing capacity factors and the three shape factors. For this purpose we had too few test results. Therefore, the shape factors were introduced according to theory, or better, according to general practice, as the theory of this problem is very incomplete. The results of this investigation were published by Naujoks (1963) and the bearing capacity factors gained are known as those of Naujoks.

Evaluating the test results in this way the magnitude of the bearing capacity factors, N, is always influenced by the size of the shape factors, s, as the product of Ns always appears in the equations to be solved, which is not very satisfactory. Therefore we performed in the last two years a new series of 14 tests in order to try to find the shape factors experimentally; beyond this the tests were to yield the bearing capacity factors at a density which had not yet been investigated by us, that is in a medium dense sand of fine to medium size.

All tests were performed in a sand with a porosity of 38 per cent ± 0.5 per cent, so that the point resistance curves of soundings in this sand were well between the curves of the earlier tests in loose and dense sand. To eliminate the influence of apparent cohesion which had proved unfortunate in the evaluation of the earlier tests, all tests were carried out with the water level at the surface of the fill. In contrast to the earlier tests, where we always had the same area of footings, the new tests were performed on footings with constant width, that is 0.5 m, but with the length varying from 0.5 m to 1.0 m to 1.5 m to 2.0 m; thus the ratio m (i.e., length to width) was between 1 and 4.

FIG. 55. Set-up used for testing a footing considered as unlimited in length.

To approach more closely a strip of unlimited length another test was arranged (Fig. 55) with three different footings 1.0, 1.5, and 1.0 m long, one behind the other, so that the length of this footing was 3.5 m and the ratio, m, was 7. These footings were loaded independently by three hydraulic presses, directed by automatic loading equipment in such a manner that all three footings were sunk approximately in the same way. As the load on each footing was measured it was possible to get the failure load of a footing with the ratio $m = 7$, but beyond this—using the failure load of the middle footing alone—to investigate the bearing capacity conditions of a strip of nearly unlimited length, since this part can be regarded as being cut out of a strip footing. Theoretically, and following the evaluation of the load-settlement curve of the central footing, the conditions of this footing can be regarded as representative of a ratio $m = 13$.

When you are carrying out loading tests on the surface of a sand layer with the water level also at the surface, the depth and the cohesion in the bearing capacity formula are zero, and as the failure load, the dimensions of the footing, and the unit weight of the sand are known you obtain the product $N_\gamma s_\gamma$. In our case the product $N_\gamma s_\gamma$ for the different footings investigated depended on the ratio m. According to theoretical aspects, for $m = \infty$, a limiting value for $N_\gamma s_\gamma$ must be reached. It must be possible to determine this limiting value by mathematical means. On the other hand by definition it is known that for $m = \infty$ the value of $s_\gamma = 1$; thus the function $s_\gamma = f(m)$ can be calculated.

To use the same method for the determination of the product $N_q s_q$ or s_q itself, when s_γ is already known, you have only to perform the tests at a certain depth but not at the surface.

Following these considerations we performed all tests, first at the surface and then at a depth of 0.3 m. The plot of the failure loads over the ratio m for the tests at the surface (Fig. 56) shows that the bearing capacity increases with higher values of m and that it approaches a limiting value for $m \to \infty$ (although the difference between the lower values at $m \sim 1$–1 compared with those at $m > 10$ is rather small). The same plot for the tests done at a depth of 0.3 m (Fig. 57) shows that a limiting value is also reached, but

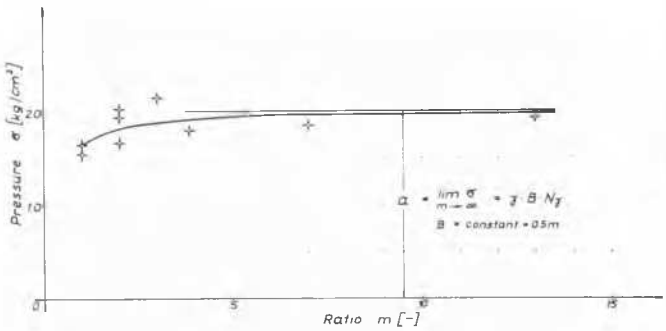

FIG. 56. Failure loads for footings on the surface of the sand.

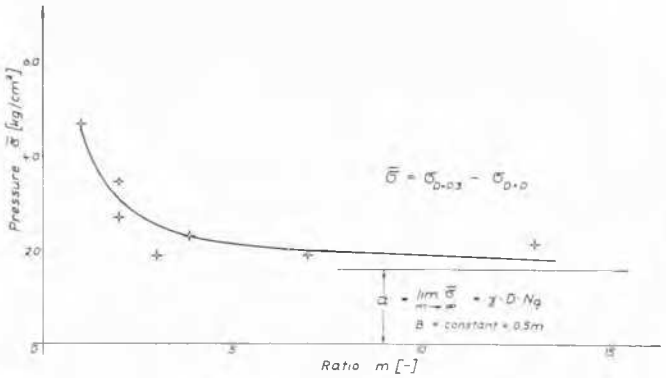

FIG. 57. Failure loads for footings embedded 0.3 m in the sand.

that the difference of the bearing capacity values between low and high m values is much greater. However, the most important fact is that the failure loads are here decreasing with increasing values of m, which means that the bearing capacity of compact footings is much higher than that of long slender footing, or generally speaking, of fundamental strips with the same width, provided that the footings are embedded into the bearing stratum. As it is a general rule not to found footings directly at the surface but at a certain depth, we can therefore conclude that the bearing capacity conditions of compact single footings are always better than those of strip footings with the same width.

You can recognize this fact immediately when you see the following photos which show the failure zones at the surface. From Fig. 58 you can see that where we have the long footing, with $m = 7$ or 13, a failure line practically parallel to the longer side of the footing exists; the same happens in the case of the same footing, when embedded in the sand. This can be taken as a proof for a practical two-dimensional state of stress in the middle part of the footing. Against that we already have the transition to a more three-dimensional state of stress around the rectangular footing with the ratio $m = 2$. In the case of the square footing (Fig. 59) it is obvious that a three-dimensional state of stress is

FIG. 58. Failure of long footing.

FIG. 59. Failure of square footing.

reached, which is the reason for the higher bearing capacity of the compact footing.

Now you will ask for the mathematical equation for the shape factor. We are still evaluating the tests, and therefore I cannot give you exact data. But it seems that the decrease of s_γ for compact footings with low m values is a little smaller, and the increase of s_q for the same conditions is much greater, than is normally assumed. I have to stress that these shape factors are different from those used by Naujoks for the evaluation of the older tests to determine the bearing capacity factors. Those factors have to be improved according to the new shape factors. We are doing this and hope to be able to present the final improved bearing capacity factors in the near future.

Y. NISHIDA (Japan)

In paper *3/7 da Costa Nunes et Porto* present an interesting example of the application of the compaction pile in practice. I presented a paper concerning this problem at the Paris Conference and I would like to ask the reason why they take the value of $4m$ for the pile space. According to my studies the zone of sands compacted by driving a pile can be estimated through the following equation, deduced from the stress and strain conditions in the ground,

$$\frac{E}{\gamma Z} = \frac{R^2}{a^2}\left[\frac{2(1 + m \sin \phi)}{m} K_0 - (1 - \sin \phi)\right] + \left[2K_0 - \frac{m(1 - \sin \phi)}{1 + m \sin \phi}\right] \times \left[\left\{\frac{1 + \sin \phi}{1 - \alpha} - \frac{m - 1}{2m}\right\}\frac{R^2}{a^2} - \left\{\frac{1 + \sin \phi}{1 - \alpha}\left(\frac{R}{a}\right)^{\alpha} - \frac{m - 1}{2m}\right\}\right]$$

where $\alpha = 2(1 + m \sin \phi)/m(1 + \sin \phi) + 2$ and ϕ is the angle of shear strength of the sand, $1/m$ is Poisson's ratio of the soil. K_0 is the coefficient of earth pressure at rest of the soil, and E is Young's modulus of the soil. According to my theoretical studies and experimental data, E can be estimated to be from 20 γZ to 170 γZ, where γZ is the vertical pressure in the ground, and is dependent on the void ratio. Based on some practical measurements, if we assume the values of $K_0 = 0.65$, $1/m = 0.25$, and $\phi = 30°$, then it follows that $R/a = 3.0 \sim 6.7$, where R is the radius of the compacted zone and a is the pile radius.

G. SANGLERAT (France)

Je désire simplement apporter un témoignage dans une question fort controversée à l'heure actuelle: la prévision des tassements à l'aide de la résistance à la pointe du pénétromètre statique. C'est avec un très grand intérêt que j'ai pris connaissance de la communication de *Bachelier et Parez (3/1)*. Ces auteurs ont généralisé la formule établie, il y a de nombreuses années, par Buismann (1940) pour les sables, au cas des argiles sous la forme: $E = (2{,}3/\alpha)\ R_p$ où R_p = résistance à la pointe et α = coefficient expérimental, ce qui correspond bien à la formule que j'ai proposée (Sanglerat, 1965): $m_v = 1/\alpha_0 R_p$.

Il est extrêmement intéressant de constater que les résultats de l'enquête statistique effectuée par ces auteurs dans la région parisienne, le nord de la France et la Belgique recoupent d'une manière très satisfaisante ceux que j'ai eu l'occasion de rassembler dans la région Rhône-Alpes (Sanglerat, 1965).

Certains s'étonnent des rapports trouvés entre le module de déformation E et la résistance à la pointe R_p du pénétromètre statique, mais, en génie civil, pour le béton armé, n'utilise-t-on pas, pour calculer les déformations, des modules d'élasticité du béton déduits de formules empiriques du genre $E = A\sqrt{\sigma}$ où A est une constante et σ la résistance à la rupture du béton? Pourquoi n'en serait-il pas de même dans chaque cas particulier pour différents types de sol d'une région donnée? Pour les sables, Buisman (1940) a montré, depuis fort longtemps, qu'il en était bien ainsi.

Signalons, par ailleurs, pour les milieux cohérents, que des essais ont mis en évidence que la cohésion apparente des argiles est proportionnelle au taux de consolidation (*Biarez, et al., 1/5*), lorsqu'il est compris entre 2 et 4 bars environ. D'autres essais ont montré que le module d'élasticité E de ces mêmes argiles est proportionnel au taux de consolidation (*Biarez, et al., 1/5;* Absi, 1965). Il en résulte que E et C sont proportionnels Ce résultat a d'ailleurs été également mentionné par Meyerhof (1953).

Comme la résistance statique à la pointe du pénétromètre R_p est directement proportionnelle à la cohésion, il est donc normal d'admettre, dans des limites données, l'essai au pénétromètre statique étant considéré comme un essai non drainé, que E et R_p peuvent être liés par une relation linéaire telle que définie ci-dessus.

Pour les milieux non cohérents, *Schultze and Melzer (2/47)* ont proposé une relation non linéaire. Il est d'ailleurs très intéressant de noter que différents géotechniciens, au Mozambique, aux U.S.A. and Afrique du Sud, en Allemagne et en Yougoslavie (Nonveiller, 1963) ont trouvé des résultats analogues à ceux de *Bachelier et Parez (3/1)*. En particulier Kantey (Afrique du Sud) a étudié les relations pouvant exister entre m_v et la résistance à la pénétration dans différents types de sols.

Devant les difficultés soulevées par la prévision des tassements, soulignées à juste titre à différentes reprises au cours du présent Congrès par de nombreux participants, il serait vivement souhaitable de poursuivre dans le plus grand nombre de pays possible, les études statistiques comparatives entre R_p et m_v ou E.

Nous n'avons, en effet, pas le droit de laisser échapper une possibilité de prévisions de tassements, peut-être grossière et approximative, mais rapide et très économique, qui peut rendre de très grands services dans les problèmes quotidiens de fondations des ouvrages courants.

RÉFÉRENCES

ABSI, E. (1965). Rhéologie des argiles. *Annales I.T.B.T.P.*, No. 213, Paris, sept.

BUISMANN, A. S. K. (1940). *Grondmechanica*. Delft.

MEYERHOF, G. G. (1953). Some recent foundation research and its application to design. *Structural Engineer*, Vol. 31, No. 6.

NONVEILLER, E. (1963). Setzungen in rolligen (körnigen) Böden, Beobachtungen und Vergleich mit der Vorhersage. *Deuxième Congrès Européen de Mécanique des Sols* (Weisbaden).

SANGLERAT, G. (1965). *Le pénétromètre et la reconnaissance des sols*. Paris, Dunod.

I. A. SIMIVOOLIDI (U.S.S.R.)

This article concerns the method for calculating a beam, L in length, with a step change in moment of inertia at arbitrary cross-sections (see Fig. 60).

Imagine that you cut the beam at the location of the inertia moment change. As a result we have two beams of definite length and constant cross-section, each of which is subjected to outer loads, unknown moments, cross-force Y_c, and bending moment M_c. For convenience in solving this problem the foundation under the beam is assumed to be a continuous flexible medium, but it is calculated for each beam independently. For determining the ground deformation under each beam the equation of the plane deformation is applied. Each of the two beams is considered to be a thin resilient bar deforming along its length.

The reactions of the foundation are in the form of algebraic functions of the third order.

$$r_x^{(n)} = a_0^{(n)} + \frac{2a_1^{(n)}}{L_n}\left(x_n - \frac{L_n}{2}\right) + \frac{4a_2^{(n)}}{L_n^2}\left(x_n - \frac{L_n}{2}\right)^2 + \frac{8a_3^{(n)}}{L_n^3}\left(x_n - \frac{L_n}{2}\right)^3, \quad (1)$$

where

$$a_0^{(n)}, a_1^{(n)}, a_2^{(n)}, a_3^{(n)}$$

are unknown parameters.

To find these unknowns a differential equation and an equation of the ground surface deformation are composed for each beam, the beginning of the co-ordinates for the first beam is on its left side, for the second on its right side.

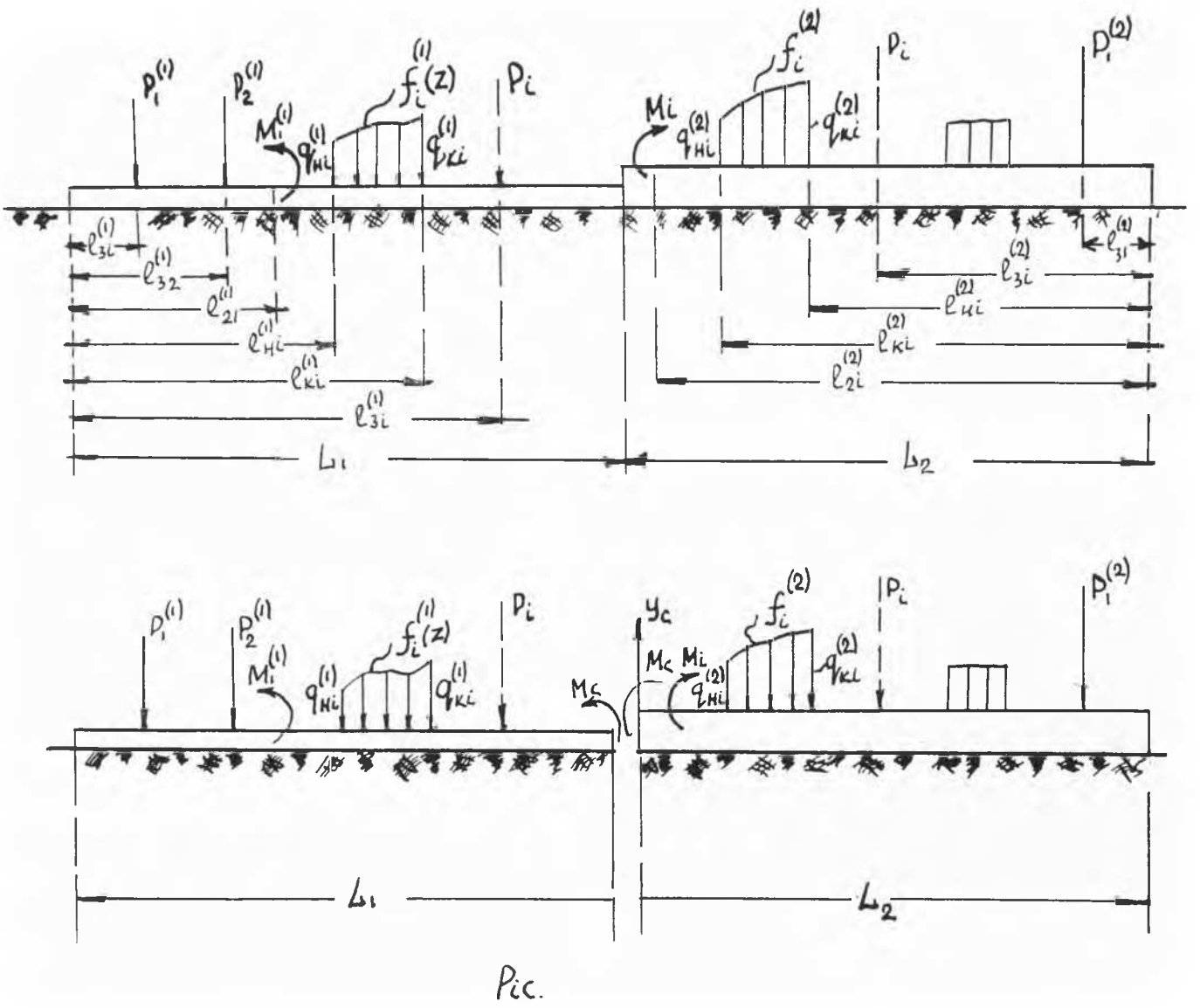

FIG. 60. Foundation beam of variable cross-section.

After quadruple integration of each of the differential equations we obtain in each of them eight unknowns. In order to determine these unknowns as well as the equations of equilibrium and boundary conditions it is necessary that:

$$Y_{x_n=0} = v_{x=0};\ Y_x = \frac{L_n}{2} = v_x = \frac{L_n}{2};$$

$$\int_0^{Ln} Y_n dx_n = \int_0^{Ln} v_n dx_n;\ \frac{d^3 Y_n}{dx_n^3} = \frac{d^3 v_n}{dx_n^3}$$

where Y_n = vertical displacement of the neutral axis of the beam, and v_n = vertical displacement of the deformed ground surface. Besides the above mentioned conditions the following requirements are to be met: (1) equality of deflections of both beams at the place of cut; (2) equality of the inclination of the tangents at the point of cut. As a result we obtain the following equations:

$$\left.\begin{aligned} \delta_{15} Y_c + \delta_{16} M_c &= \delta_1 p \\ \delta_{25} Y_c + \delta_{26} M_c &= \delta_2 p \end{aligned}\right\}, \tag{2}$$

where

$$\delta_{15} = (m_{11} + m_{13}) + \eta(m_{21} + m_{23}), \tag{3}$$

$$\delta_{16} = [(\tfrac{1}{48} m_{22} + 2m_{23} + m_{24} + \tfrac{1}{8} m_{25})\ \eta/L_2 - (\tfrac{1}{48} m_{12} + 2m_{13} + m_{14} + \tfrac{1}{8} m_{15})\ 1/L_1], \tag{4}$$

$$\delta_{25} = (d_{11} + d_{13}) - \lambda(d_{21} + d_{23}), \tag{5}$$

$$\delta_{26} = -[(d_{12}/48 + d_{13} + d_{14} + \tfrac{11}{24} d_{15})\ 1/L_1 + (d_{22}/48 + 2d_{23} + d_{24} + \tfrac{11}{24} d_{15})\ 1/L_2], \tag{6}$$

$$\delta_1 p = \eta S^{(2)} - S^{(1)}, \tag{7}$$

$$\delta_2 p = -[U^{(1)} + \lambda U^{(2)}], \tag{8}$$

$$S^{(n)} = [m_{n1}A^{(n)} + m_{n2}B^{(n)} + m_{n3}(2C^{(n)} - A^{(n)})] + m_{n4}N^{(n)} + m_{n5}\left\{\frac{1}{L_n^4}\left[\sum \int_{l_{H1}^{(n)}}^{L_n} f^{(n)}(z)\frac{(L_n - z)^3}{3!}dz - \sum \int_{l_{K1}^{(n)}}^{L_n} f^{(n)}(z)\frac{(L_n - z)^3}{3!}dz + \sum M_1^{(n)}\frac{(L_n - l_{21}^{(n)})^2}{2!} + \sum P_1^{(n)}\frac{(L_n - l_{31}^{(n)})^3}{3!}\right] + \frac{K^{(n)}}{8L_n} - 2W^{(n)}\right\}, \quad (9)$$

$$U^{(n)} = [dn_1A^{(n)} + dn_2B^{(n)} + dn_3(2C^{(n)} - A^{(n)}) + dn_4N^{(n)} + dn_5\phi^{(n)}L]b_nL_n, \quad (10)$$

$$\phi^{(n)}L = \left\{\frac{1}{L_n^4}\left[\sum \int_{l_{H1}^{(n)}}^{L_n} f^{(n)}(z)\frac{(L_n - z)^2}{2!}dz - \sum \int_{l_{K1}^{(n)}}^{L_n} f^{(n)}(z)\frac{(L_n - z)^2}{2!}dz + \sum M_1^{(n)}(L_n - l_{21}^{(n)}) + \sum P_1^{(n)}\frac{(L_n - l_{31}^{(n)})^3}{3!}\right] + \frac{11}{24L_n}K^{(n)} - 2W^{(n)}\right\}, \quad (11)$$

$$A^{(n)} = \frac{1}{L_n}\left\{\sum \int_{l_{H1}^{(n)}}^{L_n} f^{(n)}(z_n)dz_n - \sum \int_{l_{K1}^{(n)}}^{L_n} f^{(n)}(z_n)dz_n + \sum P_1^{(n)}\right\}, \quad (12)$$

$$C^{(n)} = \frac{1}{L_n^2}\left\{\sum \int_{l_{H1}^{(n)}}^{L_n} f^{(n)}(z_n)dz_n - \sum \int_{l_{K1}^{(n)}}^{L_n} f^{(n)}(z_n)dz_n + \sum P_1^{(n)}l_{31}^{(n)} - \sum M_1^{(n)}\right\}, \quad (13)$$

$$K^{(n)} = -\frac{1}{L_n}\left\{\sum \int_{l_{H1}^{(n)}}^{L_n} f^{(n)}(z_n)(L_n - z_n)dz_n - \sum \int_{l_{K1}^{(n)}}^{L_n} f^{(n)}(z_n)(L_n - z_n)dz_n + \sum M_1^{(n)} + \sum P_1^{(n)}(L_n - l_{31}^{(n)})\right\}, \quad (14)$$

$$N^{(n)} = \frac{1}{L_n}\left\{\sum \Gamma_0^{\frac{L_n}{2}} \int_{l_{H1}^{(n)}}^{\frac{L_n}{2}} f^{(n)}(z_n)dz_n - \sum \Gamma_0^{\frac{L_n}{2}} \int_{l_{K1}^{(n)}}^{\frac{L_n}{2}} f^{(n)}(z_n)dz_n + \sum \Gamma_0^{\frac{L_n}{2}} P_1^{(n)} + K^{(n)}\right\}, \quad (15)$$

$$B^{(n)} = \frac{1}{L_n^5}\left\{\sum \int_{l_{H1}^{(n)}}^{L_n} f^{(n)}(z_n)\frac{(L_n - z_n)^4}{4!}dz - \sum \int_{l_{K1}^{(n)}}^{L_n} f^{(n)}(z_n)\frac{(L_n - z_n)^4}{4!}dz + \sum M_1^{(n)}\frac{(L_n - l_{21}^{(n)})^3}{3!} + \sum P_1^{(n)}\frac{(L_n - l_{31}^{(n)})^4}{4!} + \frac{L_n^4}{48}K^{(n)} - W^{(n)}L_n^5\right\}, \quad (16)$$

$$W^{(n)} = \frac{1}{L_n^4}\left\{\sum \Gamma_0^{\frac{L_n}{2}} \int_{l_{H1}^{(n)}}^{\frac{L_n}{2}} f^{(n)}(z_n)\frac{(\frac{L_n}{2} - z_n)^3}{3!}dz_n - \sum \Gamma_0^{\frac{L_n}{2}} \int_{l_{K1}^{(n)}}^{\frac{L_n}{2}} f^{(n)}(z_n)\frac{(L_n - z_n)^3}{3!}dz_n + \sum \Gamma_0^{\frac{L_n}{2}} M_1^{(n)}\frac{(\frac{L_n}{2} - l_{21}^{(n)})^2}{2!} + \sum \Gamma_0^{\frac{L_n}{2}} P_1\frac{(\frac{L_n}{2} - l_{31}^{(n)})^3}{3!}\right\}, \quad (17)$$

$$\eta = \frac{b_1\rho_1}{b_2\rho_2}\frac{E_{01}}{E_{02}}, \quad (18)$$

$$\lambda = \frac{b_1L_1\rho_1}{b_2L_2\rho_2}\frac{E_{01}}{E_{02}}, \quad (19)$$

$$\rho_n = (2.048 + 0.001\alpha_n)(13.44 + 0.029\alpha_n), \quad (20)$$

$$m_{n1} = (665.644 + 4.796\alpha_n + 0.001344\alpha_n^2) \times (2.048 + 0.001\alpha_n), \quad (21)$$

$$m_{n2} = -(2167.6 + 6.209\alpha_n)(2.048 + 0.001\alpha_n)\alpha_n, \quad (22)$$

$$m_{n3} = (516.096 + 0.296\alpha_n)(13.44 + 0.029\alpha_n), \quad (23)$$

$$m_{n4} = 0.215(13.44 + 0.029\alpha_n)\alpha_n(2.89 + 0.00624\alpha_n)\alpha_n, \quad (24)$$

$$m_{n5} = 40.32(13.44 + 0.029\alpha_n)(2.049 + 0.001\alpha_n)\alpha_n, \quad (25)$$

$$d_{n1} = (665.644 + 23.89\alpha_n) + 0.007\alpha^2{}_n) \times (2.048 + 0.001\alpha_n), \quad (26)$$

$$d_{n2} = -(2167.6 + 15.24\alpha_n)(2.048 + 0.001\alpha_n)\alpha_n, \quad (27)$$

$$d_{n3} = (516.096 + 0.91\alpha_n + 0.000144\alpha^2{}_n) \times (13.44 + 0.029\alpha_n), \quad (28)$$

$$d_{n4} = (0.215 - 0.0077\alpha_n)(13.44 + 0.029\alpha_n)\alpha_n, \quad (29)$$

$$d_{n5} = 40.32(2.048 + 0.001\alpha_n)(13.44 + 0.029\alpha_n)\alpha_n, \quad (30)$$

$$\alpha = \frac{1 - \mu_n^2}{1 - \mu_{on}^2}\frac{\pi E_{on}b_nL_n^3}{E_nT_n}. \quad (31)$$

Everywhere for the first beam $n = 1$, and for the second beam $n = 2$, where b_n = width of the beam, L_n = length of the beam, E_{on} = deformation modulus of the soil under the beam, μ_{on} = Poisson's coefficient for the soil under the beam, μ_n = Poisson's coefficient for the material of the

beam, E_nT_n = rigidity of the beam, α_n = flexibility index, $\Gamma_0^{Ln/2}$ = bilateral disconnector by Gersevanov (1933, 1934).

After solving Eq (2) with regard to Y_c and M_c each beam is then calculated as an independent beam with a definite length and constant cross-section, resting on a flexible foundation and subjected to force Y_c and M_c as well as external loads.

Eq (2) enable one to calculate a great variety of engineering construction problems, resting on the foundation of non-variable cross-section as well as articulated beams. Let us consider a particular case, when two articulated foundation beams are to be calculated. For this it is necessary first to determine an unknown cross-force arising at the point of articulation and after that to calculate each beam separately. For this purpose it is sufficient to equate M_c to zero in the first equation of Eqs (2). Then $Y_c = \delta_1 p/\delta_{15}$.

REFERENCES

GERSEVANOV, N. M. (1933, 1934). *Functional disconnectors and their application in structural mechanics.*

SIMIVOOLIDI, I. A. (1964). Calculation of the beam of variable cross-section resting on a continuous flexible foundation. *Construction and Architecture*, Vol. 9.

A. S. STROGANOV (U.S.S.R.)

The experimental investigations of the soil properties at the complicated stress state, and the bearing capacity investigations of foundations on sand (Stroganov, in press; Stroganov, 1958), show that soils in the main are subordinated to the plastic condition of Huber and Schleicher (Schleicher, 1925) which can be expressed as:

$$\sigma_1 = (\mathrm{H} + \sigma)\tan\psi, \tag{1}$$

where σ_1 = intensity of shear stresses; H = hydrostatic pressure, equivalent to cohesion c and equal to $c/\tan\psi$, σ = mean normal stress; $\tan\psi$ = coefficient of friction on the octahedral area. It is found experimentally (Stroganov, 1958; Stroganov, 1965) that soils have a new form of plastic potential

$$\theta \equiv \sigma_1 - (\mathrm{H} + \sigma)\nu = 0, \tag{2}$$

where ν = is coefficient of dilatation and considerably less ($\nu \ll \tan\psi$) than when it is in the plastic potential of Drucker and Prager (1952).

The relationship between the components of the stresses and the strain velocities resulting from Eqs (1) and (2) and from the equation of incompressibility conditions and the deviator ratio (Stroganov, 1963), is expressed as follows:

$$\begin{aligned} \sigma_x - \sigma &= 2(H + \sigma)\tan\psi[(\xi_x + \tfrac{1}{3}\nu\xi_1)/\xi_1], \\ \tau_{xy} &= (H + \sigma)\tan\psi(\eta_{xy}/\xi_1), \text{ etc.} \end{aligned} \tag{13}$$

This relationship is the basic mechanical equation of the state of a dilating soil medium which, when $\nu = \tan\psi$, becomes the well-known equation of Drucker and Prager (1952).

Let us consider only the plane plastic flow problem of a non-dilating ($\nu = 0$) medium for which Eq (3) becomes:

$$\left.\begin{aligned} \sigma_x - \sigma &= 2(H + \sigma)\tan\psi(\xi_x/\xi_1) \\ \sigma_y - \sigma &= 2(H + \sigma)\tan\psi(\xi_y/\xi_1) \\ \tau_{xy} &= (H + \sigma)\tan\psi(\eta_{xy}/\xi_1) \end{aligned}\right\} \tag{4}$$

obtained earlier by other means (Stroganov, 1961). The incompressibility condition of the medium,

$$\xi_x + \xi_y = 0, \tag{5}$$

is identically satisfied if the function of flow $\phi(x, y)$ is introduced by means of the relationship:

$$v_x = \partial\phi/\partial y, \qquad v_y = -\partial\phi/\partial x. \tag{6}$$

By substitution of the strain velocity components and their intensity in Eq (4), and taking into account Eq (6), we obtain the following relations,

$$\left.\begin{aligned} \sigma_x, \sigma_y &= (H + \sigma)(1 \pm \tan\psi\cos 2\chi) - H, \\ \tau_{xy} &= (H + \sigma)\tan\psi\sin 2\chi, \end{aligned}\right\} \tag{7}$$

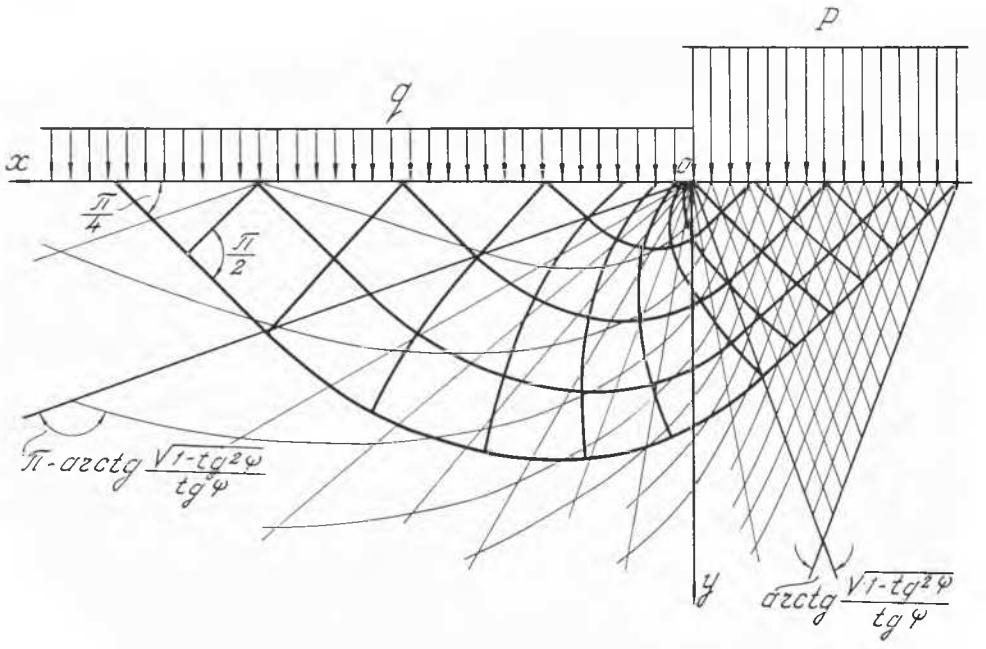

FIG. 61. Velocity and stress field of a loaded foundation.

where the new function $\chi(x, y)$ is introduced by means of the relationship:

$$\left.\begin{aligned}\sin 2\chi &= \frac{\eta_{xy}}{\xi_1} \\ &= \frac{\frac{\partial^2\phi}{\partial y^2} - \frac{\partial^2\phi}{\partial x^2}}{\sqrt{\left(2\frac{\partial^2\phi}{\partial x\partial y}\right)^2 + \left(\frac{\partial^2\phi}{\partial y^2} - \frac{\partial^2\phi}{\partial x^2}\right)^2}} \\ \cos 2\chi &= \frac{2\xi_x}{\xi_1} = -\frac{2\xi_y}{\xi_1} \\ &= \frac{2\frac{\partial^2\phi}{\partial x\partial y}}{\sqrt{\left(2\frac{\partial^2\phi}{\partial x\partial y}\right)^2 + \left(\frac{\partial^2\phi}{\partial y^2} - \frac{\partial^2\phi}{\partial x^2}\right)^2}}.\end{aligned}\right\} \quad (8)$$

By introducing the expressions of the stress components, Eq (7), identically satisfying the plastic condition, Eq (1), in the equilibrium equations,

$$\frac{\partial\sigma_x}{\partial x} + \frac{\partial\tau_{xy}}{\partial y} = 0,$$

and

$$\frac{\partial\tau_{xy}}{\partial x} + \frac{\partial\sigma_y}{\partial y} = \gamma, \quad (9)$$

the basic system of the hyperbolic type equations is obtained:

$$\left.\begin{aligned}&(\cot\psi + \cos 2\chi)\partial\sigma/\partial x + \sin 2\chi(\partial\sigma/\partial y) \\ &\quad - 2(H + \sigma)[\sin 2\chi(\partial\chi/\partial x) \\ &\quad - \cos 2\chi(\partial\chi/\partial y] = 0, \\ &\sin 2\chi(\partial\sigma/\partial x) + (\cot\psi - \cos 2\chi(\partial\sigma/\partial y) \\ &\quad + 2(H + \sigma)[\cos 2\chi(\partial\chi/\partial x) \\ &\quad + \sin 2\chi(\partial\chi/\partial y)] = \gamma\cot\psi,\end{aligned}\right\} \quad (10)$$

given earlier in some different form (Stroganov, 1961). Using the usual method of determination, we obtain for system (10) a system of differential equations of stress field characteristics:

$$\left.\begin{aligned}&dy = [\sin 2\chi \mp \sqrt{(1 - \tan^2\psi)}/(\tan\psi \\ &\quad + \cos 2\chi)]dx, \\ &d\sigma \mp 2(H + \sigma)[\tan\psi/\sqrt{(1 - \tan^2\psi)}]dx \\ &\quad = \gamma\{dy \mp [\tan\psi/\sqrt{(1 - \tan^2\psi)}]dx\}.\end{aligned}\right\} \quad (11)$$

When $\tan\psi = 0$ an Eq (10) becomes the known equations of Moris Levy, for which the equations of characteristics are well-known in the theory of an ideal plastic medium:

$$\left.\begin{aligned}dy &= [(\sin 2\chi \mp 1)/\cos 2\chi]dx \\ d\sigma \mp 2cd\chi &= \gamma dy.\end{aligned}\right\} \quad (12)$$

When $\tan\psi = \sin\rho$ and ρ is a reduced angle of internal friction under conditions of plane plastic deformation (Stroganov, 1965) Eq (10) and (11) formally become the known equations of soil plasticity theory. Hence, all known mathematical methods of the boundary problem solution for the equations of soil plasticity theory based on the Rankine-Prandtl (Coulomb) hypothesis can be used to obtain Eq (10) in the determination of the stress field.

The principal axis direction of strain velocities is determined by Eq (8), which gives the linear differential equation of hyperbolic type:

$$2(\partial^2\phi/\partial x\partial y)\tan 2\chi - (\partial^2\phi/\partial y^2 - \partial^2\phi/\partial x^2) = 0. \quad (13)$$

Equation (13) is the one of Mises. In this equation, $\chi(x, y)$ is the angle of slope to the x axis of maximum main normal stress, and consequently to that of maximum main normal strain velocity. Eq (13) is equivalent to the system of two linear first-order equations

$$\left.\begin{aligned}&\partial v_x/\partial x + \partial v_y/\partial y = 0, \\ &(\partial v_x/\partial x - \partial v_y/\partial y)\tan 2\chi - (\partial v_x/\partial y \\ &\quad + \partial v_y/\partial x) = 0,\end{aligned}\right\} \quad (14)$$

directly following from incompressibility condition (5) and from Eq (13) after reverse replacement of the flow function $\phi(x, y)$ by the velocity displacement components.

From this system of differential equations, first and second characteristic systems of velocity field are obtained,

$$dy/dx = (\sin 2\chi \mp 1)/\cos 2\chi = \tan(\chi \mp \tfrac{1}{4}\pi), \quad (15)$$

which are not identical with characteristics (11) of the stress field and are the equations of maximum shear strain velocity lines, along which, as is known, the normal strain velocity is equal to zero.

A consequence of the latter is the continuous relationship along characteristics (15) of the velocity field,

$$\left.\begin{aligned}du - vd\chi &= 0\text{—along first system,} \\ dv + ud\chi &= 0\text{—along second system,}\end{aligned}\right\} \quad (16)$$

given in the theory of an ideal plastic medium by Heiringer.

Characteristics of stress (12) and velocity (15) fields are identical in a particular case of a medium without ($\tan\psi = 0$) friction, as they are in the theory of an ideal plastic medium. Hence, the problem of determining displacement velocity is to construct velocity field characteristics (15), on the basis of preliminary solution of the stress problem (11), and then the solution of a boundary problem for equations (16) by means of well known methods. It is clear that the complete solution of the problem must satisfy the joint conditions of stress and displacement velocity fields.

The problem of Prandtl and Reisner for the weightless soil medium can illustrate the results obtained. The bearing capacity of soil for given boundary conditions (Fig. 61) may be found in the following form,

$$H + p = (H + q)[(1 + \tan\psi)/(1 - \tan\psi)] \exp[\pi\tan\psi/\sqrt{(1 - \tan^2\psi)}], \quad (17)$$

obtained by means of known methods based on the use of plasticity integrals of Eq (10) for a weightless medium. The characteristic system of the velocity field (Fig. 61, thick lines) in the soil, constructed by integrating Eq (15), and known data of the characteristic system of stress field (Fig. 61, thin lines), shows that a region of plastic flow is considerably less than the one obtained by Shield's solution.

In conclusion, it is necessary to say that the application of conditions (1) and (2) to plane plastic flow problems leads, as is shown by our investigations (Stroganov, in press; Stroganov, 1958), to considerable increase of the theoretical bearing capacity of soils and

to a quantitative agreement between theoretical and experimental data.

REFERENCES

DRUCKER, D., and W. PRAGER (1952). Soil mechanics and plastic analyses on limit design. *Quarterly Applied Mathematics*, Vol. 10, No. 2.

SCHLEICHER, F. (1925). Die energiengrenze der elastizität (Plastizitätsbedinung), *Zeits. fur ang. Math. Mech.*, Vol. 5, p. 478.

STROGANOV, A. S. (1958). Plane plastic deformation of soil. *Proc. Brussels Conference on Earth Pressure Problems*, Vol. 1, pp. 94–103.

——— (1961). Visco-plastic flow of soils. *Proc. Fifth International Conference on Soil Mechanics and Foundation Engineering*, Vol. 2, pp. 721–25.

——— (1963). *Methods of combined calculation of shaft bindings and ground pressures when grounds and materials have non-linear visco-elastic properties.* Collection on Ground Pressure and Binding of Vertical Shafts. Moscow, Gosgortechisdat (in Russian).

——— (1965). Analysis of plane plastic deformation of soil *Engineering J.* Vol. 3, Academy of Sciences, U.S.S.R. (in Russian).

——— (in press). Experimental investigations of plastic flow conditions and some problems of limit equilibrium theory of soil medium. *Engineering J.*, Academy of Sciences, U.S.S.R. (in Russian).

A. S. STROGANOV (U.S.S.R.)

Additional investigations into the strength parameter problem of soil in the condition of plane deformation arose in soil mechanics because of the quantitative divergence between experimental and theoretical data.

Experimental investigations of the plastic properties of dense (γ_0 = 1.71 tons/cu.m.) Liubercy sand at the two-stress state show (Fig. 62) that the relationship (continuous line) between the intensity of shear stresses σ_1 and the mean normal stress σ is practically independent of the kind of the stress state, and, as can be seen, follows a linear law well. At the same time the results of torsion tests on the tube samples show a break in the relationship (dotted line) at confining hydrostatic pressures exceeding approximately 4 kg/sq.cm. This effect takes place because the sample wall loses its plastic stability. As a result, a characteristic spiral neck is formed which did not form in a compact sample at the same test conditions. The failure of some investigations (Barshevscy, 1956) carried out earlier perhaps may be explained by this fact.

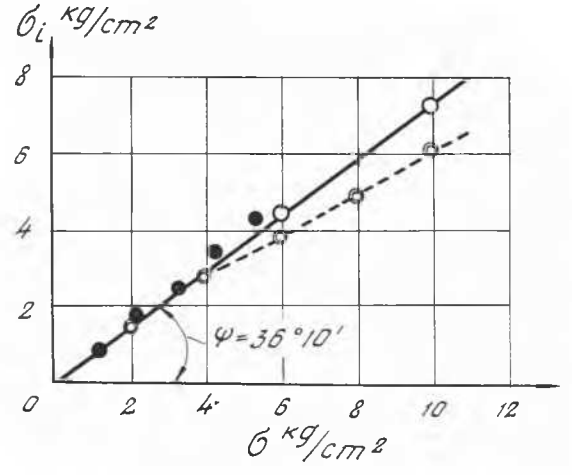

FIG. 62. Stress relationships of sand under stress and torsion.

Hence, on the basis of the experimental results and results obtained earlier by the author it is possible to suppose that investigated soils in the main follow the plastic condition of Huber and Schleicher (Schleicher, 1925) which can be expressed as

$$\sigma_1 = (H + \sigma)\tan\psi, \tag{1}$$

where σ_1 = intensity of shear stresses, σ = mean normal stress, $\tan\psi$ = coefficient of friction on the octahedral area, H = hydrostatic pressure, equivalent to cohesion c and equal to $c/\tan\psi$. It is known that condition (1) is not dependent on the kind of stress state.

The plastic condition of Rankine-Prandtl (Coulomb) can be expressed as:

$$(\sigma_1 - \sigma_3)/(\sigma_1 + \sigma_3 + 2H) = \sin\varphi, \tag{2}$$

where φ = angle of internal friction on sliding area. It is known that condition (2) depends on the kind of stress state.

Let us write the main normal stresses by trigonometrical form:

$$\begin{aligned} \sigma_1 - \sigma &= (2/\sqrt{3})\sigma_1\cos(w - \tfrac{1}{3}\pi), \\ \sigma_2 - \sigma &= (2/\sqrt{3})\sigma_1\cos(w + \tfrac{1}{3}\pi), \\ \sigma_3 - \sigma &= -(2/\sqrt{3})\sigma_1\cos w, \end{aligned} \tag{3}$$

where $\tan w = \sqrt{3}[(\sigma_1 - \sigma_2)/(\sigma_1 + \sigma_2 - 2\sigma_3)]$ = tangent of the angle of stress state kind.

Let us consider the three characteristic kinds of stress state corresponding to the methods of test: axial "tension" ($w = 0$), pure shear ($w = \frac{1}{6}\pi$), and axial compression ($w = \frac{1}{3}\pi$) at the all-round hydrostatic pressures. Moreover, we can assume that the soil follows condition (1) and the reduced stresses are expressed as follows:

$$\begin{aligned} \bar{\sigma}_1 &= H + \sigma_1 \\ \bar{\sigma}_2 &= H + \sigma_2 \\ \bar{\sigma}_3 &= H + \sigma_3 \\ \bar{\sigma} &= H + \sigma \\ \bar{\sigma}_1 &= \sigma_1. \end{aligned} \tag{4}$$

By successive substitution in Eq (3), of the assumed values of w and condition (1), taking into account (4), and by substitution of the obtained quantity of the main normal stresses in condition (2), the following relationships can be obtained.

When $w = 0$ and $w = \frac{1}{3}\pi$,

$$\tan\psi = (2/\sqrt{3'})[(\sin\varphi/(1 \pm \sin\varphi)] \tag{5) and (7}$$

When $w = \frac{1}{6}\pi$,

$$\tan\psi = \sin\varphi. \tag{6}$$

Now let us introduce the concept of the coefficient of lateral pressure at the plane of plastic deformation of the soil by means of the ratio:

$$\bar{\sigma}_2 = \xi(\bar{\sigma}_1 + \bar{\sigma}_3). \tag{8}$$

Substituting (8) in condition (1) we obtain a corresponding equation which is solved by combination with the ratio

$$(\bar{\sigma}_1 - \bar{\sigma}_3)/(\bar{\sigma}_1 + \bar{\sigma}_3) = \sin\rho, \tag{9}$$

by the exclusion of $\lambda = \bar{\sigma}_1/\bar{\sigma}_3$. Then we get the final expression for the reduced angle of internal friction ρ in the plane plastic deformation condition:

$$\sin\rho = (2/\sqrt{3})\sqrt{[\tfrac{1}{3}(1 + \xi)^2\tan^2\psi + \xi(1 - \xi) - \tfrac{1}{4}]}. \tag{10}$$

In determining ξ, the relationship between the main normal stresses and the deformation velocities (Stroganov, 1961 and 1963) can be used as follows:

$$\left.\begin{aligned} \xi_1 + \tfrac{1}{3}\nu\xi_1 &= (\xi_1/2\bar{\sigma}\tan\psi)(\bar{\sigma}_1 - \bar{\sigma}), \\ \xi_2 + \tfrac{1}{3}\nu\xi_1 &= (\xi_1/2\bar{\sigma}\tan\psi)(\bar{\sigma}_2 - \bar{\sigma}), \\ \xi_3 + \tfrac{1}{3}\nu\xi_1 &= (\xi_1/2\bar{\sigma}\tan\psi)(\bar{\sigma}_3 - \bar{\sigma}). \end{aligned}\right\} \quad (11)$$

The velocity of dilatation is introduced in this equation by means of the experimental ratio

$$\xi = -\nu\xi_1, \quad (12)$$

where ν = coefficient of dilatation of soil. Assuming $\xi_2 = 0$ in system (11) for the case of plane deformation, we get the ratio

$$\bar{\sigma}_2 = [(3 + 2\nu\tan\psi)/(\sigma - 2\nu\tan\psi)](\bar{\sigma}_1 + \bar{\sigma}_3), \quad (13)$$

obtained earlier (Stroganov, 1958) in a different manner. Introducing into (10) the value of lateral pressure obtained from (13), we get finally the basic ratio

$$\sin\rho = [\sqrt{(1 - \tfrac{1}{3}\nu^2)}/(1 - \tfrac{1}{3}\nu\tan\psi)]\tan\psi, \quad (14)$$

given earlier (Stroganov, 1958).

The reduced value of cohesion at plane deformation can be obtained using the formula

$$K = H\tan\rho. \quad (15)$$

Substituting relations (5), (6), and (7) in (14), we get, for axial tension and axial compression tests,

$$\sin\rho = \frac{2}{\sqrt{3}} \frac{\sqrt{1 - \frac{1}{3}\nu^2}}{1 \pm \frac{1}{3}\left(1 \mp \frac{2}{\sqrt{3}}\nu\right)\sin\varphi}\sin\varphi, \quad (16)$$

and

$$\quad (18)$$

and for pure shear test

$$\sin\rho = [\sqrt{(1 - \tfrac{1}{3}\nu^2)}/(1 - \tfrac{1}{3}\gamma\sin\varphi)]\sin\varphi. \quad (17)$$

The curves corresponding to the incompressibility ($\nu = 0$) of the soil are shown in Fig. 63. The dilatation

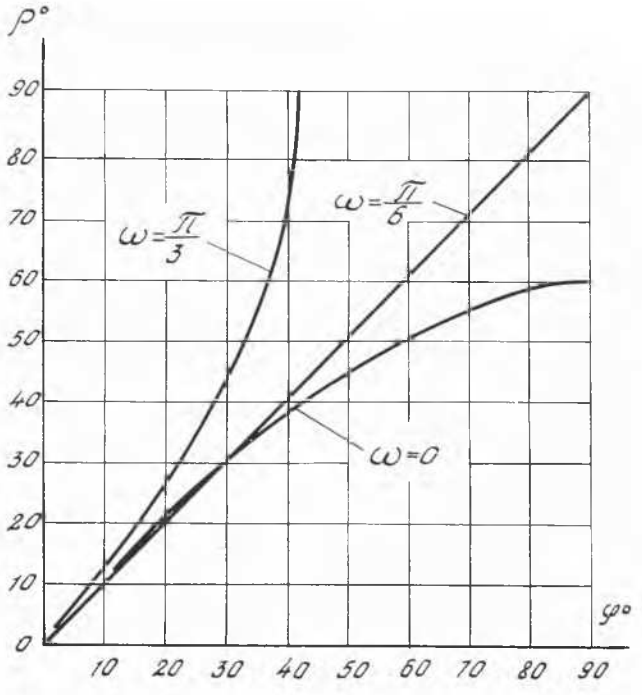

FIG. 63. Curves of incompressibility of the soil.

of soil ($\nu \neq 0$) leads to an increase in the reduced angles of internal friction. Eq (11) is obtained as a consequence of the new form of plastic potential:

$$\theta \equiv \sigma_1 - (H + \sigma)\nu = 0. \quad (19)$$

When $\nu = \tan\psi$ Eq (11) is transformed into Drucker and Prager's equations (Drucker and Prager, 1952).

The plastic potential of the Drucker and Prager form was used for the first time by Malishev (1954) to obtain the particular relationships between ρ and φ which correspond to the axial compression test. Similar relationships were given later by Takagi (1962) and Lipson (1963). Using the relation of plastic potential, excess values of ρ (Stroganov, 1965) are obtained because of $\tan\psi \gg \nu$ (Stroganov, 1958).

The results obtained show the possibility of overcoming the quantitative divergence between experimental and theoretical data in the plane problems of soil plasticity theory, while retaining all the mathematical methods of the solution of the problems mentioned.

REFERENCES

Barshevscy, B. N. (1956). About the strength hypothesis of cohesionless soil. *Izvestia OTN*, Academy of Sciences, U.S.S.R., No. 4 (in Russian).

Drucker, D., and W. Prager (1952). Soil mechanics and plastic analyses on limit design. *Quart. Applied Mathematics*, Vol. 10, No. 2.

Lipson, M. A. (1963). On the strength theory of plane-deformed solids. *Engineering J.*, Academy of Sciences, U.S.S.R., Vol. 3, No. 1 (in Russian).

Malishev, M. V. (1954). About the determination of the angle of internal friction and cohesion in loose soil at ultimate stress state. *Izvestia OTN*, Academy of Sciences, U.S.S.R., No. 7 (in Russian).

Schleicher, F. (1925). Die energiengrenze der elastizität (Plastizitätsbedinung). *Zeits. für ang. Math. Mech.*, Vol. 5, p. 478.

Stroganov, A. S. (1958). Plane plastic deformation of soil. *Proc. Brussels Conference on Earth Pressure Problems*, Vol. 1, pp. 94–103.

——— (1961). Visco-plastic flow of soils, *Proc. Fifth International Conference Soil Mechanics and Foundation Engineering*. Vol. 2, pp. 721–25.

——— 1963). *Methods of combined design of shaft bindings and ground pressures when grounds and materials have non-linear visco-elastic properties*. Collection on Ground Pressure and Binding of Vertical Shafts. Moscow, Gosgortechisdat (in Russian).

——— (1965). Analysis of plane plastic deformation of soil. *Engineering J.*, Academy of Sciences, U.S.S.R., Vol. 5, No. 3 (in Russian).

Takagi, S. (1962). Plane plastic deformation of soils. *J. Engineering Mechanics Division, Proc. A.S.C.E.*, Vol. 83, EM3, pp. 107–51.

C. Széchy (Hungary)

Some laboratory and photo-elastic studies have been carried out with the purpose in mind of determining the influence of the shape of contact surface of spread foundations upon their bearing capacity and settlement. They have indicated that convex-shaped contact surfaces have a favourable effect upon the propagation of stresses, transmitting them upon a larger area and thus leading to a certain reduction in settlement. On the other hand, this shape of contact surface facilitates lateral displacement and thus leads to a certain reduction of bearing capacity. Contact surfaces with a concave shape act just in the opposite sense in concentrating the stress-propagation zone and counteracting the lateral displacements.

Deviations were not in excess of 10–20 per cent, however, and were understandably diminished with foundation depth, that is, when the foundation depth was double the foundation width, differences became negligible. For further details the reader may refer to the following literature.

REFERENCES

SZÉCHY, C. (1964). The influence of the shape of surface upon the bearing capacity and settlement of strip foundations. *Proc. Seminar on Soil Mechanics*. Lodz, Polish Academy of Sciences.

——— (1965). *Proc. Fifth Symposium Civil and Hydraulic Engineering Department, Bangalore, India, Indian Institute of Science.*

V. USHKALOV (U.S.S.R.)

It is well known that the compressibility of ground thawing under pressure is characterized by a thawing coefficient A_0, and by a consolidation coefficient α_0, and that the strain for the thawing ground is determined by the equation:

$$e = A_0 + \alpha_0 p. \tag{1}$$

Consolidation coefficients were determined at two pressures of thawing: $p_1 = 1$ and $p_3 = 3$ kg/sq. cm. in accordance with the procedure suggested by Tsytovich. Consolidation tests were carried out in a big consolidometer with a diameter of 200 mm. A hot settlement plate with an area of 5000 sq. cm. was used in the field test.

In accordance with the procedure (1) the following data were determined.

$$e_1 = (E_m^I - E_{c1})/(1 + E_m^I) = A_0 + \alpha_0 p_1, \tag{2}$$

$$e_3 = (E_m^{II} - E_{c3})/(1 + E_m^{II}) = A_0 + \alpha_0 p_3, \tag{3}$$

in which e_1 and e_3 stand for the compression of the ground monolith during the thawing under the pressure of p_1 and p_3, E_m^I and E_m^{II} stand for the initial porosity coefficients of the frozen monoliths; E_{c1} and E_{c3} stand for porosity coefficients of the thawed ground monoliths.

Using Eqs (2) and (3) we determined consolidation coefficients α_0 and A_0:

$$\alpha_0 = [(E_m^{II} - E_{c3})(1 + E_m^I) - (E_m^I - E_{c1})(1 + E_m^{II})]/[(1 + E_m^I) \times (1 + E_m^{II})(p_3 - p_1)] \tag{4}$$

or

$$\alpha_0 = {}_3(e - e_1)/(p_3 - p_1), \tag{5}$$

and

$$A_0 = e_3 - \alpha_0 p_3 \tag{6}$$

The correlation of the value e_p and the initial value of the porosity coefficient E_{om} was determined statistically by generalizing the data obtained in the experiment. From the analysis of the experimental data we may write: $E_{om} = E_m(\zeta_i/\zeta_m)$, in which $\zeta_i = E_m - E_{min}$ (or E_{wp})$/E_m$, and where E_{min} stands for the minimum coefficient value for the porosity of the sandy soil, E_{wp} stands for the porosity coefficient with the moisture at the expansion limit, and $\zeta_m = \sum_1^n \zeta_i/n$, n standing for the number of the tests (for loam $\zeta_m = 0.51$, for sandy loam 0.40, for sand 0.37, and for sandy grit 0.36).

The change in the e_p value in accordance with the above equation may be expressed in the following way:

$$e_p = M_p E_{om} \pm b_p, \tag{7}$$

in which M_p and b_p stand for the parameters of the equation.

The plotting of the experimental data in the co-ordinated field $e_p - E_{om}$ gave the linear relationship between the given values stated by Tsytovich (1941), who was the first to discover this relationship. Calculated data for the relationship between e_p and E_{om} may be expressed by the correlation factor equal to 0.86 and the quadratic deviation of the experimental data e_{fi} and the calculated data e_{ci} which amounts to ±12 per cent, the latter meeting the requirements of engineering calculations (Ushkalov, 1962). The data

TABLE II. COMPARISON OF LABORATORY AND FIELD TESTS

Type of soil	Coefficient	Field tests: p = 1 kg/sq. cm.	Field tests: p = 3 kg/sq. cm.	Consolidation tests: p = 1 kg/sq. cm.	Consolidation tests: p = 3 kg/sq. cm.	Ratio of coefficients α/α_{0o}: p = 1 kg/sq. cm.	Ratio of coefficients A/A_{0o}: p = 3 kg/sq. cm.
loam	α_0	*0.031*/0.042	*0.092*/0.127	*0.033*/0.047	*0.100*/0.141	*0.92*/0.90	*0.928*/0.90
	A_0	*0.060*/0.137	*0.060*/0.137	*0.068*/0.148	*0.068*/0.148	*0.88*/0.93	*0.88* /0.93
sandy loam	α_0	*0.029*/0.043	*0.089*/0.131	*0.031*/0.047	*0.096*/0.142	*0.93*/0.92	*0.93* /0.92
	A_0	*0.054*/0.117	*0.054*/0.119	*0.062*/0.131	*0.062*/0.133	*0.87*/0.89	*0.87* /0.89
sand	α_0	*0.017*/0.030	*0.052*/0.090	*0.021*/0.031	*0.062*/0.093	*0.81*/0.96	*0.84* /0.97
	A_0	*0.025*/0.086	*0.025*/0.086	*0.037*/0.095	*0.037*/0.095	*0.68*/0.90	*0.68* /0.90
sandy grit	α_0	*0.017*/0.027	*0.050*/0.080	*0.018*/0.028	*0.053*/0.085	*0.94*/0.96	*0.94* /0.94
	A_0	*0.018*/0.079	*0.018*/0.079	*0.033*/0.080	*0.033*/0.080	*0.55*/0.99	*0.55* /0.99

NOTE: Indices "f" and "c" stand for the coefficients obtained from the data of field and consolidation tests. In the fraction, the consolidation coefficient in the numerator (in italics) is given at $E_{om} = 0.3 \div 0.8$, and in the denominator at $E_{om} = 1.3 \div 1.8$.

obtained by the equations determining the calculated parameters of the correlation between e_p, α_0, and A_0 and E_{om} have been already published (Ushkalov, 1962).

TABLE III. SUMMARY OF RESULTS

Type of soil	Coefficient	Correlation factor $E_{om} = 0.5 \div 0.8$	Correlation factor $E_{om} = 1.3 \div 1.8$
loam	α_0	0.92	0.90
	A_0	0.88	0.93
	e_p	0.90	0.91
sandy loam	α_0	0.93	0.92
	A_0	0.87	0.89
	e_p	0.90	0.91
sand	α_0	0.81	0.96
	A_0	0.68	0.9
	e_p	0.75	0.93
sandy grit	α_0	0.94	0.96
	A_0	0.55	0.99
	e_p	0.75	0.98

Table II shows the comparative data for the calculated consolidation coefficients of thawing ground obtained from the data of consolidation and field tests. In the laboratory experiments with a large consolidometer it was necessary to interpolate the correction factor K_r (the ratio of the calculated values obtained as a result of field tests and those obtained in consolidation tests). The figures are summarized in Table III. Thus, the study of the data obtained gives grounds for believing that the large consolidometer may be successfully used for the testing of thawing ground, on the condition that the above correlation factors are taken into account.

REFERENCES

TSYTOVICH, N. (1941). Calculation of foundation settlement. Moscow, Stroiizdat.

USHKALOV, V. (1962). *Investigations of the thawing foundations and their computation on threshold structure strains.* Moscow, Academy of Sciences U.S.S.R.

R. V. WHITMAN (U.S.A.)

This discussion deals with the development of plastic zones beneath a footing. Traditionally, the engineer has been able only to estimate the initial slope of the load-settlement curve using elastic theory and to estimate the ultimate load using a bearing capacity theory. Until now, there has been no method for analysing the behaviour once yielding starts but before the ultimate load is reached. Such an analysis now is possible using the finite difference iterative techniques developed by Bendel (1962) and Ang and Harper (1964).

In a study at M.I.T. (Whitman and Höeg, 1965) the Harper-Ang technique has been applied to the problem shown in Fig. 64. The numerical properties correspond to steel rather than to soil, but the general nature of the results emerges nonetheless. Fig. 65 shows the calculated load-settlement relation, while Figs. 66 through 69 show the extent of the plastic zone and the motion field at four different stages of the loading. In the final stage, the load has virtually reached the ultimate load predicted by the Prandtl theory, and the motion field is very similar to that predicted by that theory. Note that the plastic zone spreads to considerable depth before it begins to spread sideways beyond the loaded area.

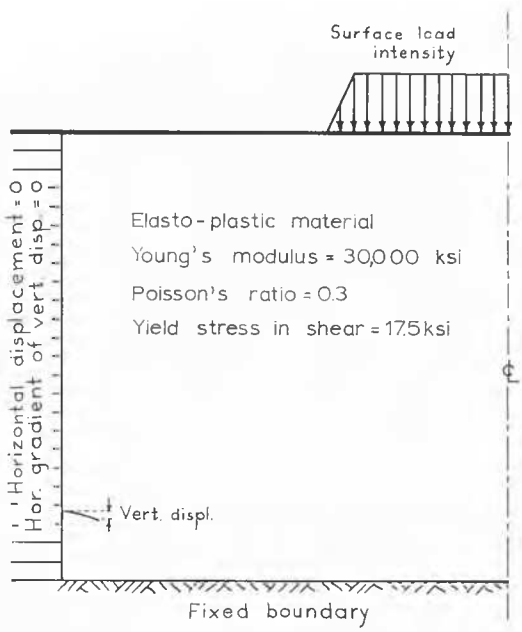

FIG. 64. Details of problem to be analysed.

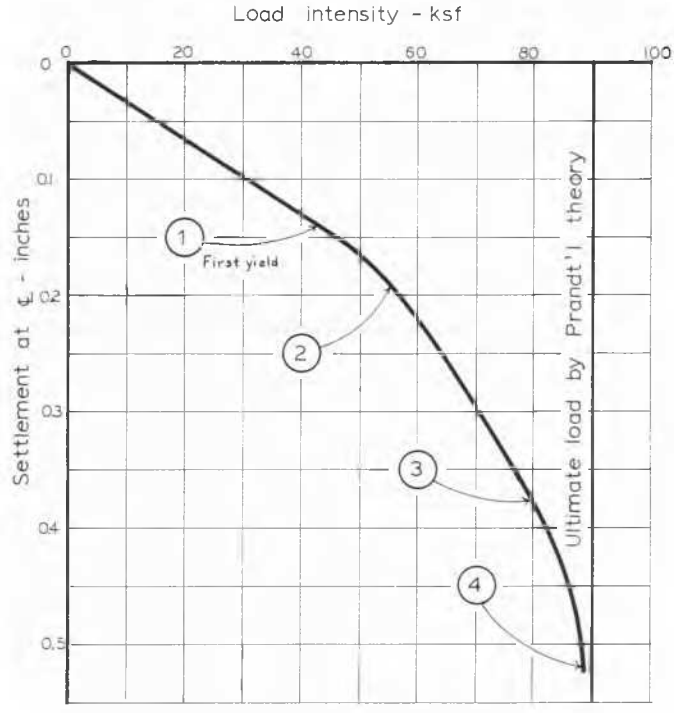

FIG. 65. Computed load-settlement relation.

REFERENCES

ANG, A. H. S., and G. N. Harper (1964). Analysis of contained plastic flow in plane solids. *J. Engineering Mechanics Division, Proc. A.S.C.E.*, Vol. 90, No. EM5, pp. 397–418.

BENDEL, H. (1962). Die berechnung von spannungen und verschiebungen in erddämmen. *Mitteilungen der Versuchsanstalt für Fasserbau und Erdbau*, Zürich, No. 55.

WHITMAN, R. V., and HÖEG (1965). *Development of plastic zone beneath a footing.* Report by M.I.T. Department of Civil Engineering to U.S. Army Engineer Waterways Experiment Station.

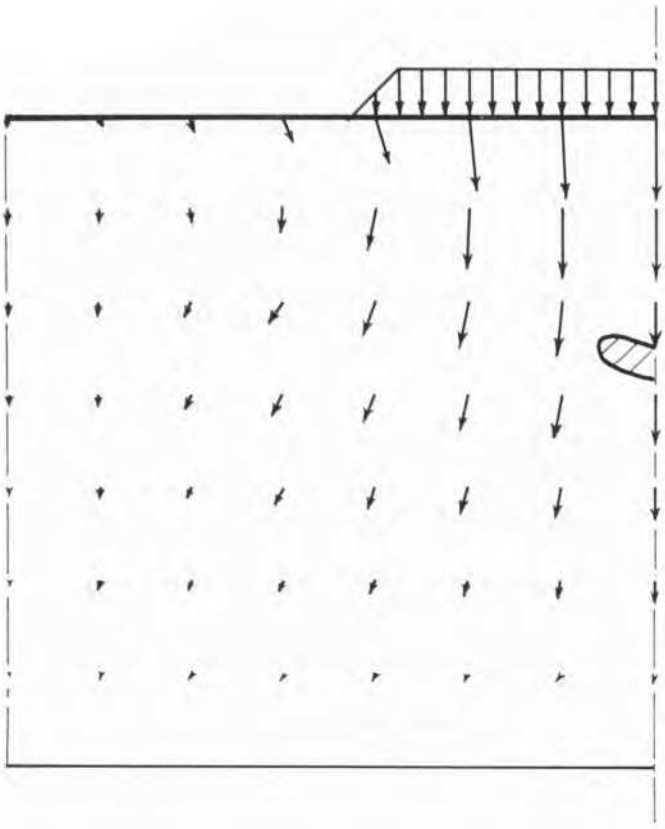

FIG. 66. Load = 46 kg/sq.in. (point 1); point of initial yielding and motions during elastic increment.

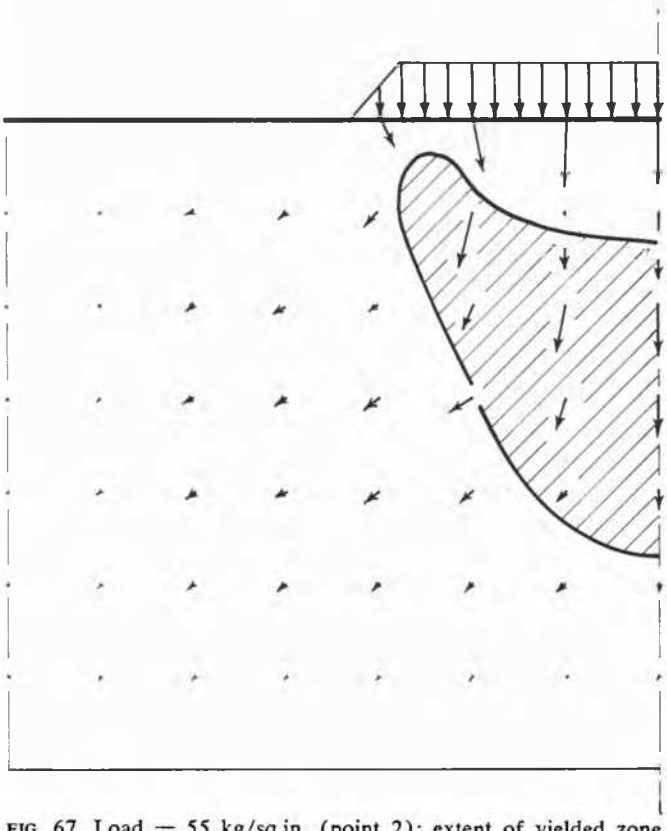

FIG. 67. Load = 55 kg/sq.in. (point 2); extent of yielded zone and motions during small increment of load.

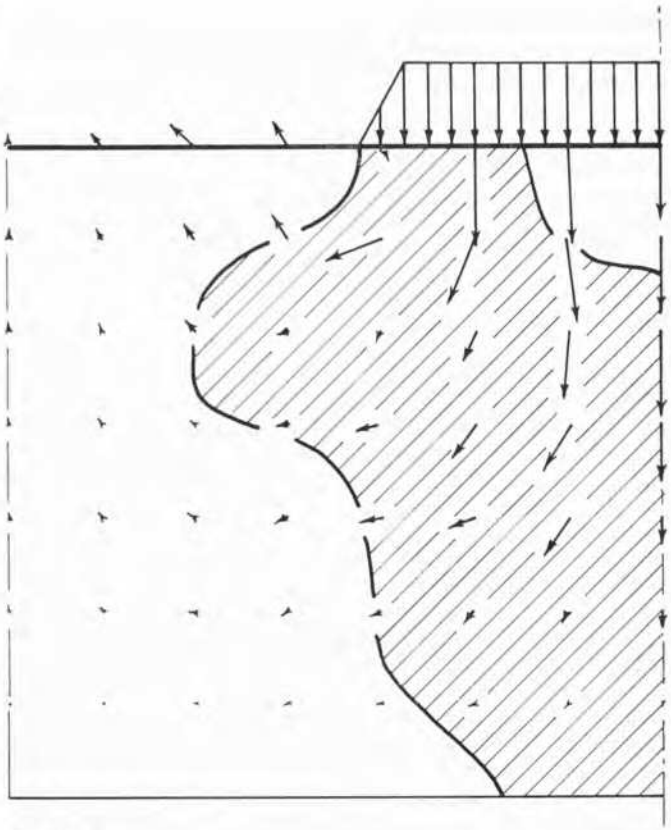

FIG. 68. Load = 80 kg/sq.in. (point 3); extent of yielded zone and motions during small increment of load.

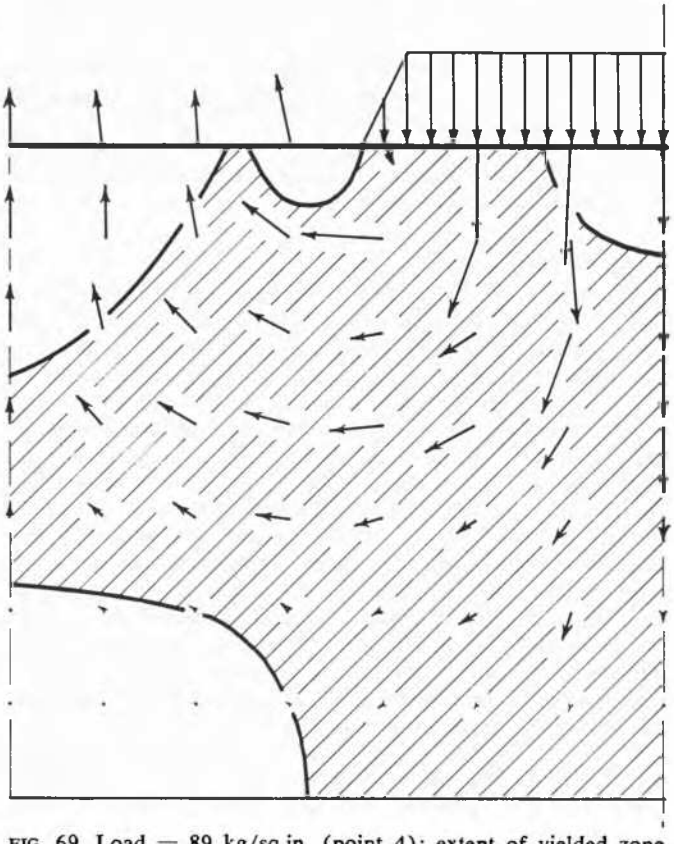

FIG. 69. Load = 89 kg/sq.in. (point 4); extent of yielded zone and motions during small increment of load.